



Fisheries New Zealand

Tini a Tangaroa

Temporal and spatial distribution of non-target catch and non-target catch species in deepwater fisheries

New Zealand Aquatic Environment and Biodiversity Report No. 303

C.T.T. Edwards,
S. Mormede

ISSN 1179-6480 (online)
ISBN 978-1-99-106267-3 (online)

January 2023



Te Kāwanatanga o Aotearoa
New Zealand Government

Disclaimer

This document is published by Fisheries New Zealand, a business unit of the Ministry for Primary Industries (MPI). The information in this publication is not government policy. While every effort has been made to ensure the information is accurate, the Ministry for Primary Industries does not accept any responsibility or liability for error of fact, omission, interpretation, or opinion that may be present, nor for the consequence of any decisions based on this information. Any view or opinion expressed does not necessarily represent the view of Fisheries New Zealand or the Ministry for Primary Industries.

Requests for further copies should be directed to:

Fisheries Science Editor
Fisheries New Zealand
Ministry for Primary Industries
PO Box 2526
Wellington 6140
NEW ZEALAND

Email: Fisheries-Science.Editor@mpi.govt.nz

Telephone: 0800 00 83 33

This publication is also available on the Ministry for Primary Industries websites at:

<http://www.mpi.govt.nz/news-and-resources/publications>

<http://fs.fish.govt.nz> go to Document library/Research reports

© **Crown Copyright - Fisheries New Zealand**

Please cite this report as:

Edwards, C.T.T.¹; Mormede, S.² (2023). Temporal and spatial distribution of non-target catch and non-target catch species in deepwater fisheries. *New Zealand Aquatic Environment and Biodiversity Report No. 303*. 81 p.

TABLE OF CONTENTS

EXECUTIVE SUMMARY	1
1. INTRODUCTION	2
2. METHODOLOGY	2
3. DATA AND METHODS	6
3.1. Data request	6
3.2. Data grooming and preparation	7
3.2.1. Effort data	7
3.2.2. Catches	8
3.2.3. Trawl survey data	8
3.3. Grid specification and environmental data	10
3.4. Model specifications	11
3.4.1. Model fits and diagnostics	13
3.4.2. Model selection	13
3.4.3. Prediction of the catch	13
3.4.4. Prediction of the density	14
3.5. Model analyses	14
4. RESULTS	15
4.1. Prediction of known target catches	15
4.2. Cross validation using observer sampling data	23
4.3. Estimated catches for and biomass distributions for non-target species	26
4.3.1. Barracouta (<i>Thyrsites atun</i>)	26
4.3.2. Rattails (Macrouridae)	28
4.3.3. Spiny dogfish (<i>Squalus acanthias</i>)	30
4.3.4. Frostfish (<i>Lepidopus caudatus</i>)	32
4.3.5. Blue mackerel (<i>Scomber australasicus</i>)	34
4.3.6. Morid cods (Moridae)	36
4.3.7. Redbait (<i>Emmelichthys nitidus</i>)	38
4.3.8. Common warehou (<i>Seriolella brama</i>)	40
4.3.9. Smooth red swimming crab (<i>Nectocarcinus bennetti</i>)	42
4.3.10. Sea perch (<i>Helicolenus</i> spp.)	44
4.3.11. Pale ghost shark (<i>Hydrolagus bemisi</i>)	46
4.3.12. Gemfish (<i>Rexea solandri</i>)	48
4.3.13. Ghost shark (<i>Hydrolagus novaezealandiae</i>)	50
4.3.14. Silver dory (<i>Cyttus novaezealandiae</i>)	52
4.3.15. Giant stargazer (<i>Kathetostoma</i> spp.)	54
4.3.16. Shovelnose spiny dogfish (<i>Deania calcea</i>)	56
4.3.17. Lookdown dory (<i>Cyttus traversi</i>)	58
4.3.18. Smooth skate (<i>Dipturus innominatus</i>)	60
4.3.19. Slender tuna (<i>Allothunnus fallai</i>)	62
4.3.20. Ray's bream (<i>Brama brama</i>)	64
4.3.21. Rough skate (<i>Zearaja nasuta</i>)	66
4.3.22. Baxter's lantern dogfish (<i>Etmopterus baxteri</i>)	68

4.3.23. Hydrocorals (Stylasteridae)	70
4.4. Summary of estimated catches	73
4.5. Summary of density estimates	75
5. DISCUSSION	77
6. POTENTIAL RESEARCH	77
7. ACKNOWLEDGEMENTS	78
8. REFERENCES	79
APPENDIX 1	81

EXECUTIVE SUMMARY

Edwards, C.T.T.¹; Mormede, S.² (2023). Temporal and spatial distribution of non-target catch and non-target catch species in deepwater fisheries.

New Zealand Aquatic Environment and Biodiversity Report No. 303. 81 p.

Bycatch estimation in New Zealand has previously focused on large species groups (i.e., Quota Management System, non-Quota Management System and invertebrate categories) and been performed per fishery. However, for effective ecosystem based fisheries management, catches are required per species for all fisheries combined. To further this aim, we have developed a framework for application on a species-specific basis that is able to integrate across fishing effort and sampling data from multiple fisheries, operating in different locations and with different gear types.

The model follows a two-part structure, using a binomial distribution to describe the probability of a positive catch fishing event, and a log-normal distribution to describe the size of the positive catch component. The model is spatially resolved and has a hierarchical structure, including the biomass density as a predictor of the catch. Using a Bayesian approach, it is able to co-estimate both the catch and the biomass density across space. We included a seasonal component to the spatial biomass distribution, but assumed it to be constant across years. The changing distribution and magnitude of fishing effort over time allowed us to predict catches temporally.

The model was applied to the top non-target species by biomass (and hydrocorals) represented in observer data from the major deepwater Tier 1 fisheries in the New Zealand Exclusive Economic Zone. Application of the model to ling (*Genypterus blacodes*) catches, which were assumed to be well documented, as well as cross-validation of predicted catches using the observer data, demonstrate that the model is internally consistent and able to perform well when provided with reasonable data. In general, it provided a good fit to the observer catch data and was able to generate distributions of the total catch and biomass density spatially and over time. Comparison of these predictions with total landings and vessel reported catch estimates generally demonstrated good performance. However, some shortcomings were identified in instances where the model was not able to adequately accommodate the statistical properties of the observer data, notably infrequent large catches that can lead to a strong positive skew in the catch rates. Given the overall framework, these could be addressed in future work using a species-specific, focused approach to the modelling.

In being able to estimate both the biomass and catch for non-target species within a statistically coherent framework, the model represents a step towards estimation of a spatially resolved exploitation rate for data-poor bycatch fisheries. We discuss shortcomings and improvements that could be made for the approach to provide a basis for future risk assessments of this kind.

¹CEscape Consultancy Services, Otaki, New Zealand

²soFish Consulting Ltd., Wellington, New Zealand

1. INTRODUCTION

Ecosystem based fisheries management is becoming recognised internationally as a pre-requisite for responsible stewardship of the marine environment (Pikitch et al. 2004). Estimation of catch and the exploitation rate for non-target species is central to this paradigm being upheld. In New Zealand, non-target catch is considered equivalent to bycatch and includes all fish and invertebrates caught that were not the target species of the fishing event, whether or not they were discarded (a definition consistent with that presented by McCaughan 1992). In the offshore fisheries, bycatch and discards are routinely estimated (Anderson et al. 2017a,b, Anderson & Edwards 2018, Anderson et al. 2019, Finucci et al. 2020) and trends over time are monitored qualitatively (Fisheries New Zealand 2020). However, non-target catch is usually organised into coarse species groups (e.g., Quota Management System (QMS) or non-QMS species) and is only specific to the fishery, rather than the population or species being caught. The total catch per species is not estimated.

To monitor the exploitation of a population, which may be caught as both target and non-target catch, the total catch across all fisheries must be calculated. The work of Anderson (2017) and Finucci et al. (2019), for example, estimated the catches per fishery at the species level and non-target catch estimates for each species could be added across fisheries to generate a total over time. However, models were applied independently to each fishery and species combination. In the current project we aimed to develop a new model that could estimate the total catch from multiple fisheries simultaneously. The overall project objective was to deliver an analysis of temporal and spatial patterns of non-target catch in deepwater fisheries and model the spatial distribution of some of the most representative non-target species.

Specific objectives were that the project should deliver:

1. A spatially- and temporally-detailed representation of non-target catch in deepwater fisheries around New Zealand, coupled with catch data and fishery information on the location of non-target catch hotspots; the influence of seasonal factors on non-target catch hotspots; and the species and fishing methods that may be driving these hotspots.
2. A spatial distribution of some of the most representative non-target species, modelled from catch and survey data, as well as environmental data.

Previous work has demonstrated that a total catch per non-target species can be estimated by simultaneous integration of the data from multiple fisheries, and that the spatial biomass density distribution can be included as an estimated parameter (Edwards et al. 2018, Edwards 2021). Because these fisheries have different spatial definitions, the estimation model is also spatial. This work was restricted to a limited subset of the available catch data, and our intention was to further develop the approach, increasing both the volume of data and the breadth of application. Our intention was to develop a widely applicable, coherent statistical framework that is able to estimate both the biomass and catch across multiple fisheries operating simultaneously.

2. METHODOLOGY

At a conceptual level, prediction of the non-target catch using a statistical model involves the estimation of the catch rate from observer data and then the application of this rate to the unobserved effort component to calculate the total bycatch. The bycatch data recorded by observers typically follows a semi-continuous distribution, characterised by a high proportion of zeros and a positive skewed continuous distribution of non-zero catches. The appropriate model therefore has two

parts: a binomial model to represent the occurrence of zeros in the data and either a gamma or log-normal model for the non-zero catch component. Previous work in New Zealand has so far implemented a log-normal model for the non-zero catches (e.g., Anderson et al. 2019). The model is fitted to tow-by-tow observer sampling data X_i (in tonnes) using a Bayesian estimation framework (implemented using stan: Stan Development Team 2020, R Core Team 2020). We briefly describe how estimated parameters are currently used to predict the catch for unobserved commercial fishing effort, before describing modifications to the approach and how a new bycatch model is developed for the current project.

Observed and unobserved components of the fishing effort are given the notation o and r , the latter being referred to as the residual effort. The total effort for stratum j is therefore:

$$n_j = r_j + o_j$$

The strata typically represent discrete combinations of the region, fishing year and any features of the fishery considered relevant (e.g., the gear type and presence of a meal plant on a vessel can be relevant to its discard rate, Anderson et al. 2019).

The binomial model part estimates the proportion of positive catches per stratum θ_j using the summed count of non-zero observations, Y_j . For example, for stratum j :

$$Y_j = \sum_{i=1}^{o_j} I(X_i > 0) \sim \text{Binomial}(o_j, \theta_j)$$

where $I(\cdot)$ is an indicator function equal to one if the condition inside the parentheses is met.

Fitting to the sum of the binomial data component introduces a considerable computational saving, which increases as the catches become less frequent. For the positive catch, data are included on a tow-by-tow basis, which is necessary for correct estimation of the standard error term σ . Given observer record i in stratum j , we therefore have:

$$X_i | X_i > 0 \sim \text{LogNormal}(\mu_j, \sigma^2) \quad \text{for } i \in j$$

The two-model parts are independent (i.e., the likelihoods for Y_j and $X_i | X_i > 0$ can be maximised independently), and the full likelihood for stratum j is:

$$\mathbb{L}[\theta_j, \mu_j, \sigma] = \prod_{i=1}^{o_j} \left\{ (1 - \theta_j) \cdot I(X_i = 0) + \theta_j \cdot f_{LN}(X_i | X_i > 0, \mu_j, \sigma) \right\}$$

where $f_{LN}(\cdot)$ is the probability density function of a log-normal distribution evaluated at X_i , θ_j is the probability mass function of a Bernoulli distribution evaluated at one, and the product is across all observed effort in stratum j . The expected values are, for the conditionally positive catch:

$$\mathbb{E}[X_i | X_i > 0] = \exp(\mu_j + \sigma^2/2)$$

and for the unconditional catch:

$$\mathbb{E}[X_i] = \theta_j \cdot \exp(\mu_j + \sigma^2/2)$$

For previous implementations of this model, covariates have been selected based on prior knowledge of the fishery, rather than formal statistical techniques. Due to the quantity of data, formal methods tend to include any covariate with even a small effect size and can therefore complicate the

modelling procedure without additional benefit to the predictions. For this reason, both θ_j and μ_j are typically predicted using shared, pre-selected covariates, including as a minimum the fishing year and area:

$$\begin{aligned}\text{logit}(\theta_j) &= \gamma_0 + \mathbf{x}'_{i \in j} \cdot \boldsymbol{\gamma} \\ \mu_j &= \beta_0 + \mathbf{x}'_{i \in j} \cdot \boldsymbol{\beta}\end{aligned}$$

where $\mathbf{x}'_{i \in j}$ represents a row from the design matrix for record i in stratum j . Parameterisation of the model involves estimation of the intercept terms β_0 and γ_0 , and coefficient vectors $\boldsymbol{\beta}$ and $\boldsymbol{\gamma}$.

Following fits of the model, catch from the residual (unobserved) commercial fishing effort can be predicted. Because observed and unobserved effort cannot be matched by fishing event, the residual effort is calculated on an aggregated scale by model strata (i.e., the sum of the unobserved effort for a particular stratum j):

$$r_j = n_j - o_j$$

At this aggregated scale, the unobserved non-target catch is the summed catch across unobserved effort. Prediction of the total catch per stratum therefore involves the simulation of catch rates per tow \tilde{X}_i (using posterior prediction), and adding these to the observed values X_i :

$$\text{catch}_j = \sum_{i=1}^{r_j} \tilde{X}_i + \sum_{i=1}^{o_j} X_i$$

Because of the large volume of data, posterior predictive simulation of \tilde{X}_i can be computer intensive. It is helpful therefore to predict the summation of the non-zero catches:

$$\tilde{Z}_j = \sum_{i=1} \tilde{X}_i | \tilde{X}_i > 0$$

for which we need the statistical distribution. Unfortunately, the sum of log-normals does not follow a well defined probability distribution, although various approximations exist. A common assumption is to assume that Z_j also follows a log-normal distribution. If $X_i | X_i > 0$ are independent and identically distributed within the stratum (which is an assumption of the modelling), then an approximation for the first two moments of $\ln(Z_j)$ is:

$$\begin{aligned}\eta_j &= \ln(Y_j \cdot \exp(\mu_j)) + \sigma^2/2 - \tau^2/2 \\ \tau &= \sqrt{\ln\left((\exp(\sigma^2) - 1) \cdot \frac{1}{Y_j} + 1\right)}\end{aligned}$$

which is known as the Fenton-Wilkinson method, and gives the familiar expectation:

$$\begin{aligned}\mathbb{E}[Z_j] &= \exp(\eta_j + \tau^2/2) \\ &= \exp(\mu_j + \ln(Y_j) + \sigma^2/2)\end{aligned}$$

If we replace Y_j with the binomial expectation $\mathbb{E}[Y_j] = \theta_j \cdot o_j$, then:

$$\mathbb{E}[Z_j] = \theta_j \cdot \exp(\mu_j + \ln(o_j) + \sigma^2/2)$$

We can therefore use posterior prediction to simulate values for Z_j using a log-normal distribution directly with parameters η_j and τ . The η_j and τ can be functions of $\mathbb{E}[Y_j]$ (the expectation) or \tilde{Y}_j (the simulated number of non-zero events). Posterior prediction of \tilde{Z}_j yields the total unobserved catch for that stratum.

The above modelling framework was appropriate for the question it was designed to answer, namely the low-resolution prediction of absolute, unobserved catches per fishery. It was extended by Anderson et al. (2019) to include a finer spatial representation than the fishery management areas typically requested by Fisheries New Zealand, instead applying the model to a regular grid. A higher spatial resolution requires the inclusion of spatially correlated random effects to represent the catch rate per grid cell. Because of the extra parameters, priors have to be developed to constrain the estimation procedure appropriately. If we first re-specify the subscript j to represent the year and other non-spatial covariates, and use k to represent the spatial effects, the model was modified by Anderson et al. (2019) to include a spatial random effect in the log-normal model part:

$$\begin{aligned}\text{logit}(\theta_j) &= \gamma_0 + \mathbf{x}'_{i \in j} \cdot \boldsymbol{\gamma} \\ \mu_{jk} &= \beta_0 + \mathbf{x}'_{i \in j} \cdot \boldsymbol{\beta} + \phi_k\end{aligned}$$

where ϕ_k is a random effect used to predict the non-zero catch rate at spatial grid cell k . The vector $\boldsymbol{\phi}$ was represented by a Gaussian Random Field:

$$\boldsymbol{\phi} \sim MVN(0, \Sigma)$$

which is a multivariate normal prior distribution with a covariance matrix structured to allow spatially dependent correlation between the estimated coefficients. Intuitively, this spatial dependence allowed information to be shared between neighbouring locations, which aligns with the assumption that areas in close geographical proximity are likely to have similar biophysical properties and therefore similar catches. Because neighbouring grid cells are defined as sharing a common boundary, the approach naturally accounts for land barriers that may separate two grid cells. This model was shown to perform reasonably well under limited testing (Anderson et al. 2019). We note however that parameterisation is too high to allow for a year-area interaction, and application to a species group may therefore not be appropriate if the group has changed species composition over the duration of the time series (because by changing the species composition of a group the spatial distribution of catches could also have changed).

A notable feature of bycatch modelling in New Zealand, and in general, is that prediction of the catch of a certain species is independent of any representation of the biomass of that species, despite it clearly being important. Without explicit representation of the biomass hierarchically as an estimated parameter, these models cannot be used to reconstruct the density surface except under very restricted conditions. For example, using the model of Anderson et al. (2019), we can extract the relative biomass density surface using an assumption that the density is proportional to the expected catch rate:

$$d_k \propto \mathbb{E}[x_{jk}] = \theta_j \cdot \exp(\mu_{jk} + \sigma^2/2)$$

We note however that the density estimate d_k will be strictly dependent on the covariates within each stratum, j . We may have fleet, or fishing method covariates for example, which would equate to multiple density predictions at the same location. If only a single fleet or fishing method is used, then this may be appropriate, but the approach would otherwise be unsuitable. For the current project we instead propose an alternative hierarchical model, that still fits a two-part model to the data, but simultaneously allows explicit representation of the biomass density surface. This is an approach that was first developed and presented by Edwards et al. (2018) and Edwards (2021).

The model proposed by Edwards (2021) represented the catches as a function of the available biomass density per tow d_i , using a two-part marginalised regression:

$$\text{cloglog}(\theta_i) = \log(\gamma_j \cdot a_i \cdot d_i)$$

$$\mu_i = \log(\pi_j \cdot a_i \cdot d_i) - \log(\theta_i) - \sigma_j^2/2$$

for $i \in j$, where a_i is the gear affected area per fishing event i , and γ_j and π_j are rate parameters specific to the fishery j . The available, relative biomass density per event d_i , was predicted using event specific covariates, namely depth and latitude, with regression coefficients estimated during the model fit. Using environmental data as a predictor of the density stabilised the estimation and allowed prediction of both the density surface and catch rates into regions of limited data coverage.

Binomial and log-normal distributional assumptions were used to fit to the observational data which gives the model an expected catch per fishing event i , of:

$$\mathbb{E}[x_i] = \pi_j \cdot a_i \cdot d_i$$

which is the familiar catch equation of Paloheimo & Dickie (1964), where π_j is an “efficiency” term that predicts the proportion of the biomass within the gear affected area that is typically retained. In so much as a_i and d_i represent the mechanics of the fishing event, the product $\pi_j \cdot a_i$ is usually referred to as the “catchability.”

The model has been shown to be capable of predicting the catches at a fine spatial resolution. For example, Edwards (2021) fitted it to vessel reported catch data per $0.2^\circ \times 0.2^\circ$ grid cell for a range of species, showing that it can predict the observed catches across a spatial extent within the New Zealand Exclusive Economic Zone (EEZ). For the current project we used a similar two-part modelling approach to co-estimate both the non-target catches, spatially resolved, and the underlying biomass density surface.

3. DATA AND METHODS

3.1 Data request

Commercial catch and effort data, observer data, and landings data were requested for all years from 1 October 1990 up to 30 September 2020, in all areas, for all form types and by any fishing method, where the target species was one of: ORH, HOK, HAK, LIN, JMA, JMD, JMN, JMM, OEO, SSO, BOE, SOR, WOE, SBW, SQU, ASQ, NOS, NOG, SCI, SWA, WWA. This aligned with the approach of Finucci et al. (2019), who in their comprehensive assessment considered bycatch in the major offshore Tier 1 fisheries: the arrow squid (SQU), hoki, hake, ling (HHL), southern blue whiting (SBW), orange roughy (ORH), oreo (OEO), and scampi (SCI) trawl fisheries; and the ling bottom longline (LLL) fishery. A list of the target species is given in Table 1. In addition, all bottom trawl data from the RV *Tangaroa* and RV *Kaharoa* trawl surveys were requested. These provide an important source of information for estimation of the catch and biomass density surface using the proposed method (Edwards et al. 2018). A list of the fishing methods and gear types is given in Table 2. For reference, a copy of the data request is provided in Appendix 3.1.

Table 1: Target species for the major offshore Tier 1 fisheries, in order of decreasing catch biomass (see Figure 1). Note that SQU also includes the codes: ASQ, NOS and NOG; JMA also includes the codes: JMD, JMN and JMM; and, OEO also includes the codes: SSO, BOE, SOR and WOE.

Species code	Common name	Scientific name	Family
HOK	Hoki	<i>Macruronus novaezelandiae</i>	Merlucciidae
SQU	Arrow squid	<i>Nototodarus sloanii</i> & <i>N. gouldi</i>	Ommastrephidae
SBW	Southern blue whiting	<i>Micromesistius australis</i>	Gadidae
JMA	Jack mackerel	<i>Trachurus declivis</i> , <i>T. murphyi</i> & <i>T. novaezelandiae</i>	Carangidae
ORH	Orange roughy	<i>Hoplostethus atlanticus</i>	Trachichthyidae
OEO	Oreos	<i>Pseudocyttus maculatus</i> , <i>Allocyttus niger</i> , <i>A. verrucosus</i> & <i>Neocyttus rhomboidalis</i>	Oreosomatidae
LIN	Ling	<i>Genypterus blacodes</i>	Ophidiidae
SWA	Silver warehou	<i>Seriolella punctata</i>	Centrolophidae
HAK	Hake	<i>Merluccius australis</i>	Merlucciidae
WWA	White warehou	<i>Seriolella caerulea</i>	Centrolophidae
SCI	Scampi	<i>Metanephrops challengeri</i>	Nephropidae

Table 2: Notation and description for fishing methods and gear types.

Method	Gear	Description
BLL	AUT	Bottom autoline
BLL	MAN	Bottom manual longline
TWL	BT	Bottom trawl
TWL	MB	Mid-water trawl within 5 m of the bottom
TWL	MW	Mid-water trawl
TWL	PRB	Precision trawl harvesting (bottom)
TWL	PRM	Precision trawl harvesting (mid-water)
TWL	TAN	RV <i>Tangaroa</i> trawl survey
TWL	KAH	RV <i>Kaharoa</i> trawl survey

3.2 Data grooming and preparation

An R-package **nzce** was developed as a repository of code for the preparation of all data necessary for this type of bycatch analysis. Due to changes in the observer recording protocols in the early 2000s, only data from fishing years 2000/01 onwards were retained for analysis. The temporal range was for fishing years 2000/01 to 2018/19 inclusive, which was up to the most recent year of complete landings data. Data were further partitioned by season, specifically: Summer (October to March) and Winter (April to September).

3.2.1 Effort data

Both commercial effort and observer data effort fields were groomed in the following manner:

- Check for and if possible correct inconsistencies in the start and end times of fishing;
- Remove obvious errors in the positional data;
- Calculate preliminary distance covered using groomed positional data;
- Trim and if necessary impute missing effort variables (e.g., speed, duration and distance);
- Re-calculate the distance covered if reliable speed and duration data are present.
- Identify mid-water bottom trawls and assign to new MB gear category;

This procedure involved an initial calculation of the distance covered per trawl tow using positional data. However, because of non-straight tow paths, it was re-calculated using speed and duration data if these data were present. This latter calculation took precedent.

Two fishing methods were represented in the data, namely trawl and bottom longline (consistent with Finucci et al. 2019), for which we measured effort using the distance covered by the tow and the number of thousand hooks, respectively.

3.2.2 Catches

Non-target species to be included in the current analysis were selected based on the observed catch. Species categories that comprised 90% of the observed non-target catches were retained for analysis. In Figure 1, the total catches for all target and non-target species included in this analysis are shown, with the top 90% of non-target species listed in Table 3. In addition to those species, we further included the hydrocoral species group (code COR) at the request of Fisheries New Zealand.

Catches used in the analysis were as follows:

- Observer reported catches comprise the data used to fit the model and were therefore the primary source of information for the analysis.
- Vessel reported catches are the catches “estimated” per event by the vessel during fishing. Only the top five or eight species caught in an event (by weight, depending on the reporting form) are recorded and these records are therefore incomplete. For some fishing events, there will be both vessel reported and observed catches, but since these two sources of data are not matched by event they cannot be reliably compared directly. Nevertheless, vessel reported catches still have associated spatial and temporal information and were retained for purposes of comparison with the observer catch data and model estimated catches. For example, comparison of the total observed and vessel reported catches can give an indication of the degree to which vessel catches are represented in the observer data being used to fit the model.
- Landings are the catches reported per trip and fish stock. They are weighed on shore and are therefore the most reliable record of the total. For purposes of model validation, we also included the discards in these totals. This allowed comparison with the model estimated total catches.

3.2.3 Trawl survey data

All bottom trawl survey data from the RV *Tangaroa* and RV *Kaharoa*, and with a gear performance code of “Excellent” or “Satisfactory,” were retained.

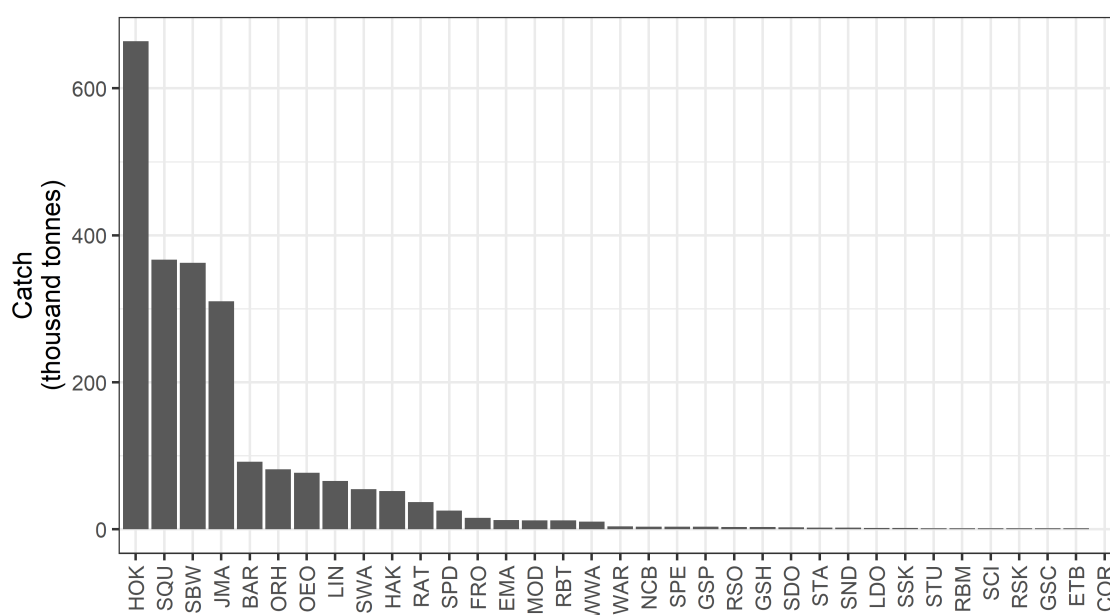


Figure 1: Total observed catches for the top 33 species recorded in the Centralised Observer Database 2000/01 to 2019/20. Species codes are listed in Table 1 and 3.

Table 3: Non-Target species comprising the top 90% of observer recorded catches, plus hydrocorals, in order of decreasing observed catch biomass.

Species code	Common name	Scientific name	Family
BAR	Barracouta	<i>Thyrsites atun</i>	Gempylidae
RAT	Rattails	Macrouridae	Macrouridae
SPD	Spiny dogfish	<i>Squalus acanthias</i>	Squalidae
FRO	Frostfish	<i>Lepidopus caudatus</i>	Trichiuridae
EMA	Blue mackerel	<i>Scomber australasicus</i>	Scombridae
MOD	Morid cods	Moridae	Moridae
RBT	Redbait	<i>Emmelichthys nitidus</i>	Emmelichthyidae
WAR	Common warehou	<i>Seriolella brama</i>	Centrolophidae
NCB	Smooth red swimming crab	<i>Nectocarcinus bennetti</i>	Portunidae
SPE	Sea perch	<i>Helicolenus</i> spp.	Scorpaenidae
GSP	Pale ghost shark	<i>Hydrolagus bemisi</i>	Chimaeridae
RSO	Gemfish	<i>Rexea solandri</i>	Gempylidae
GSH	Ghost shark	<i>Hydrolagus novaezealandiae</i>	Chimaeridae
SDO	Silver dory	<i>Cyttus novaezealandiae</i>	Zeidae
STA	Giant stargazer	<i>Kathetostoma</i> spp.	Uranoscopidae
SND	Shovelnose spiny dogfish	<i>Deania calcea</i>	Centrophoridae
LDO	Lookdown dory	<i>Cyttus traversi</i>	Zeidae
SSK	Smooth skate	<i>Dipturus innominatus</i>	Rajidae
STU	Slender tuna	<i>Allothunnus fallai</i>	Scombridae
RBM	Rays bream	<i>Brama brama</i>	Bramidae
RSK	Rough skate	<i>Zearaja nasuta</i>	Rajidae
GSC	Giant spider crab	<i>Jacquintotia edwardsii</i>	Majidae
ETB	Baxters lantern dogfish	<i>Etmopterus baxteri</i>	Etmopteridae
COR	Hydrocorals	Stylasteridae	Stylasteridae

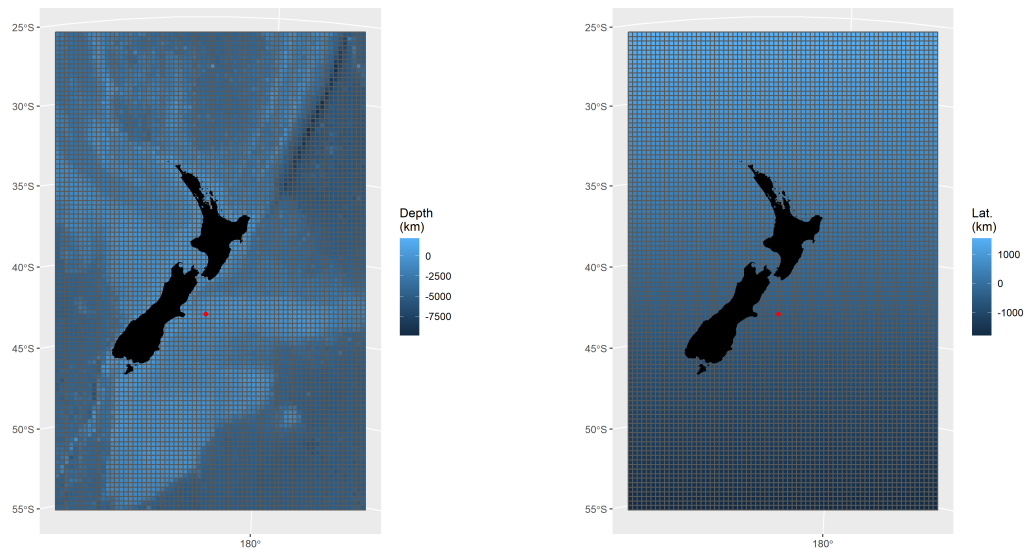


Figure 2: Grid cell covariates supplied to the model, with mean depth per cell in the left panel, and latitude in kilometres on the right. The origin specified by the projection is shown as a red dot, with latitude given relative to this point.

3.3 Grid specification and environmental data

The standard Fisheries New Zealand grid was applied, using code presented by Mormede et al. (2022). The square cell size was set to 32 km, giving an area per grid cell of 1024 km². Depth data were obtained from the publicly available 2016 bathymetric data: <https://niwa.co.nz/our-science/oceans/bathymetry/download-the-data>; and the average depth was calculated per cell. Latitude was calculated in metres using the mid-point per cell, relative to the origin point of the projection (Figure 2). Prior to being used in the model, each covariate was re-normalised by subtracting the mean and dividing by the standard deviation.

Observer and commercial effort data were assigned to each of the grid cells within the New Zealand EEZ. For each species we discarded grids with no observed catches. This provided a means by which the model could be bounded spatially, based on an assumption that if the species has never been observed within a given grid cell, then it is unlikely to be present or only present at a negligible density. Commercial effort within those grid cells was also omitted on the assumption that it is unlikely to yield any significant catches of that species. This is a simplification that could be addressed in further work by using environmental relationships to extend the estimated biomass density distribution into regions where catches have not been observed.

3.4 Model specifications

We modified the model proposed by Edwards (2021) to make it more efficient computationally, and to better represent the total effort by changing the effort metric per fishing event. Computational savings were achieved by assuming a uniform distribution of the biomass density within each grid cell, which can then be represented by a grid cell specific (rather than event specific) biomass density parameter d_k . We also introduce an effort scalar parameter s_i , which is proportional to the gear affected area rather than equal to it. For trawl, effort was the distance of the tow; for longline, effort was measured as the number of thousand hooks. This is more data inclusive, since the covariates needed to calculate the gear affected area are often missing. In addition, we introduced a seasonal component to the biomass distribution, using the subscript l . Model terms and subscripts are summarised in Table 4.

The model is written as:

$$\begin{aligned} \text{cloglog}(\theta_{jkl}) &= \log(\gamma_j \cdot s_{jkl} \cdot d_{kl}) \\ \mu_{jkl} &= \log(\pi_j \cdot s_{jkl} \cdot d_{kl}) - \log(\theta_{jkl}) - \sigma_j^2/2 \end{aligned}$$

using the average effort scalar per fishery, grid cell and season: $s_{jkl} = \sum s_i / n'_{jkl}$, where n'_{jkl} is the number of observed fishing events. The distributional assumptions used to fit the model were:

$$\begin{aligned} I(X_i > 0) &\sim \text{Bernoulli}(\theta_{jkl}) \\ X_i | X_i > 0 &\sim \text{LogNormal}(\mu_{jkl}, \sigma_j) \end{aligned}$$

for $i \in jkl$, giving the expectation per event:

$$\mathbb{E}[X_i] = \pi_j \cdot s_{jkl} \cdot d_{kl}$$

The terms γ_j and π_j are specified per fishery group j using two sub-models. The fishery group is a unique combination of the method (i.e., trawl or bottom longline) and the gear type, with the gear type coefficients constrained to sum to zero within each method.

$$\begin{aligned} \gamma_j &= \gamma_{\text{method}} + \gamma_{\text{gear}|\text{method}} \\ \pi_j &= \pi_{\text{method}} + \pi_{\text{gear}|\text{method}} \end{aligned}$$

For instances in which the catches of a target species were being modelled, we introduced additional γ_{target} and π_{target} terms, also constrained to sum to zero.

The density d_{kl} was modelled as a regression on coefficient vector α :

$$\log(d_{kl}) = \underbrace{\mathbf{x}'_k \cdot \alpha}_{\bar{d}_k} + \phi_{kl}$$

where \mathbf{x}'_k represents the latitude and depth covariates per grid cell, and with a correlated random effect term centred on zero for each season:

$$\phi_l \sim \text{MVN}(0, \Sigma_l)$$

The Σ covariance matrix was constructed so that ϕ_l follows a conditional autoregressive (CAR) prior distribution (Gelfand & Vounatsou 2003, Jin et al. 2005), meaning that each ϕ_{kl} has a prior that is dependent on the value for ϕ_{kl} in neighbouring grid cells.

Table 4: Summary of model terms

Notation	Description
Subscripts	
i	Fishing event
j	Fishing group (method and gear)
k	Grid
l	Season
Estimated parameters	
$\gamma_{\text{method}; \gamma_{\text{gear} \text{method}}$	Encounter rate parameters
$\pi_{\text{method}; \pi_{\text{gear} \text{method}}$	Efficiency parameters
α	Vector of regression coefficients
ϕ_l	Vector of density random effects
τ, ρ	Precision and correlation for conditional autoregressive (CAR) prior
Derived parameters	
γ_j	Encounter rate
π_j	Catch efficiency
θ_{jkl}	Probability of non-zero catch per event
μ_{jkl}	Expectation of the log of the catch per event
d_{kl}	Biomass density
Input covariates	
s_{jkl}	Mean effort scalar per event
x_{depth}	Depth (m)
x_{lat}	Latitude (km)
Input data	
X_i	Catch
$I(X_i > 0)$	Binary indicator of non-zero catch
$X_i X_i > 0$	Non-zero catch
Y_{jkl}	Count of non-zero catch records
Z_{jkl}	Sum of non-zero catch records
n'_{jkl}	Number of observed fishing events
n_{jkl}	Number of commercial fishing events
Model outputs	
\tilde{Y}_{jkl}	Count of non-zero catch records
\tilde{Z}_{jkl}	Sum of non-zero catch records

Prior probability distributions for the remaining parameters were:

$$\gamma_{\text{gear}|\text{method}} \sim \text{Normal}(0, 1)$$

$$\pi_{\text{gear}|\text{method}} \sim \text{Normal}(0, 1)$$

$$\sigma_j \sim \text{Normal}(0, 1)$$

$$\tau \sim \text{Gamma}(2, 2)$$

The γ_{method} and π_{method} parameters were given improper (unbounded) uniform priors.

3.4.1 Model fits and diagnostics

All analyses and estimation procedures were performed using Bayesian methods within R using the **rstan** package (Stan Development Team 2020, R Core Team 2020). For each model fit, two Monte-Carlo Markov chains were run for 1000 iterations with the first half discarded. To check performance of the model, the convergence of all parameter chains was first verified using visual inspection and consideration of the \hat{R} statistic (Gelman & Rubin 1992). In addition, posterior prediction of the data was performed to ensure that the model was capable of reproducing the observations.

3.4.2 Model selection

For each species-specific application of the model, six model runs were performed, each with a different regression relationship between the predicted density per grid cell \bar{d}_k , and the depth and latitude covariates. Further details on these models and their selection for use are given in the supplementary information for this report by Edwards & Mormede (2023). In each case, only results from the best performing model were retained.

3.4.3 Prediction of the catch

We use posterior prediction to generate catches for the total commercial fishing effort, aggregated by fishery, grid cell and season and represented as the number of fishing events multiplied by the average effort scalar per event; $s_{jkl} \cdot n_{jkl}$. This differs from the approach implemented by, for example, Anderson et al. (2019) in which catches are only predicted for the unobserved effort component (see Section 2). This was to allow better diagnosis of the model performance: by predicting over the total commercial effort rather than the residual (unobserved effort), we are better able to diagnose performance of the model when observer coverage is high. For actual model application, prediction would be restricted to the residual effort only and summed with the observed catches (as done previously).

Using the Fenton-Wilkinson method, total commercial catches were generated using posterior predictive simulation from a log-normal distribution:

$$\eta_{jkl} = \ln(\bar{Y}_{jkl} \cdot \exp(\mu_{jkl})) + \sigma_j^2/2 - \tau_{jkl}^2/2$$

$$\tau_{jkl} = \sqrt{\ln\left(\left(\exp(\sigma_j^2) - 1\right) \cdot \frac{1}{\bar{Y}_{jkl}} + 1\right)}$$

$$\tilde{Z}_{jkl} \sim \text{LogNormal}(\eta_{jkl}, \tau_{jkl})$$

If we replace \tilde{Y}_{jkl} with the binomial expectation $n_{jkl} \cdot \theta_{jkl}$ then we can verify the expected catches to be:

$$\begin{aligned}\mathbb{E}[\tilde{Z}_{jkl}] &= \exp(\eta_{jkl} + \tau_{jkl}^2/2) \\ &= \exp(\mu_{jkl} + \ln(\tilde{Y}_{jkl}) + \sigma_j^2/2) \\ &= \exp(\ln(\pi_j \cdot s_{jkl} \cdot d_{kl}) - \ln(\theta_{jkl}) - \sigma_j^2/2 + \ln(n_{jkl} \cdot \theta_{jkl}) + \sigma_j^2/2) \\ &= \pi_j \cdot s_{jkl} \cdot d_{kl} \cdot n_{jkl}\end{aligned}$$

3.4.4 Prediction of the density

For each species, the spatial extent of the model was constrained to grid cells in which at least one positive catch had been recorded in the observer data. The species-specific biomass density for those grid cells, per season, was extracted from the model fit as a posterior distribution of the predicted value:

$$d_{kl} = \exp(\mathbf{x}'_k \cdot \boldsymbol{\alpha} + \phi_{kl})$$

The biomass density has a seasonal component, allowing a distributional change in the biomass between the Summer and Winter. However, there is currently no annual variation. Although this could be included, for the current project we opted to estimate a constant biomass distribution over years.

Previous work by Edwards (2021) has shown that the biomass density is inversely correlated with the estimated catch efficiency coefficient (π_j), i.e., similar catch values can be predicted by the model for a high biomass and low catch efficiency or *vice versa*. Reliability of the d_{kl} parameter as a measure of the absolute biomass density is improved by prior information on the catchability for at least one of the gear types (from surveys for example), and the absolute density estimate is only reliable to the extent that this is known. In the current work we do not make any prior assumptions of this type and the density should therefore be considered a relative rather than an absolute measure. Uncertainty in the biomass density surface was quantified using the 95% equal-tailed credibility interval. The difference between the upper and lower quantile, normalised to four times the median value, provides a Bayesian measure of the uncertainty analogous to the coefficient of variation.

If we assume that the density is measured in tonnes per square kilometre, then the units for π_j can be specified accordingly. For trawls, effort s_{jkl} is measured in units of kilometres and units for π_j are therefore also kilometres. Intuitively, π_{BT} for example, can be thought of as the effective width of the trawl net, under the assumption that the width is proportional to the catch and the biomass density is uniformly distributed. For the longline fishery, since effort is measured in units of a thousand hooks, π_j is in units of square kilometres per thousand hooks. In this case, π_{AUT} for example, would be a measure of the effective area covered per thousand hooks, again assuming that the area covered is proportional to the catches.

3.5 Model analyses

A sequence of analyses were performed to first, investigate and validate performance of the model (Sections 4.1 and 4.2), and second to produce predictions of the total catch for non-target species (Section 4.3). The intention is to introduce the method and present the framework as broadly applicable to a wide range of non-target species, with minimal consideration of the species or fishery specific characteristics. Within each of the applications presented, there remains scope for further exploration of the model structure and how the data are represented.

4. RESULTS

We present here illustrative results that will allow us to describe the validity and performance of the model. Detailed results for each of the non-target species are given by Edwards & Mormede (2023) in a supplement to this report. Validation of the model is achieved through prediction of catches for ling: a target species with accurate landings data. A second validation was performed using cross-validation, in which a subset of the observer data was used to predict the remainder of the observed catches. These are described in further detail below, following which we present species-specific summary estimates of the total bycatch and biomass density distribution.

4.1 Prediction of known target catches

We first evaluated model performance by predicting known catches for ling (LIN), an important commercial target species that is targeted by both the HHL trawl fishery and the ling bottom longline fishery (LLL). This served to validate the approach and also allowed us to introduce some of the model diagnostics.

Visual convergence diagnostics are shown for the catchability parameters in Figure 3. Despite only a small number of posterior samples, convergence was good. We do not report the catchability parameter estimates in numeric form, but we can see visually the relationship between gear types. For example, the TAN and KAH surveys have the highest catchability out of the trawl fishing methods, and BT has a higher catchability than MB or MW, as might be expected. Catchability estimates for the longline gear types cannot be compared with those for the trawl gear types, because they have different units (see Section 3.4.4). For the longlines, it appears that catchability for MAN is higher than for AUT, as might be expected from our understanding that manual longlines are more carefully placed by fishing vessels.

Model fit is given in Figure 4. In the top panel, the model estimated average annual catch per grid cell and gear type is plotted against the empirically observed values used to fit the data. There is a close relationship, indicating that the model is capable of reproducing the data. We also show the relationship to empirical vessel reported catches. The model is not fitted to these data. Rather the tight correlation is an emergent property and indicates that the vessel reported catches are themselves tightly correlated with the observer data. This observation is further illustrated in Figure 5, which shows the sum of the observed and vessel reported catches per gear type, with corresponding model predictions. Despite vessel reported catches being substantially larger (i.e., only a small proportion of the catches are represented in the observer data), the model is able to reliably predict these data.

Spatial fit of the model is illustrated in Figure 6. Here, the model estimated and observed average annual catches per grid cell and method are shown. Both the spatial coverage and magnitude of the catch appeared to be well predicted by the model.

As a further validation of the model, we predicted the vessel reported catches and landings (Figure 7). From Figure 4 we can infer a close relationship between the observed and vessel reported catches, and it can be seen in Figure 7 that the model is able to predict the vessel reported catches over time. However, the vessel reported catches were slightly less than the landings, and model predictions of the landings data were a slight under-estimate. Nevertheless, the model estimates were clearly a valid approximation, and further work would be required to understand the differences between the landings and observed and vessel reported catch data and how these can be represented within the modelling framework. We further note that the biomass density included in the model currently has

no annual effect; it is constant over years. This could account for some of the deficiencies in the model fit, particularly if the stock biomass is fluctuating in different regions of its distribution.

Finally, as additional model outputs we present the total catches distributed spatially, and disaggregated by fishing method and season (Figure 8). The underlying biomass density distribution is given per season in Figure 9, including an estimate of the uncertainty. This is included to emphasise that the density is an estimated parameter rather than a model input, with a statistically coherent representation of the uncertainty throughout. There appears to be very little seasonal change in either the catch or biomass density distributions.

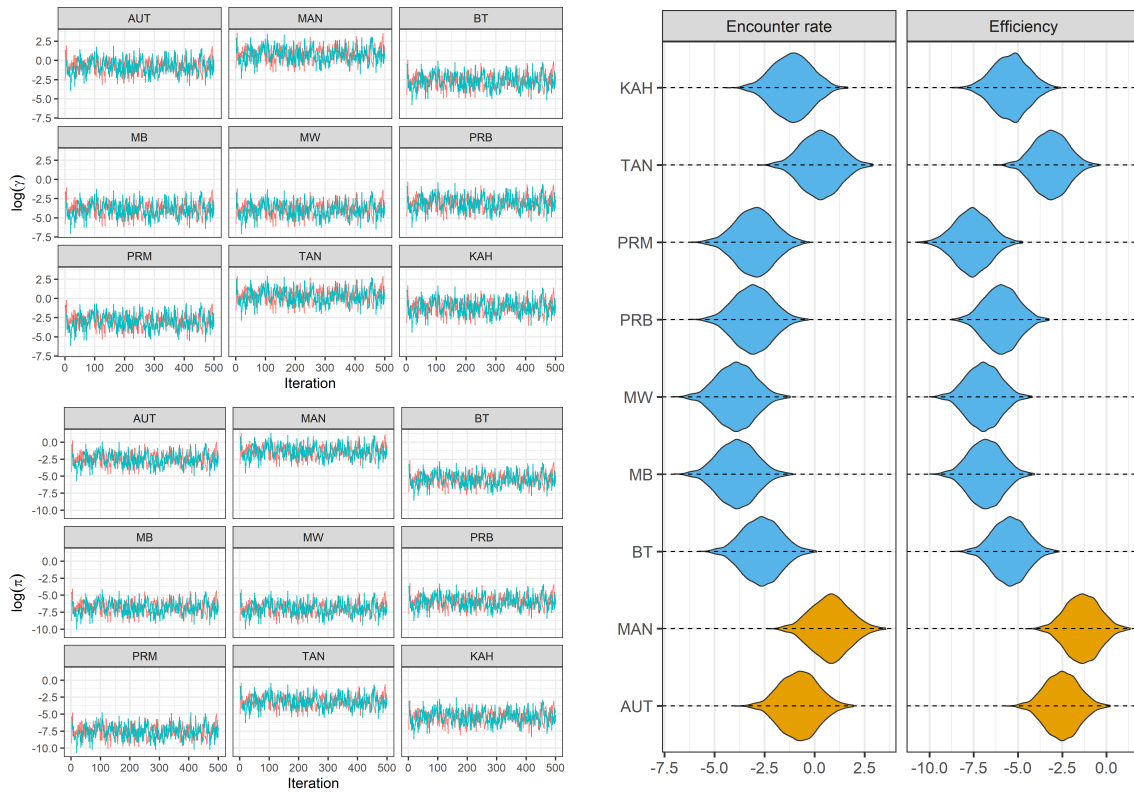


Figure 3: Trace diagnostics and posterior density distributions for LIN catchability parameters per gear type: the encounter rate $\log(\gamma_j)$, and efficiency $\log(\pi_j)$. Gear types are listed in Table 2.

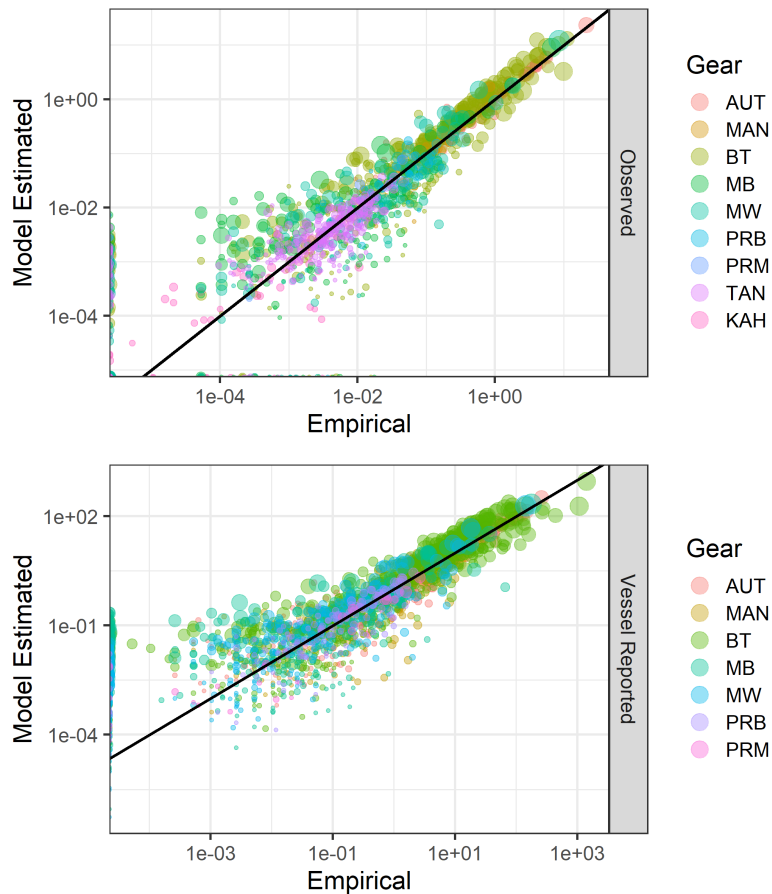


Figure 4: Prediction of observed (top) and vessel reported (bottom) catch data for LIN. Model estimated values were obtained as the median of the posterior predicted distribution of the average annual catch per grid cell and gear type. Catch values are given in tonnes on a log10 scale. Gear types are listed in Table 2.

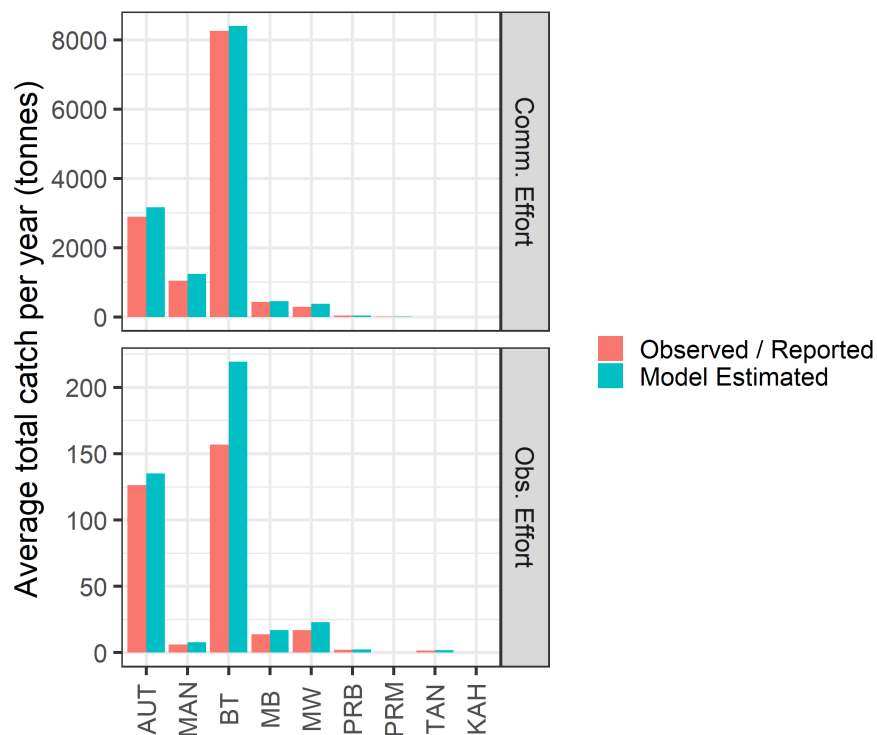


Figure 5: Prediction of vessel reported (top) and observed (bottom) catch data for LIN, noting that vessel reported catches are an order of magnitude larger than the observed catches. Catches are given as the posterior median of the average annual catch per gear type. Gear types are listed in Table 2.

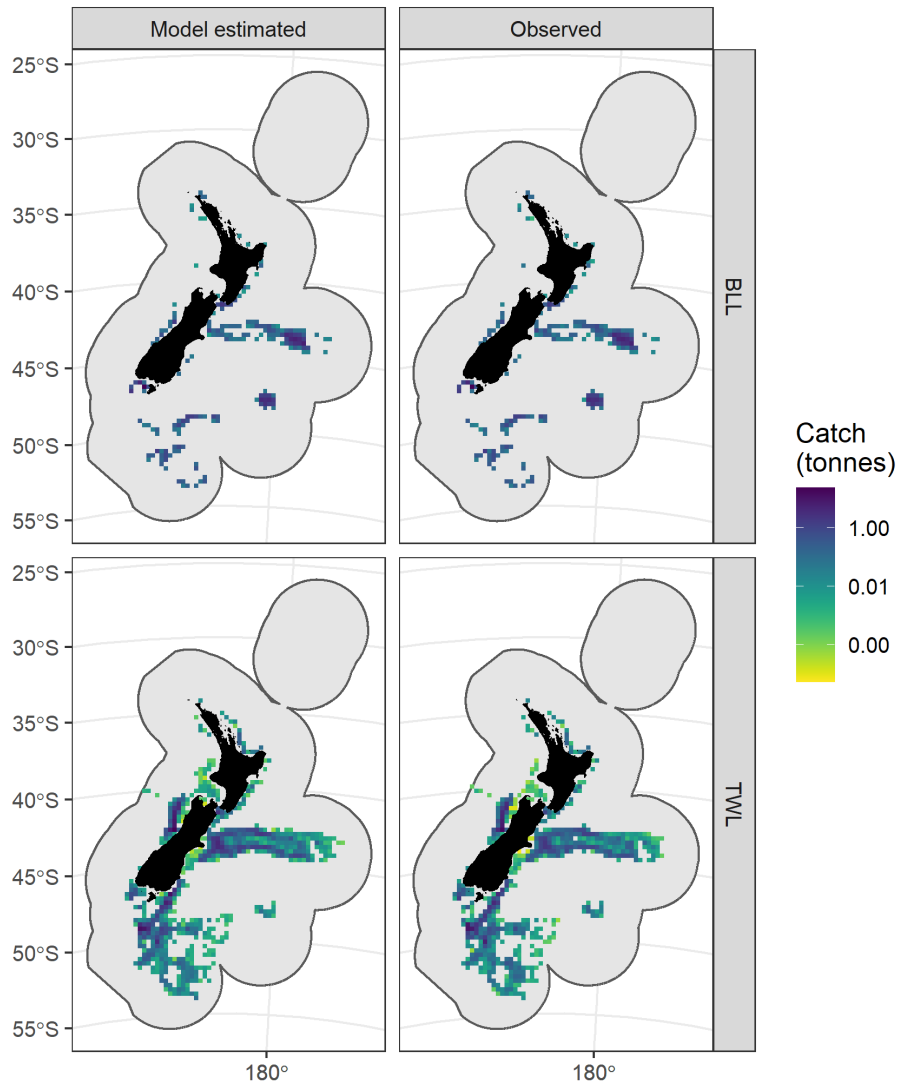


Figure 6: Spatial comparison of observed and predicted catches for LIN. Model estimated values were obtained as the median of the posterior predicted distribution of the average annual catch per grid cell and method. Catch values are given in tonnes on a log₁₀ scale.

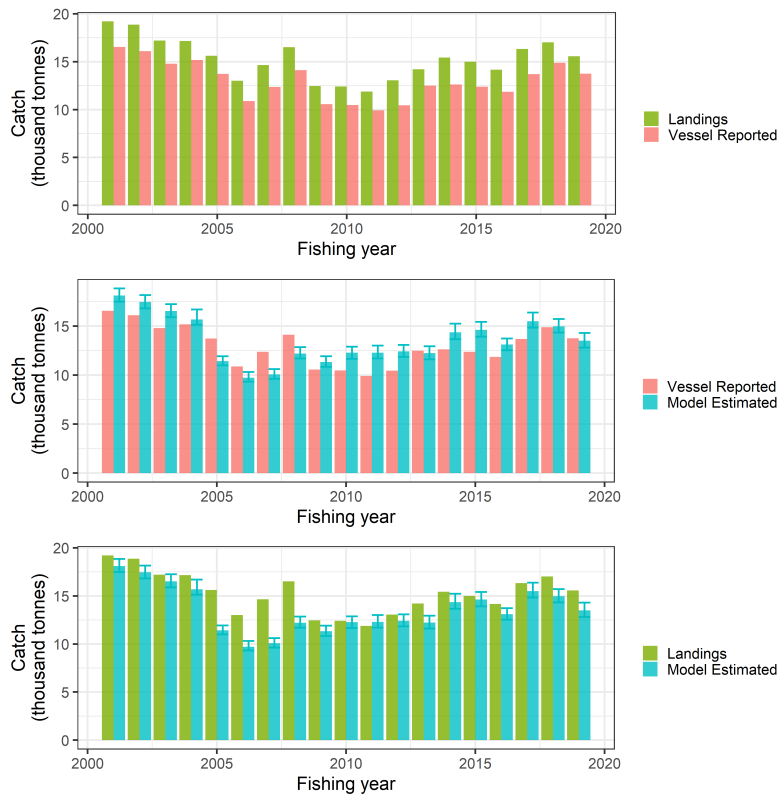


Figure 7: Prediction of total catches for LIN. The median of the total posterior predicted catch per year is shown and compared with the sum of the vessel reported catches and landings data. Vessel reported catches and landings are also compared directly for reference.

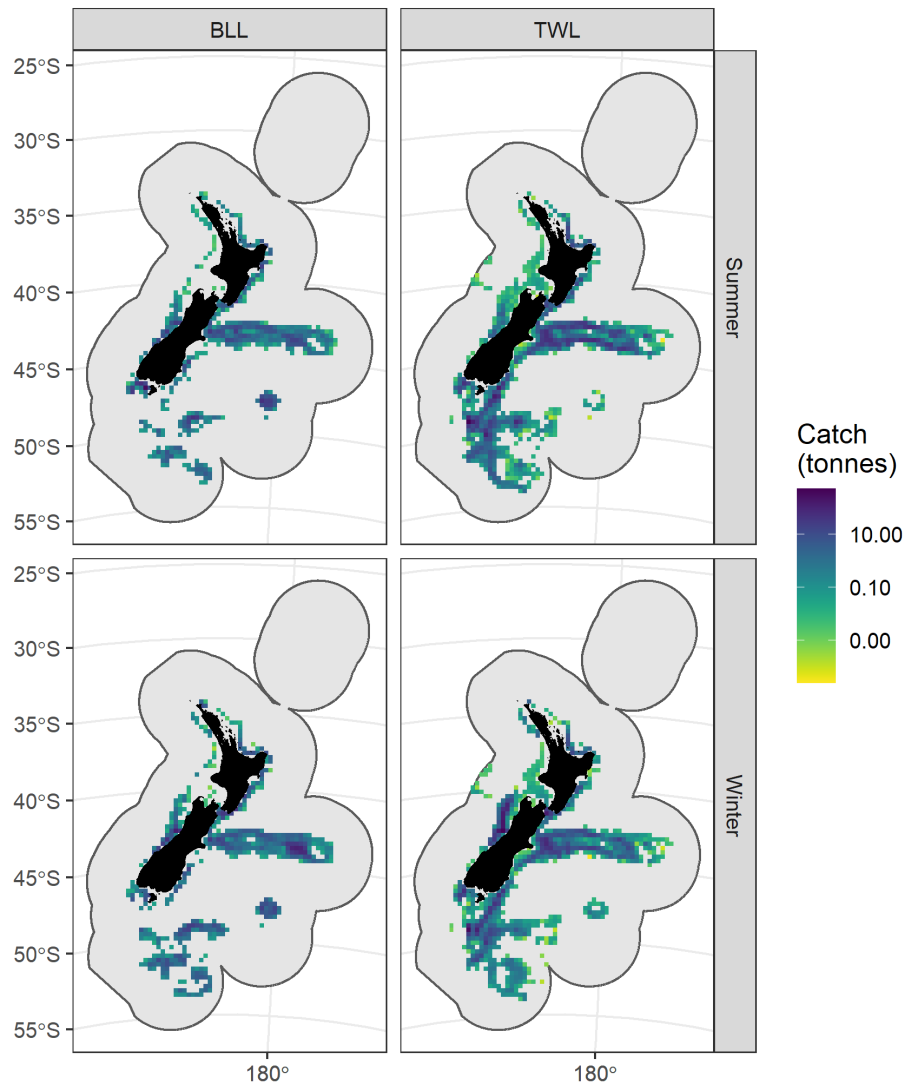


Figure 8: Model estimated spatial distribution of total catches for LIN per method and season. Model estimated values were obtained as the median of the posterior predicted distribution of the average annual catch per grid cell, method and season. Catch values are given in tonnes on a log₁₀ scale.

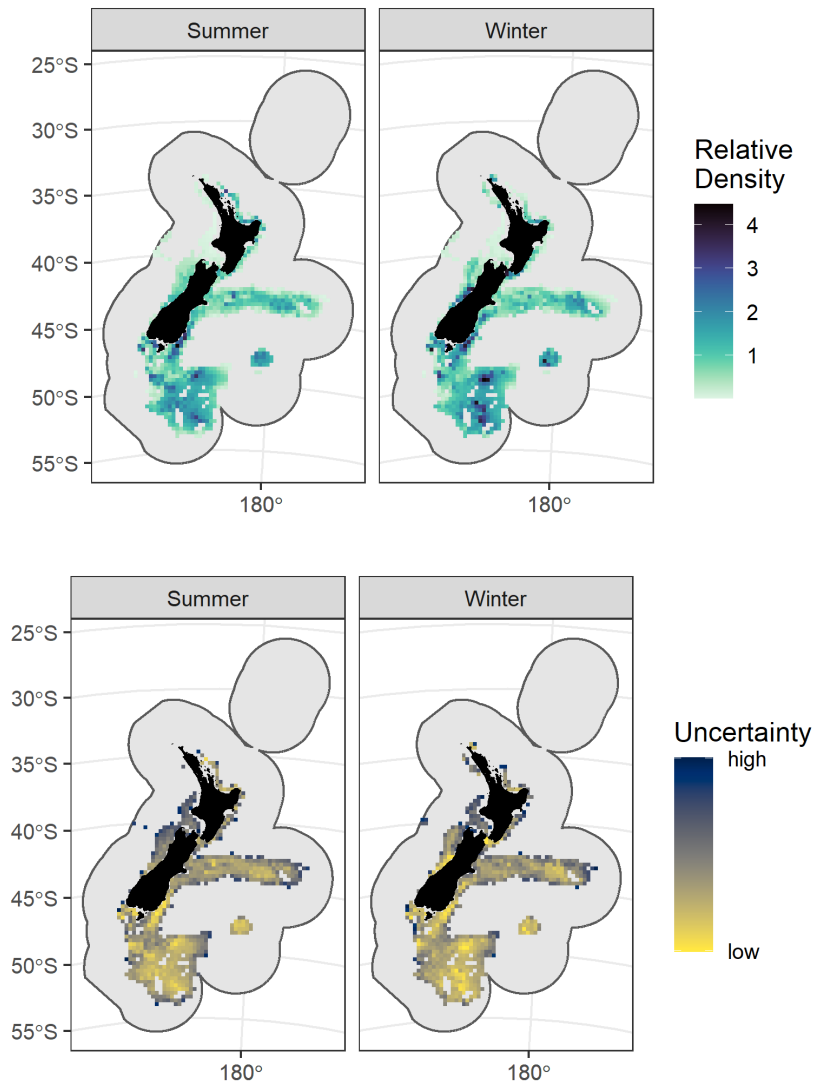


Figure 9: Model estimated biomass density for LIN d_{kt} , per grid cell and season in tonnes per square kilometre. Estimates were obtained as median posterior values. The uncertainty was quantified using the difference between the upper and lower bounds of the 95% credibility interval (see Section 3.4.4).

4.2 Cross validation using observer sampling data

We used cross validation as a means to evaluate performance of the model through its ability to predict known observer sampling data. Accurate prediction of known data confers confidence that the model will be able to predict the unobserved catches. A random 20% subset of the observer data was used to fit the model (the Insample) and the model was evaluated relative to its ability to predict the complete data set (the Outsample). Non-target species selected for this purpose, in order of total observed catch biomass and representing a range of values (Figure 1), were: rattails (RAT), spiny dogfish (SPD), frostfish (FRO), Baxter’s lantern dogfish (ETB), shovelnose dogfish (SND) and rough skate (RSK).

From Figure 10, we first illustrate the ability of the model to fit the Insample observer data, using the average annual catch per grid cell and gear type. We then used the estimated density and catchability parameters to extrapolate the catches across the Outsample effort. Results are shown in Figure 11, illustrating the ability of the model to predict the unobserved catch data. Finally, we compared the model estimated and observer Outsample catches over time (Figure 12), which showed a close correlation between the two.

In summary, these results demonstrate that the model was able to predict catch data that exhibit a similar structure to the observer data used to fit the model. This is a necessary condition for use of the model in predicting the total unobserved catches. Actual ability of the model to perform this function will however be dependent on how representative the observer data are of real world fishing practices.

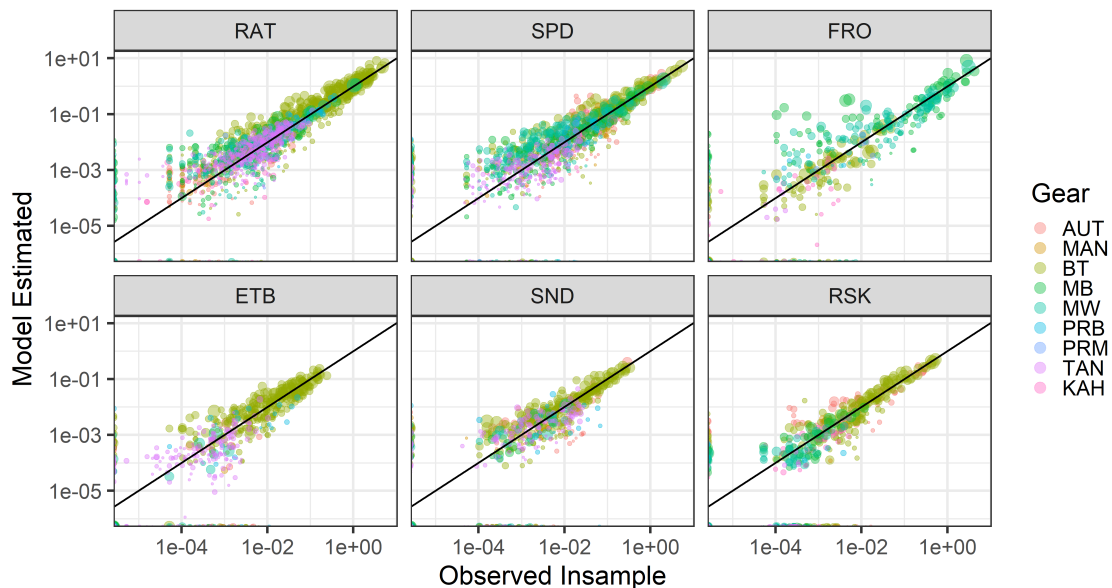


Figure 10: Model fit to empirical Insample catches. Model estimated values were obtained as the median of the posterior predicted distribution of the average annual catch per grid cell and gear type. Catch values are given in tonnes on a log₁₀ scale. Gear types are listed in Table 2. Species codes are listed in Table 3.

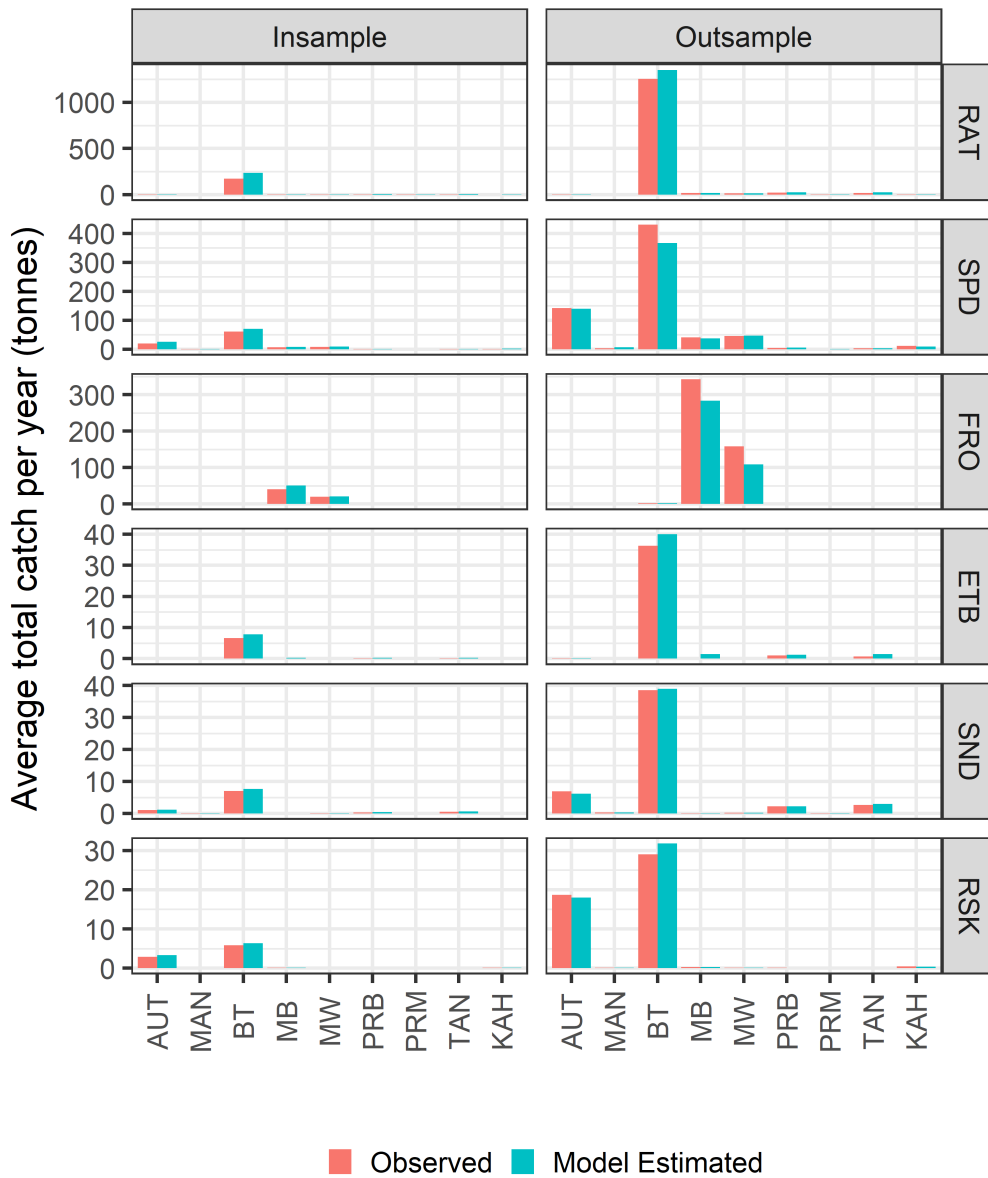


Figure 11: Average annual catch per year per species and gear type. Insample observed catches were used to fit the data. Outsample observed catches were not used to fit the data. They are assumed known and allowed us to validate the ability of the model to predict the unobserved catches. Catches are reported as posterior median values of the average annual catch per gear type. Gear types are listed in Table 2. Species codes are listed in Table 3.

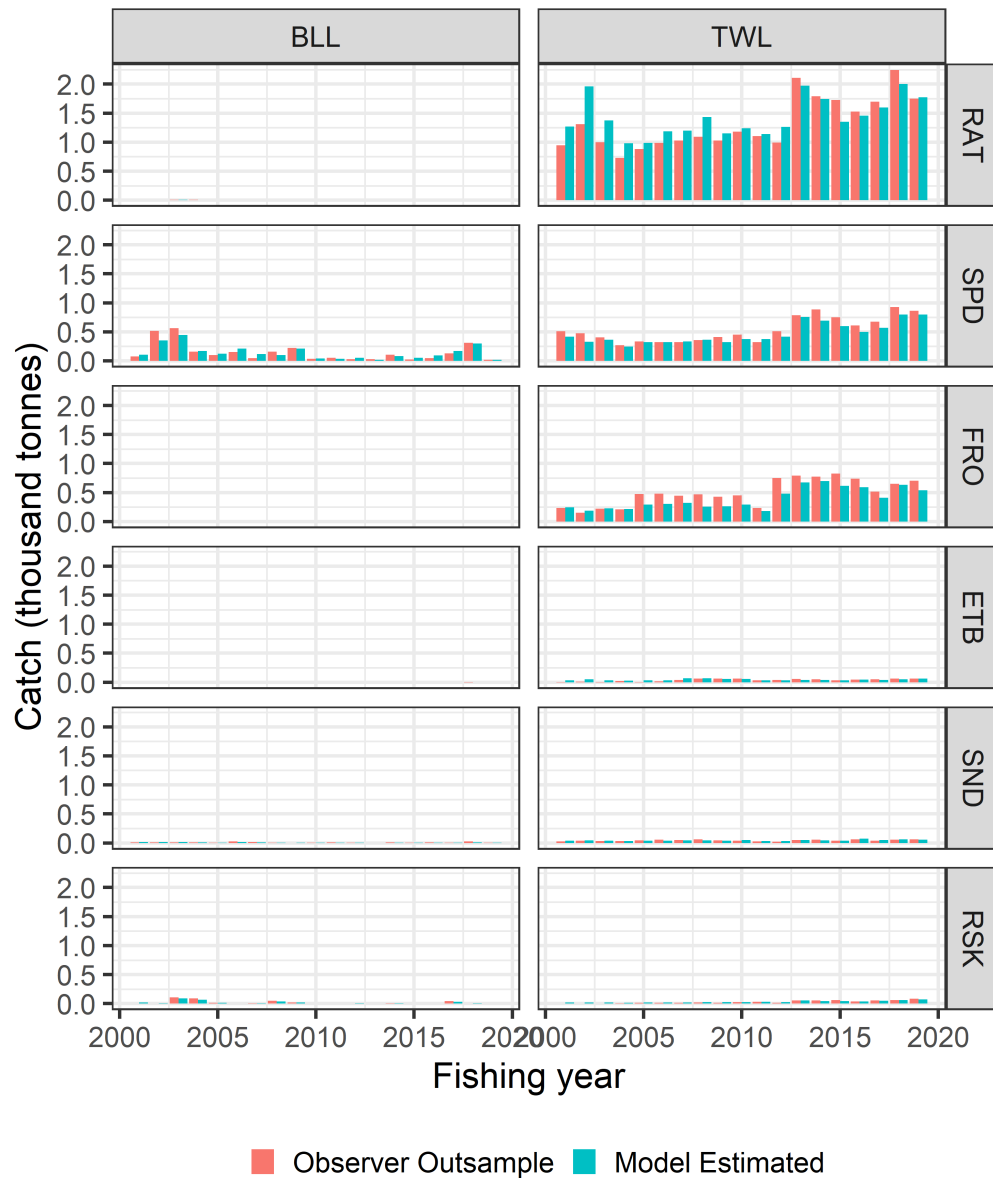


Figure 12: Catch time series per method and species, comparing the observer Outsample with the model estimated values. Catches are reported as posterior median values of the total annual catches summed across grid cells and gear types per method. Gear types are listed in Table 2. Species codes are listed in Table 3.

4.3 Estimated catches for and biomass distributions for non-target species

We present summary tables (Tables 5 to 27) and figures (Figures 13 to 58) to report the catch and biomass density estimates for non-target species, as specified by the project objectives (see Introduction). Detailed model fits, selection criteria and diagnostics are provided in the supplementary information (Edwards & Mormede 2023). For purposes of comparison across species, we further provide a summary of the average annual catches per species and gear type in Table 28 and summed by species in Figure 59.

4.3.1 Barracouta (*Thyrsites atun*)

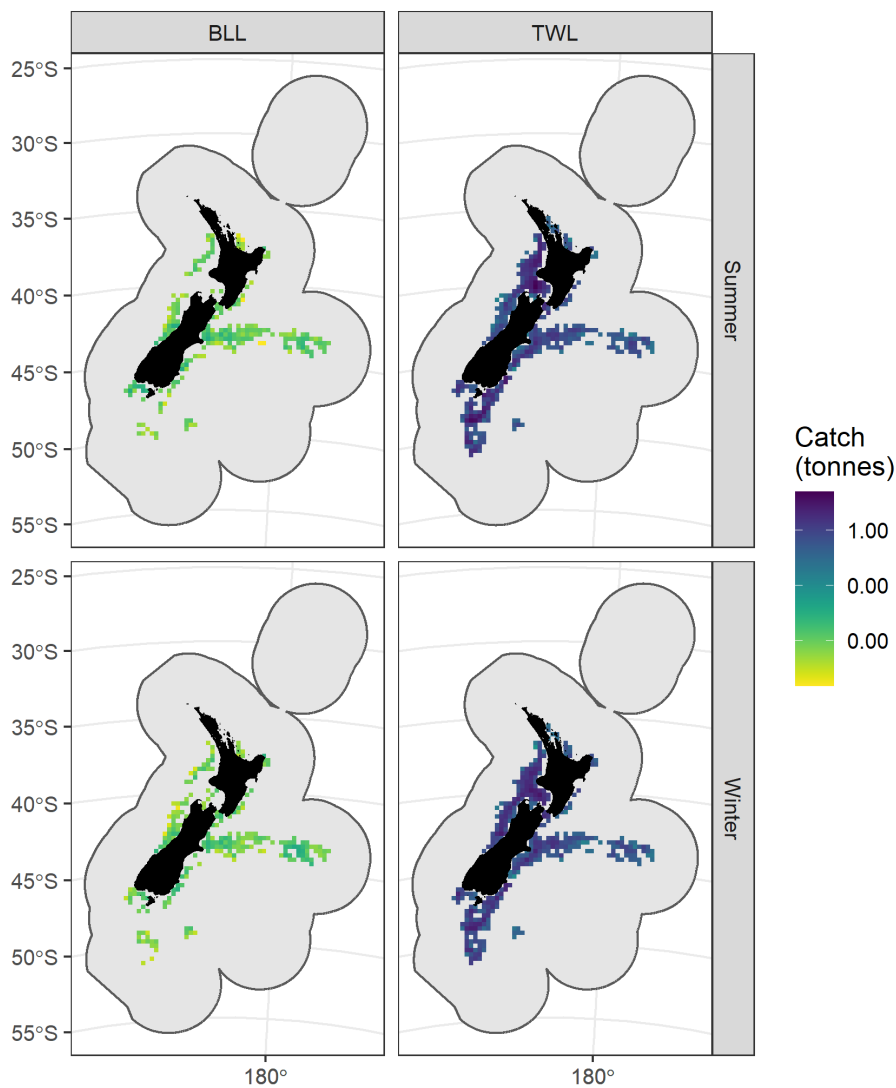


Figure 13: Posterior prediction of the average total catches for barracouta by grid cell and method for each season. Average annual catches per season were calculated as the sum across gear types per grid cell and method. Posterior median values are shown, with catches in tonnes on a log₁₀ scale.

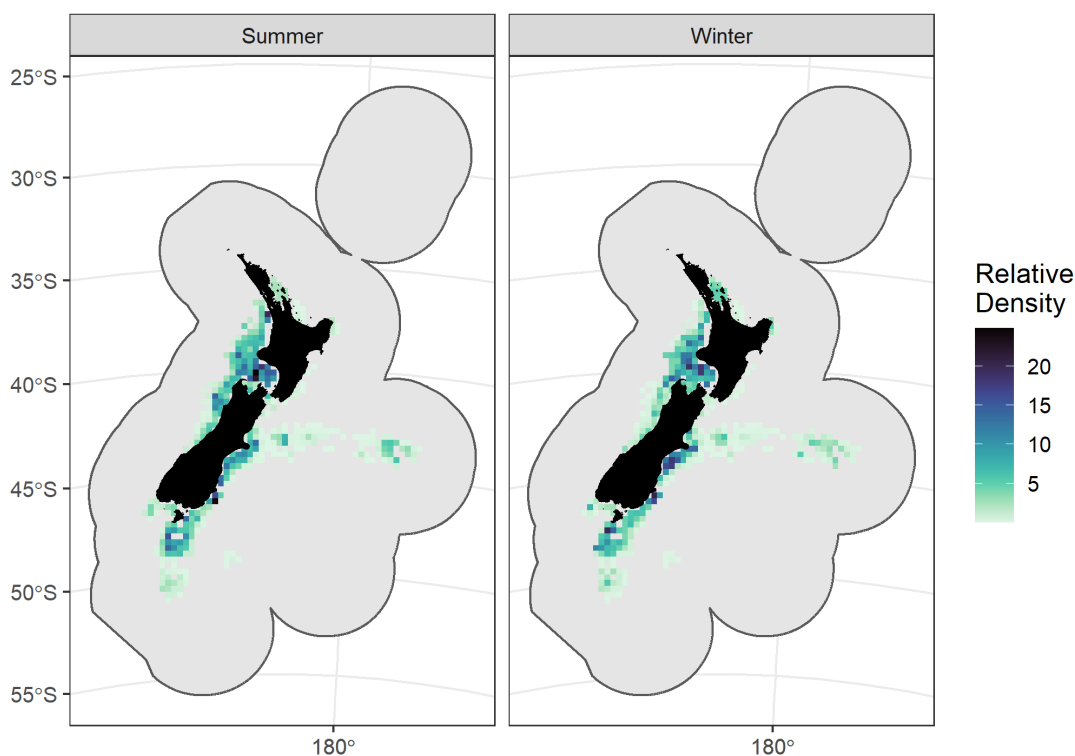


Figure 14: Posterior prediction of the relative density per grid cell and season for barracouta. Posterior median values are shown on a natural scale in tonnes per square kilometre.

Table 5: Total predicted bycatch (tonnes) per method for barracouta. Posterior median values are given, with the 95% equal-tailed credibility intervals in brackets.

Fishing year	BLL	TWL	Total
2000/01	0 (0 - 0)	5 965 (4 999 - 8 151)	5 965 (4 999 - 8 151)
2001/02	0 (0 - 0)	6 167 (5 169 - 7 931)	6 167 (5 169 - 7 931)
2002/03	0 (0 - 0)	6 926 (5 844 - 8 594)	6 926 (5 844 - 8 594)
2003/04	0 (0 - 0)	5 099 (4 276 - 6 395)	5 099 (4 276 - 6 395)
2004/05	0 (0 - 0)	5 410 (4 605 - 6 689)	5 410 (4 605 - 6 689)
2005/06	0 (0 - 0)	5 915 (5 055 - 7 482)	5 915 (5 055 - 7 482)
2006/07	0 (0 - 0)	5 268 (4 413 - 6 756)	5 268 (4 413 - 6 756)
2007/08	0 (0 - 0)	4 916 (4 088 - 6 156)	4 916 (4 088 - 6 156)
2008/09	0 (0 - 0)	4 482 (3 633 - 6 098)	4 482 (3 633 - 6 098)
2009/10	0 (0 - 0)	5 653 (4 547 - 7 799)	5 653 (4 547 - 7 799)
2010/11	0 (0 - 0)	4 238 (3 407 - 5 639)	4 238 (3 407 - 5 639)
2011/12	0 (0 - 0)	4 931 (3 928 - 6 743)	4 931 (3 928 - 6 743)
2012/13	0 (0 - 0)	4 109 (3 327 - 5 385)	4 109 (3 327 - 5 385)
2013/14	0 (0 - 0)	4 072 (3 289 - 5 524)	4 072 (3 289 - 5 524)
2014/15	0 (0 - 0)	3 515 (2 704 - 5 049)	3 515 (2 704 - 5 049)
2015/16	0 (0 - 0)	3 293 (2 520 - 4 637)	3 293 (2 520 - 4 637)
2016/17	0 (0 - 0)	3 791 (2 873 - 5 629)	3 791 (2 873 - 5 629)
2017/18	0 (0 - 0)	3 898 (3 029 - 5 523)	3 898 (3 029 - 5 523)
2018/19	0 (0 - 0)	4 255 (3 463 - 5 782)	4 255 (3 463 - 5 782)

4.3.2 Rattails (Macrouridae)

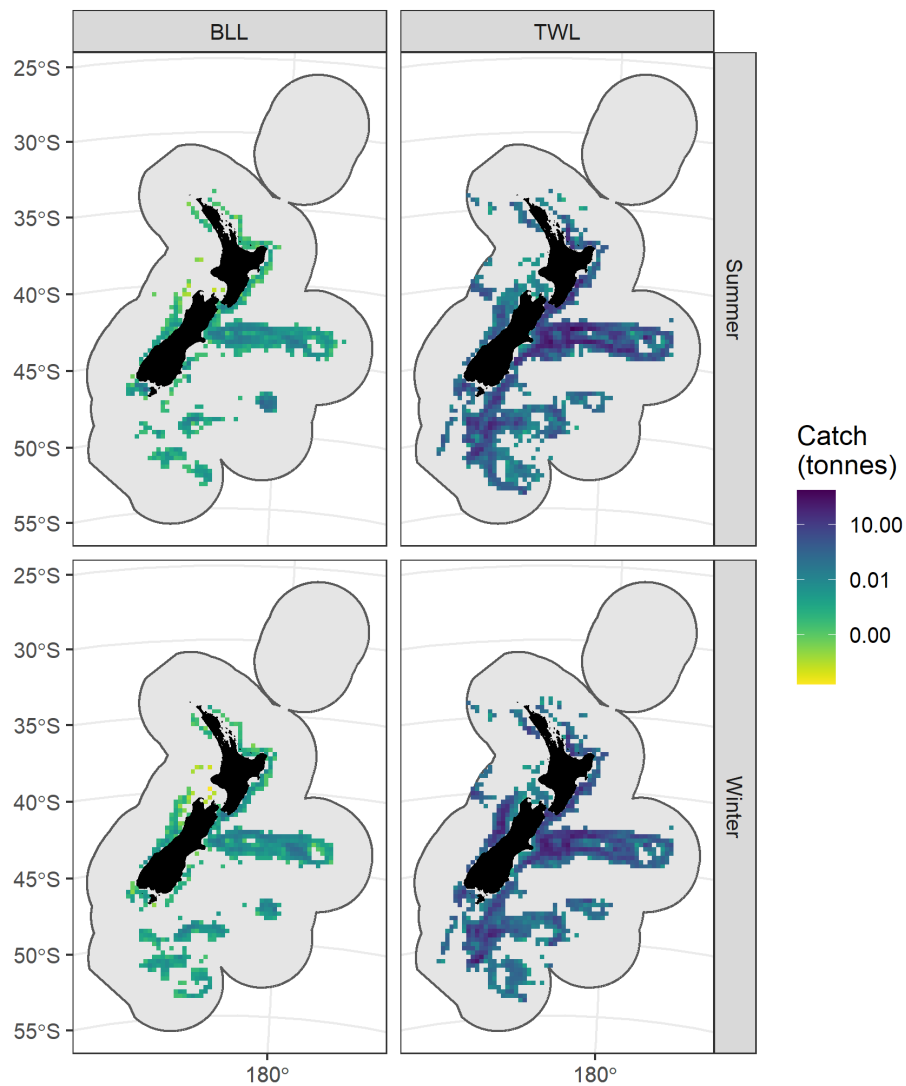


Figure 15: Posterior prediction of the average total catches for rattails by grid cell and method for each season. Average annual catches per season were calculated as the sum across gear types per grid cell and method. Posterior median values are shown, with catches in tonnes on a log₁₀ scale.

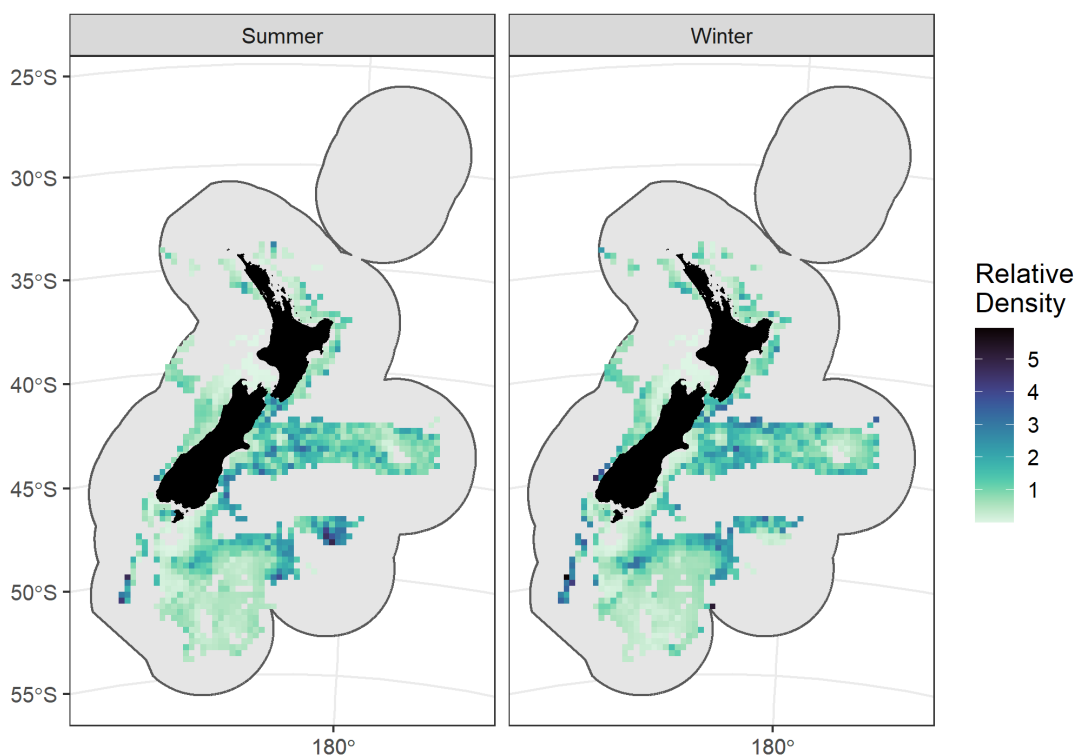


Figure 16: Posterior prediction of the relative density per grid cell and season for rattails. Posterior median values are shown on a natural scale in tonnes per square kilometre.

Table 6: Total predicted bycatch (tonnes) per method for rattails. Posterior median values are given, with the 95% equal-tailed credibility intervals in brackets.

Fishing year	BLL	TWL	Total
2000/01	13 (11 - 14)	14 482 (13 442 - 15 694)	14 495 (13 454 - 15 708)
2001/02	12 (11 - 14)	14 421 (13 378 - 15 708)	14 433 (13 391 - 15 720)
2002/03	8 (7 - 9)	14 830 (13 716 - 16 230)	14 838 (13 724 - 16 239)
2003/04	11 (10 - 12)	11 784 (10 881 - 12 773)	11 795 (10 891 - 12 784)
2004/05	8 (7 - 9)	9 464 (8 756 - 10 276)	9 473 (8 763 - 10 283)
2005/06	6 (5 - 6)	9 219 (8 509 - 9 977)	9 224 (8 514 - 9 983)
2006/07	7 (6 - 8)	9 135 (8 388 - 9 964)	9 142 (8 394 - 9 970)
2007/08	7 (6 - 8)	10 549 (9 633 - 11 561)	10 556 (9 640 - 11 568)
2008/09	7 (6 - 8)	10 263 (9 397 - 11 288)	10 270 (9 404 - 11 296)
2009/10	6 (5 - 7)	11 362 (10 485 - 12 475)	11 368 (10 491 - 12 481)
2010/11	6 (5 - 6)	11 268 (10 342 - 12 435)	11 273 (10 348 - 12 441)
2011/12	5 (4 - 5)	11 815 (10 793 - 13 033)	11 820 (10 798 - 13 038)
2012/13	4 (3 - 4)	11 391 (10 348 - 12 634)	11 395 (10 351 - 12 638)
2013/14	7 (6 - 8)	12 320 (11 193 - 13 571)	12 328 (11 201 - 13 579)
2014/15	5 (4 - 6)	13 125 (11 959 - 14 548)	13 130 (11 964 - 14 553)
2015/16	6 (6 - 7)	13 269 (12 079 - 14 613)	13 275 (12 085 - 14 619)
2016/17	9 (8 - 10)	12 808 (11 658 - 16 793)	12 817 (11 667 - 16 802)
2017/18	8 (7 - 9)	13 146 (12 088 - 14 509)	13 153 (12 098 - 14 517)
2018/19	7 (6 - 8)	12 658 (11 558 - 14 044)	12 665 (11 566 - 14 052)

4.3.3 Spiny dogfish (*Squalus acanthias*)

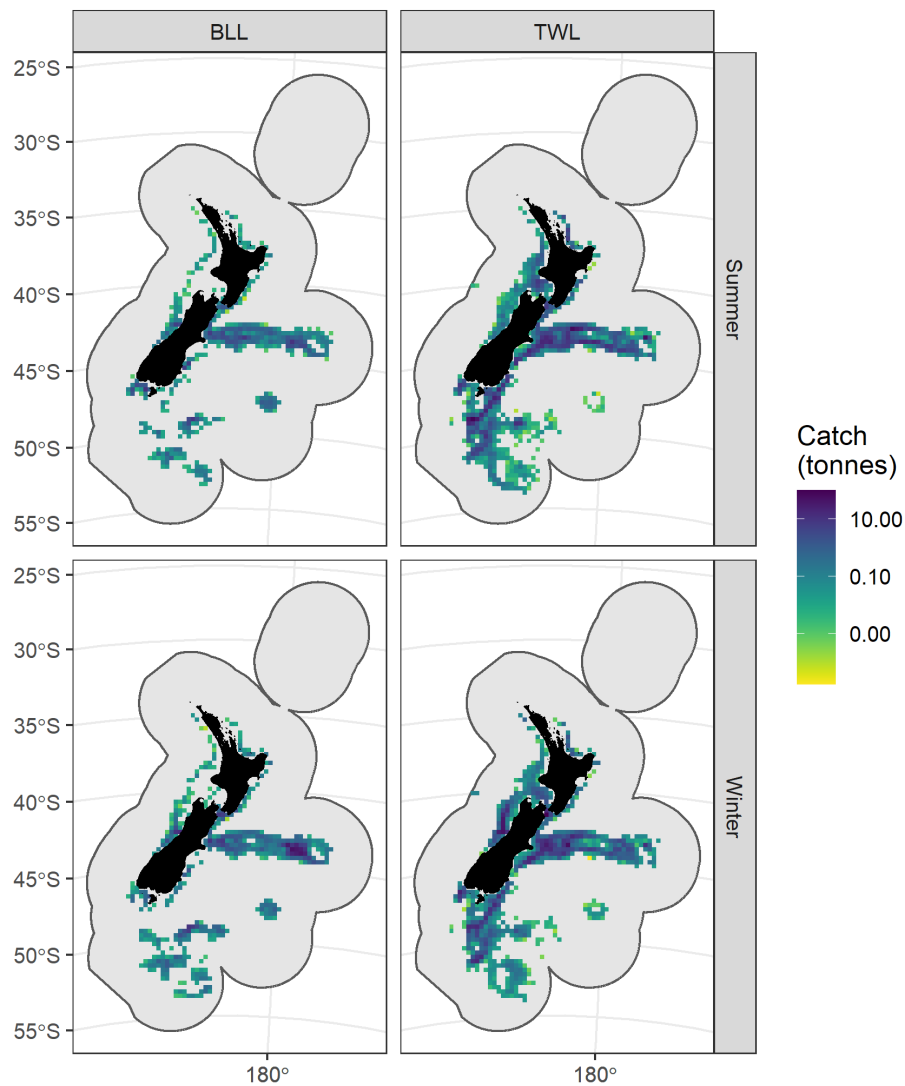


Figure 17: Posterior prediction of the average total catches for spiny dogfish by grid cell and method for each season. Average annual catches per season were calculated as the sum across gear types per grid cell and method. Posterior median values are shown, with catches in tonnes on a log₁₀ scale.

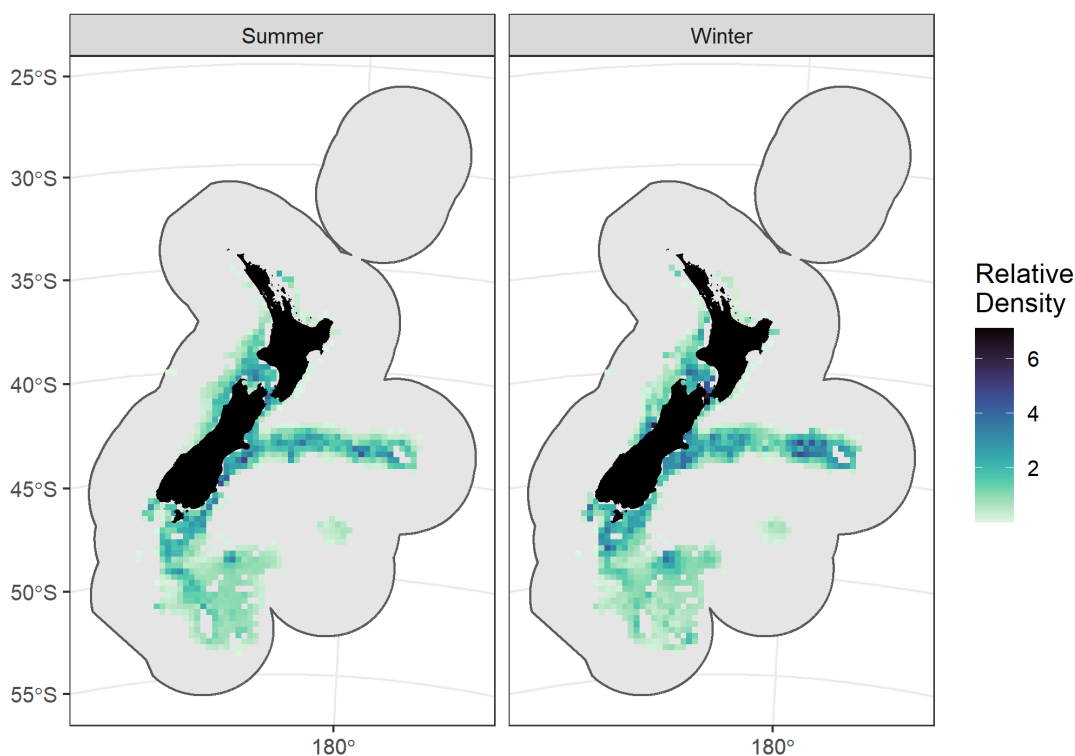


Figure 18: Posterior prediction of the relative density per grid cell and season for spiny dogfish. Posterior median values are shown on a natural scale in tonnes per square kilometre.

Table 7: Total predicted bycatch (tonnes) per method for spiny dogfish. Posterior median values are given, with the 95% equal-tailed credibility intervals in brackets.

Fishing year	BLL	TWL	Total
2000/01	897 (768 - 1 163)	3 739 (3 457 - 4 561)	4 639 (4 300 - 5 663)
2001/02	994 (851 - 1 200)	3 388 (3 142 - 3 728)	4 392 (4 103 - 4 782)
2002/03	664 (551 - 808)	3 773 (3 469 - 4 199)	4 440 (4 115 - 4 877)
2003/04	932 (784 - 1 127)	2 860 (2 636 - 3 094)	3 800 (3 529 - 4 105)
2004/05	716 (595 - 882)	2 969 (2 740 - 3 376)	3 687 (3 437 - 4 098)
2005/06	599 (499 - 743)	2 773 (2 581 - 3 006)	3 377 (3 157 - 3 658)
2006/07	539 (449 - 658)	2 572 (2 363 - 2 872)	3 118 (2 882 - 3 443)
2007/08	740 (593 - 1 831)	2 739 (2 529 - 3 042)	3 494 (3 201 - 4 905)
2008/09	764 (617 - 1 097)	2 335 (2 160 - 2 575)	3 114 (2 867 - 3 503)
2009/10	773 (649 - 1 044)	2 695 (2 503 - 2 970)	3 479 (3 242 - 3 858)
2010/11	875 (705 - 1 617)	2 582 (2 379 - 2 820)	3 465 (3 192 - 4 214)
2011/12	834 (678 - 1 650)	2 571 (2 379 - 2 779)	3 418 (3 142 - 4 258)
2012/13	709 (557 - 1 050)	2 433 (2 225 - 2 646)	3 147 (2 882 - 3 562)
2013/14	994 (788 - 1 566)	2 551 (2 367 - 2 791)	3 551 (3 258 - 4 204)
2014/15	873 (702 - 1 581)	2 664 (2 461 - 2 923)	3 552 (3 262 - 4 324)
2015/16	1 036 (848 - 1 816)	2 535 (2 336 - 2 792)	3 574 (3 284 - 4 423)
2016/17	1 131 (923 - 1 642)	2 566 (2 378 - 2 778)	3 700 (3 418 - 4 235)
2017/18	1 097 (902 - 1 584)	2 530 (2 342 - 2 724)	3 630 (3 351 - 4 126)
2018/19	1 004 (827 - 1 360)	2 561 (2 356 - 2 765)	3 570 (3 300 - 3 972)

4.3.4 Frostfish (*Lepidopus caudatus*)

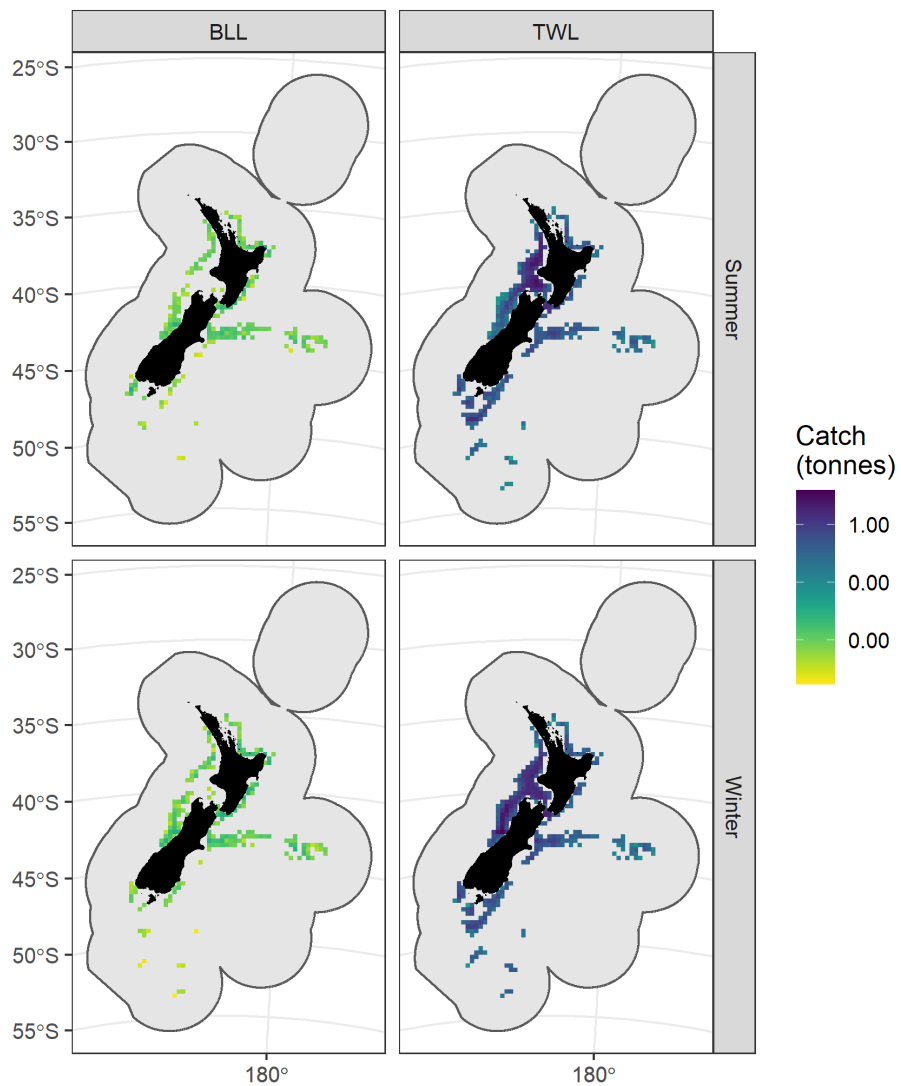


Figure 19: Posterior prediction of the average total catches for frostfish by grid cell and method for each season. Average annual catches per season were calculated as the sum across gear types per grid cell and method. Posterior median values are shown, with catches in tonnes on a log₁₀ scale.

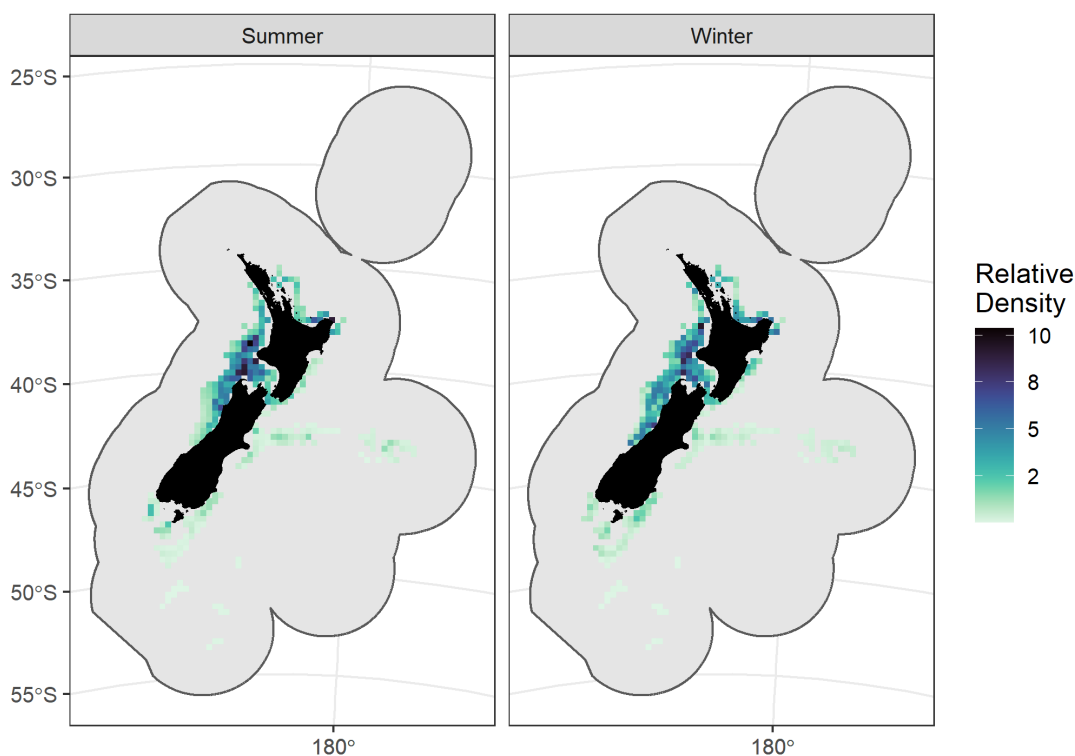


Figure 20: Posterior prediction of the relative density per grid cell and season for frostfish. Posterior median values are shown on a natural scale in tonnes per square kilometre.

Table 8: Total predicted bycatch (tonnes) per method for frostfish. Posterior median values are given, with the 95% equal-tailed credibility intervals in brackets.

Fishing year	BLL	TWL	Total
2000/01	0 (0 - 0)	1 536 (1 383 - 1 724)	1 536 (1 383 - 1 724)
2001/02	0 (0 - 0)	1 504 (1 335 - 1 712)	1 504 (1 335 - 1 712)
2002/03	0 (0 - 0)	1 894 (1 674 - 2 169)	1 894 (1 674 - 2 169)
2003/04	0 (0 - 0)	1 694 (1 470 - 2 024)	1 694 (1 470 - 2 024)
2004/05	0 (0 - 0)	1 256 (1 099 - 1 451)	1 256 (1 099 - 1 451)
2005/06	0 (0 - 0)	1 297 (1 121 - 1 547)	1 297 (1 121 - 1 547)
2006/07	0 (0 - 0)	1 222 (1 045 - 1 457)	1 222 (1 045 - 1 457)
2007/08	0 (0 - 0)	1 103 (922 - 1 303)	1 103 (922 - 1 303)
2008/09	0 (0 - 0)	1 082 (911 - 1 333)	1 082 (911 - 1 333)
2009/10	0 (0 - 0)	1 266 (1 086 - 1 507)	1 266 (1 086 - 1 507)
2010/11	0 (0 - 0)	941 (800 - 1 117)	941 (800 - 1 117)
2011/12	0 (0 - 0)	1 068 (917 - 1 274)	1 068 (917 - 1 274)
2012/13	0 (0 - 0)	1 152 (1 000 - 1 353)	1 152 (1 000 - 1 353)
2013/14	0 (0 - 0)	1 312 (1 152 - 1 514)	1 312 (1 152 - 1 514)
2014/15	0 (0 - 0)	1 160 (1 032 - 1 340)	1 160 (1 032 - 1 340)
2015/16	0 (0 - 0)	1 085 (943 - 1 251)	1 085 (943 - 1 251)
2016/17	0 (0 - 0)	1 151 (983 - 1 383)	1 151 (983 - 1 383)
2017/18	0 (0 - 0)	1 116 (956 - 1 320)	1 116 (956 - 1 320)
2018/19	0 (0 - 0)	1 149 (1 001 - 1 348)	1 149 (1 001 - 1 348)

4.3.5 Blue mackerel (*Scomber australasicus*)

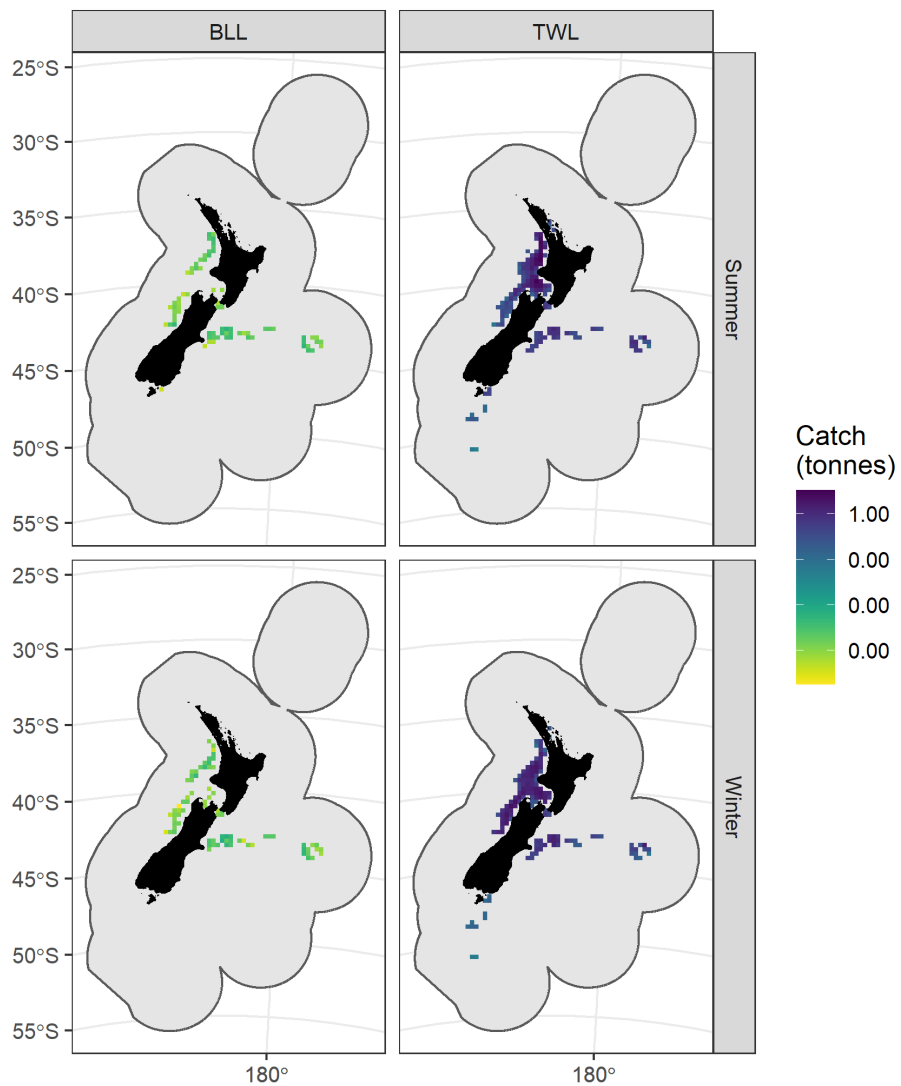


Figure 21: Posterior prediction of the average total catches for blue mackerel by grid cell and method for each season. Average annual catches per season were calculated as the sum across gear types per grid cell and method. Posterior median values are shown, with catches in tonnes on a log₁₀ scale.

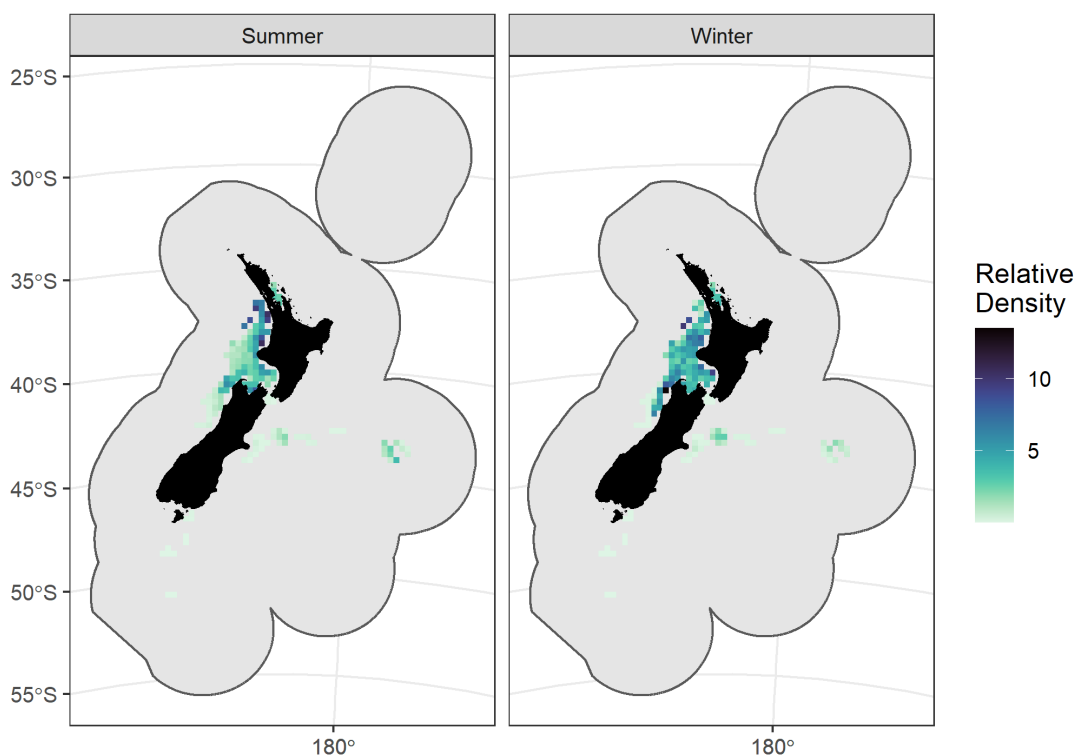


Figure 22: Posterior prediction of the relative density per grid cell and season for blue mackerel. Posterior median values are shown on a natural scale in tonnes per square kilometre.

Table 9: Total predicted bycatch (tonnes) per method for blue mackerel. Posterior median values are given, with the 95% equal-tailed credibility intervals in brackets.

Fishing year	BLL	TWL	Total
2000/01	0 (0 - 0)	408 (219 - 2 447)	408 (219 - 2 447)
2001/02	0 (0 - 0)	477 (292 - 2 308)	477 (292 - 2 308)
2002/03	0 (0 - 0)	539 (366 - 1 900)	539 (366 - 1 900)
2003/04	0 (0 - 0)	527 (374 - 1 137)	527 (374 - 1 137)
2004/05	0 (0 - 0)	686 (492 - 1 409)	686 (492 - 1 409)
2005/06	0 (0 - 0)	545 (392 - 1 293)	545 (392 - 1 293)
2006/07	0 (0 - 0)	713 (511 - 1 557)	713 (511 - 1 557)
2007/08	0 (0 - 0)	608 (422 - 1 804)	608 (422 - 1 804)
2008/09	0 (0 - 0)	450 (323 - 836)	450 (323 - 836)
2009/10	0 (0 - 0)	606 (442 - 1 078)	606 (442 - 1 078)
2010/11	0 (0 - 0)	586 (396 - 1 296)	586 (396 - 1 296)
2011/12	0 (0 - 0)	501 (341 - 1 282)	501 (341 - 1 282)
2012/13	0 (0 - 0)	618 (432 - 1 225)	618 (432 - 1 225)
2013/14	0 (0 - 0)	642 (458 - 1 444)	642 (458 - 1 444)
2014/15	0 (0 - 0)	579 (390 - 1 720)	579 (390 - 1 720)
2015/16	0 (0 - 0)	523 (330 - 1 908)	523 (330 - 1 908)
2016/17	0 (0 - 0)	488 (313 - 1 353)	488 (313 - 1 353)
2017/18	0 (0 - 0)	493 (336 - 1 210)	493 (336 - 1 210)
2018/19	0 (0 - 0)	478 (329 - 1 212)	478 (329 - 1 212)

4.3.6 Morid cods (Moridae)

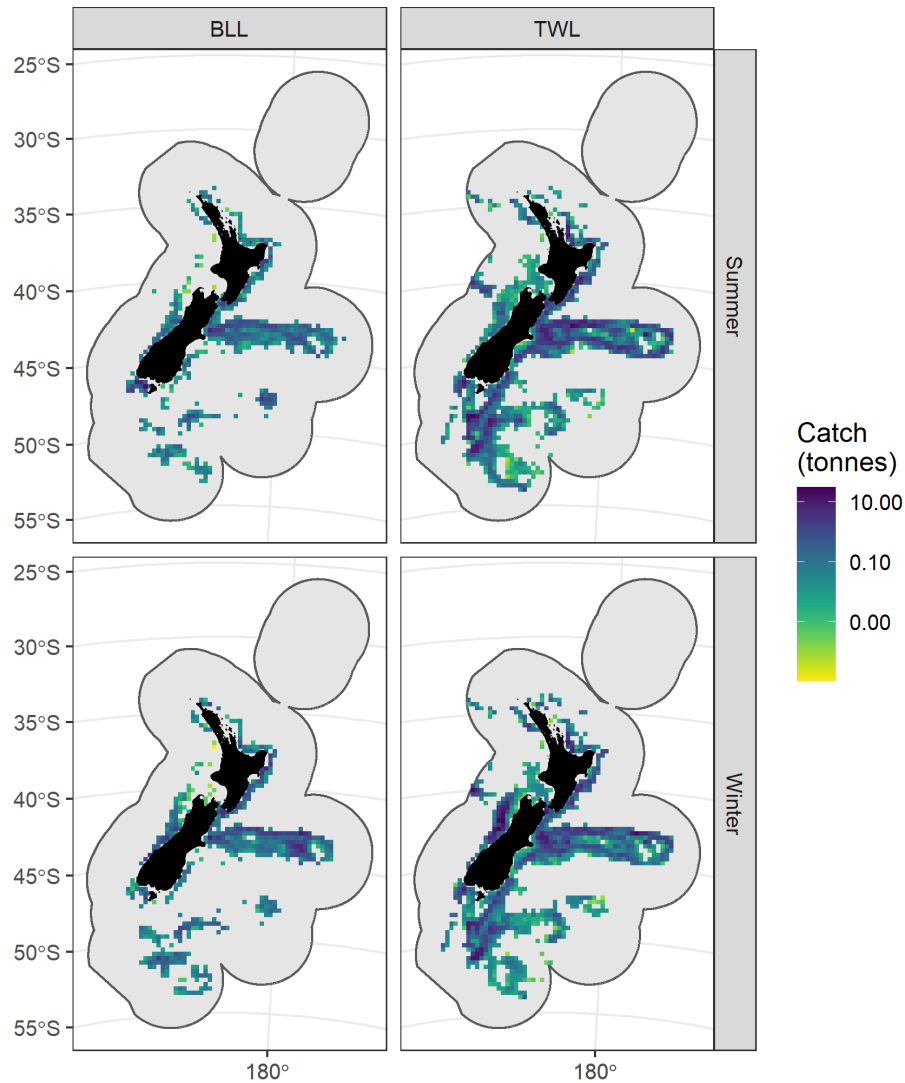


Figure 23: Posterior prediction of the average total catches for morid cods by grid cell and method for each season. Average annual catches per season were calculated as the sum across gear types per grid cell and method. Posterior median values are shown, with catches in tonnes on a log₁₀ scale.

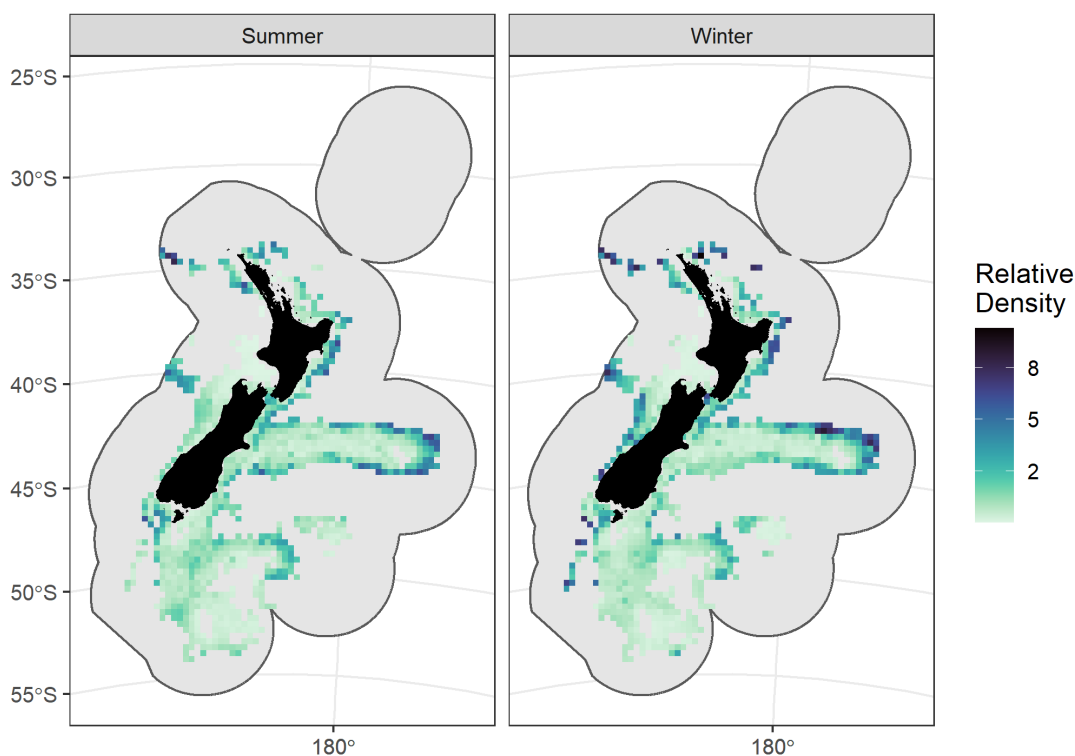


Figure 24: Posterior prediction of the relative density per grid cell and season for morid cods. Posterior median values are shown on a natural scale in tonnes per square kilometre.

Table 10: Total predicted bycatch (tonnes) per method for morid cods. Posterior median values are given, with the 95% equal-tailed credibility intervals in brackets.

Fishing year	BLL	TWL	Total
2000/01	429 (356 - 536)	1 977 (1 831 - 2 240)	2 408 (2 238 - 2 700)
2001/02	479 (382 - 661)	2 103 (1 962 - 2 759)	2 592 (2 400 - 3 287)
2002/03	216 (177 - 272)	2 013 (1 872 - 3 493)	2 236 (2 079 - 3 687)
2003/04	364 (290 - 902)	1 862 (1 746 - 2 007)	2 234 (2 086 - 2 783)
2004/05	326 (262 - 423)	1 673 (1 557 - 1 817)	2 004 (1 872 - 2 178)
2005/06	247 (203 - 312)	1 485 (1 389 - 1 657)	1 737 (1 625 - 1 932)
2006/07	283 (230 - 364)	1 350 (1 258 - 1 469)	1 637 (1 530 - 1 786)
2007/08	361 (289 - 470)	1 484 (1 377 - 1 620)	1 851 (1 710 - 2 015)
2008/09	355 (285 - 570)	1 494 (1 390 - 1 623)	1 856 (1 713 - 2 097)
2009/10	379 (300 - 556)	1 535 (1 428 - 1 679)	1 923 (1 762 - 2 166)
2010/11	407 (324 - 670)	1 424 (1 328 - 1 688)	1 836 (1 694 - 2 435)
2011/12	358 (284 - 505)	1 296 (1 201 - 1 394)	1 654 (1 538 - 1 851)
2012/13	323 (250 - 633)	1 255 (1 163 - 1 383)	1 589 (1 459 - 1 961)
2013/14	615 (464 - 907)	1 492 (1 380 - 1 628)	2 111 (1 921 - 2 408)
2014/15	456 (347 - 731)	1 608 (1 483 - 1 786)	2 078 (1 902 - 2 412)
2015/16	477 (379 - 945)	1 604 (1 487 - 1 778)	2 095 (1 922 - 2 697)
2016/17	474 (367 - 771)	1 802 (1 667 - 1 959)	2 281 (2 099 - 2 609)
2017/18	424 (332 - 712)	1 780 (1 645 - 4 712)	2 215 (2 039 - 5 118)
2018/19	433 (340 - 632)	1 495 (1 389 - 1 636)	1 935 (1 785 - 2 189)

4.3.7 Redbait (*Emmelichthys nitidus*)

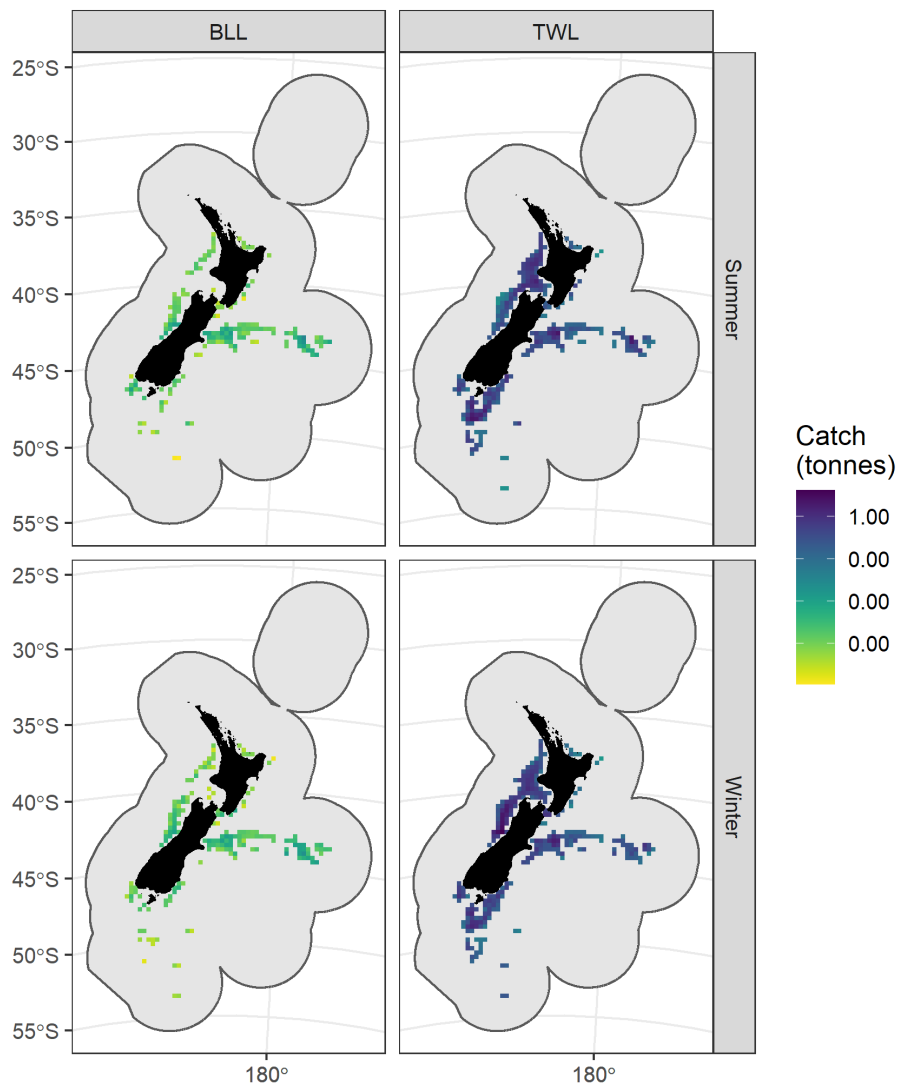


Figure 25: Posterior prediction of the average total catches for redbait by grid cell and method for each season. Average annual catches per season were calculated as the sum across gear types per grid cell and method. Posterior median values are shown, with catches in tonnes on a log₁₀ scale.

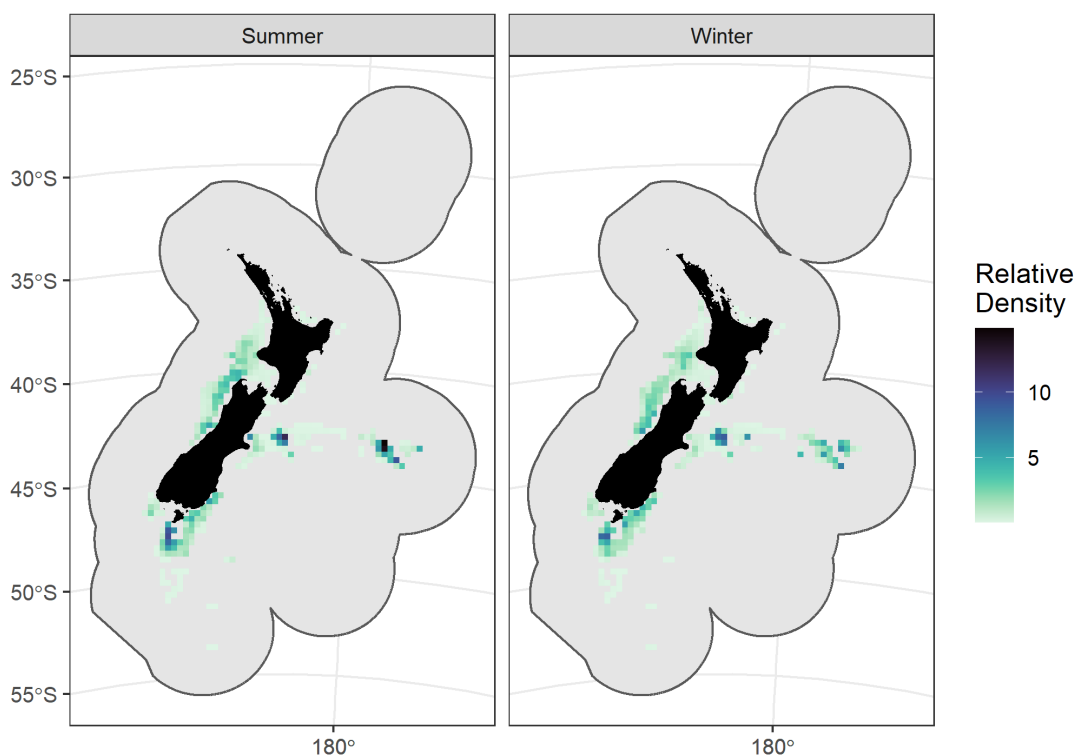


Figure 26: Posterior prediction of the relative density per grid cell and season for redbait. Posterior median values are shown on a natural scale in tonnes per square kilometre.

Table 11: Total predicted bycatch (tonnes) per method for redbait. Posterior median values are given, with the 95% equal-tailed credibility intervals in brackets.

Fishing year	BLL	TWL	Total
2000/01	0 (0 - 0)	588 (479 - 743)	588 (479 - 743)
2001/02	0 (0 - 0)	474 (381 - 608)	474 (381 - 608)
2002/03	0 (0 - 0)	547 (442 - 759)	547 (442 - 759)
2003/04	0 (0 - 0)	458 (367 - 599)	458 (367 - 599)
2004/05	0 (0 - 0)	326 (260 - 433)	326 (260 - 433)
2005/06	0 (0 - 0)	408 (303 - 718)	408 (303 - 718)
2006/07	0 (0 - 0)	266 (211 - 394)	266 (211 - 394)
2007/08	0 (0 - 0)	280 (209 - 401)	280 (209 - 401)
2008/09	0 (0 - 0)	211 (155 - 349)	211 (155 - 349)
2009/10	0 (0 - 0)	196 (145 - 314)	196 (145 - 314)
2010/11	0 (0 - 0)	180 (138 - 261)	180 (138 - 261)
2011/12	0 (0 - 0)	238 (181 - 350)	238 (181 - 350)
2012/13	0 (0 - 0)	277 (203 - 421)	277 (203 - 421)
2013/14	0 (0 - 0)	337 (251 - 588)	337 (251 - 588)
2014/15	0 (0 - 0)	349 (260 - 568)	349 (260 - 568)
2015/16	0 (0 - 0)	286 (223 - 412)	286 (223 - 412)
2016/17	0 (0 - 0)	355 (242 - 1 837)	355 (242 - 1 837)
2017/18	0 (0 - 0)	365 (240 - 2 020)	365 (240 - 2 020)
2018/19	0 (0 - 0)	510 (375 - 987)	510 (375 - 987)

4.3.8 Common warehou (*Seriolella brama*)

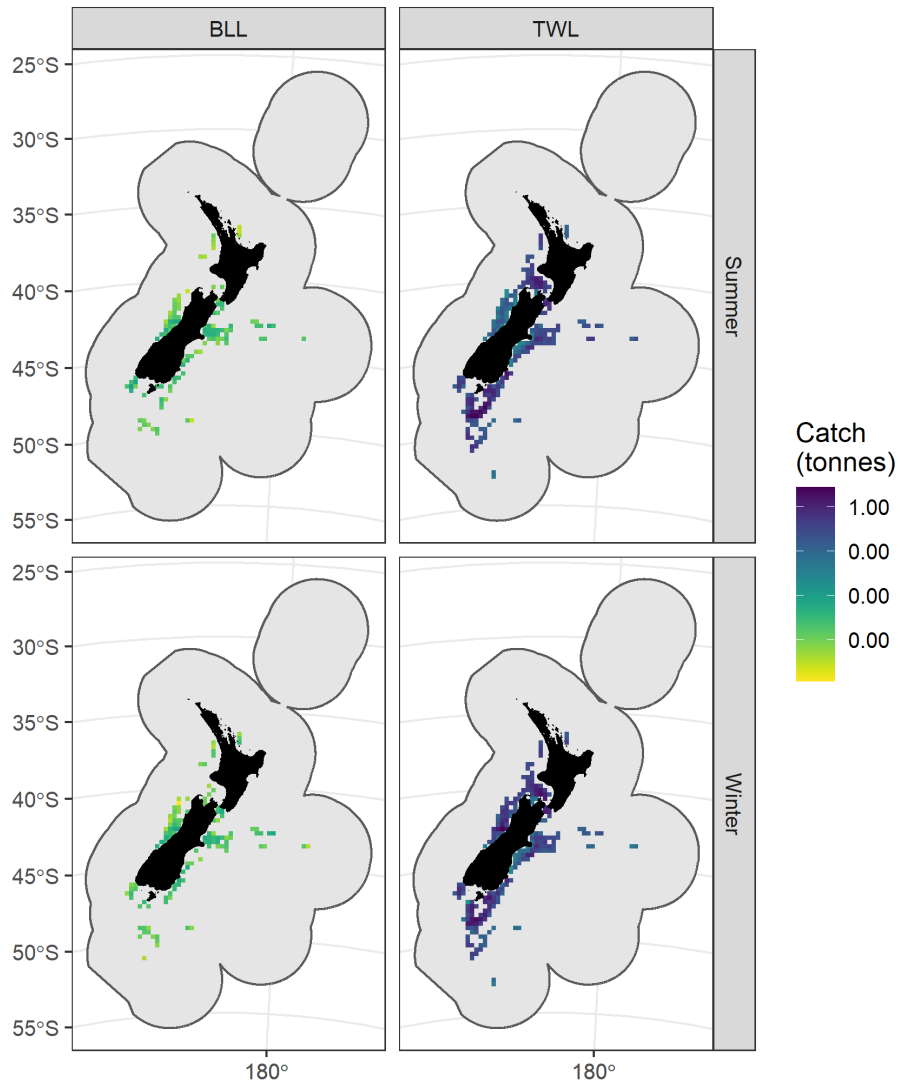


Figure 27: Posterior prediction of the average total catches for common warehou by grid cell and method for each season. Average annual catches per season were calculated as the sum across gear types per grid cell and method. Posterior median values are shown, with catches in tonnes on a log₁₀ scale.

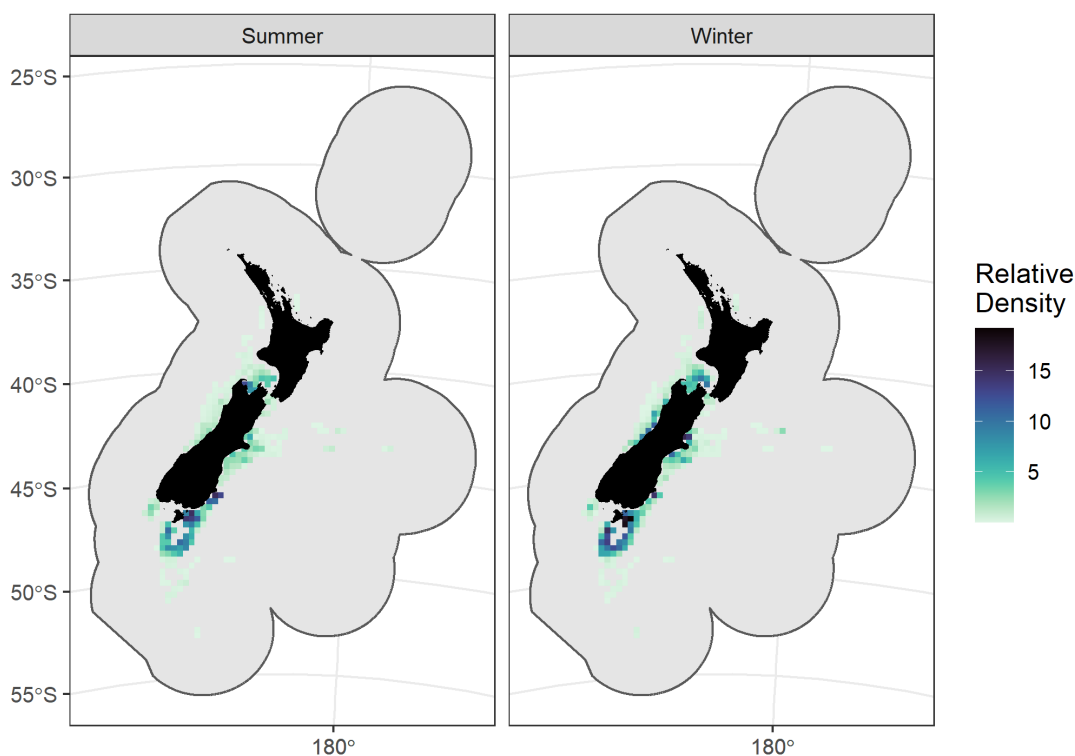


Figure 28: Posterior prediction of the relative density per grid cell and season for common warehou. Posterior median values are shown on a natural scale in tonnes per square kilometre.

Table 12: Total predicted bycatch (tonnes) per method for common warehou. Posterior median values are given, with the 95% equal-tailed credibility intervals in brackets.

Fishing year	BLL	TWL	Total
2000/01	0 (0 - 0)	424 (309 - 730)	424 (309 - 730)
2001/02	0 (0 - 0)	342 (259 - 595)	342 (259 - 595)
2002/03	0 (0 - 0)	336 (245 - 659)	336 (245 - 659)
2003/04	0 (0 - 0)	343 (242 - 646)	343 (242 - 646)
2004/05	0 (0 - 0)	304 (230 - 471)	304 (230 - 471)
2005/06	0 (0 - 0)	283 (202 - 447)	283 (202 - 447)
2006/07	0 (0 - 0)	233 (165 - 414)	233 (165 - 414)
2007/08	0 (0 - 0)	244 (162 - 409)	244 (162 - 409)
2008/09	0 (0 - 0)	176 (118 - 297)	176 (118 - 297)
2009/10	0 (0 - 0)	157 (110 - 279)	157 (110 - 279)
2010/11	0 (0 - 0)	148 (103 - 256)	148 (103 - 256)
2011/12	0 (0 - 0)	200 (137 - 334)	200 (137 - 334)
2012/13	0 (0 - 0)	147 (101 - 268)	147 (101 - 268)
2013/14	0 (0 - 0)	146 (107 - 236)	146 (107 - 236)
2014/15	0 (0 - 0)	137 (98 - 244)	137 (98 - 244)
2015/16	0 (0 - 0)	128 (91 - 202)	128 (91 - 202)
2016/17	0 (0 - 0)	137 (94 - 296)	137 (94 - 296)
2017/18	0 (0 - 0)	215 (156 - 347)	215 (156 - 347)
2018/19	0 (0 - 0)	265 (181 - 473)	265 (181 - 473)

4.3.9 Smooth red swimming crab (*Nectocarcinus bennetti*)

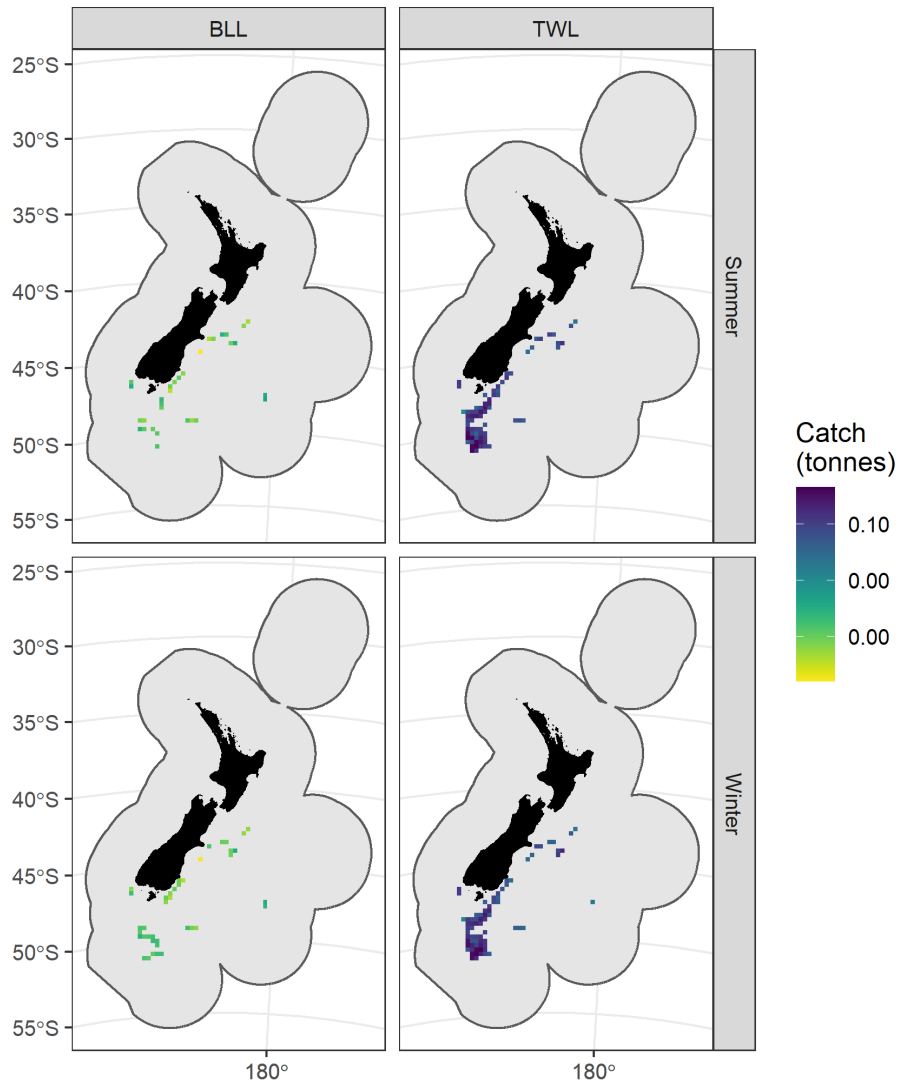


Figure 29: Posterior prediction of the average total catches for smooth red swimming crab by grid cell and method for each season. Average annual catches per season were calculated as the sum across gear types per grid cell and method. Posterior median values are shown, with catches in tonnes on a log₁₀ scale.

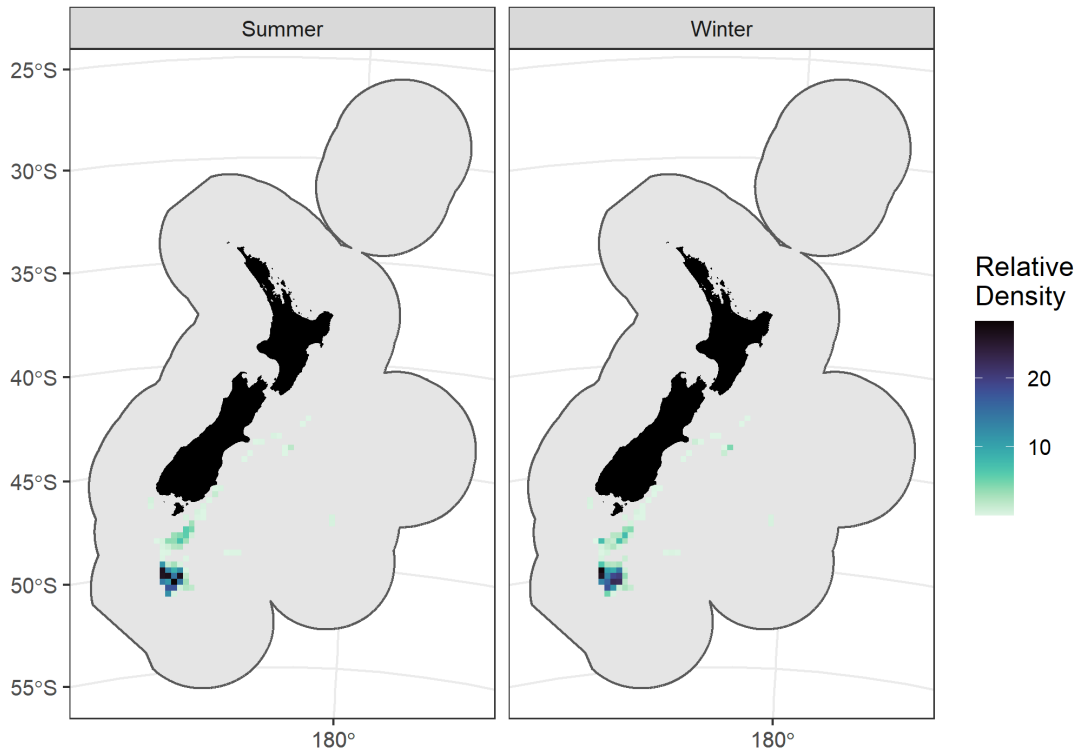


Figure 30: Posterior prediction of the relative density per grid cell and season for smooth red swimming crab. Posterior median values are shown on a natural scale in tonnes per square kilometre.

Table 13: Total predicted bycatch (tonnes) per method for smooth red swimming crab. Posterior median values are given, with the 95% equal-tailed credibility intervals in brackets.

Fishing year	BLL	TWL	Total
2000/01	0 (0 - 0)	163 (119 - 240)	163 (119 - 240)
2001/02	0 (0 - 0)	289 (211 - 415)	289 (211 - 415)
2002/03	0 (0 - 0)	306 (232 - 455)	306 (232 - 455)
2003/04	0 (0 - 0)	506 (365 - 726)	506 (365 - 726)
2004/05	0 (0 - 0)	593 (448 - 829)	593 (448 - 829)
2005/06	0 (0 - 0)	642 (477 - 901)	642 (477 - 901)
2006/07	0 (0 - 0)	345 (252 - 518)	345 (252 - 518)
2007/08	0 (0 - 0)	349 (248 - 543)	349 (248 - 543)
2008/09	0 (0 - 0)	615 (457 - 887)	615 (457 - 887)
2009/10	0 (0 - 0)	458 (333 - 693)	458 (333 - 693)
2010/11	0 (0 - 0)	509 (379 - 739)	509 (379 - 739)
2011/12	0 (0 - 0)	429 (307 - 668)	429 (307 - 668)
2012/13	0 (0 - 0)	376 (258 - 579)	376 (258 - 579)
2013/14	0 (0 - 0)	289 (191 - 443)	289 (191 - 443)
2014/15	0 (0 - 0)	208 (139 - 347)	208 (139 - 347)
2015/16	0 (0 - 0)	366 (262 - 548)	366 (262 - 548)
2016/17	0 (0 - 0)	624 (455 - 927)	624 (455 - 927)
2017/18	0 (0 - 0)	459 (328 - 656)	459 (328 - 656)
2018/19	0 (0 - 0)	369 (261 - 548)	369 (261 - 548)

4.3.10 Sea perch (*Helicolenus* spp.)

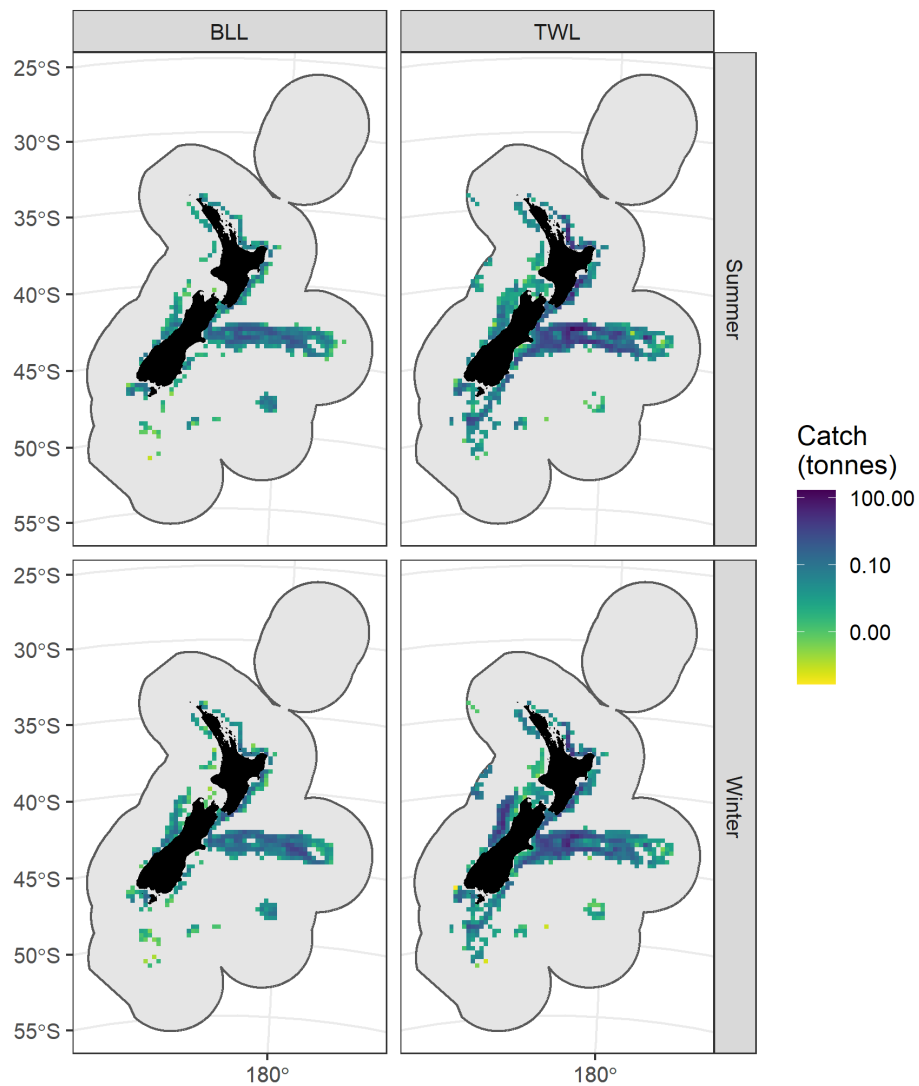


Figure 31: Posterior prediction of the average total catches for sea perch by grid cell and method for each season. Average annual catches per season were calculated as the sum across gear types per grid cell and method. Posterior median values are shown, with catches in tonnes on a log₁₀ scale.

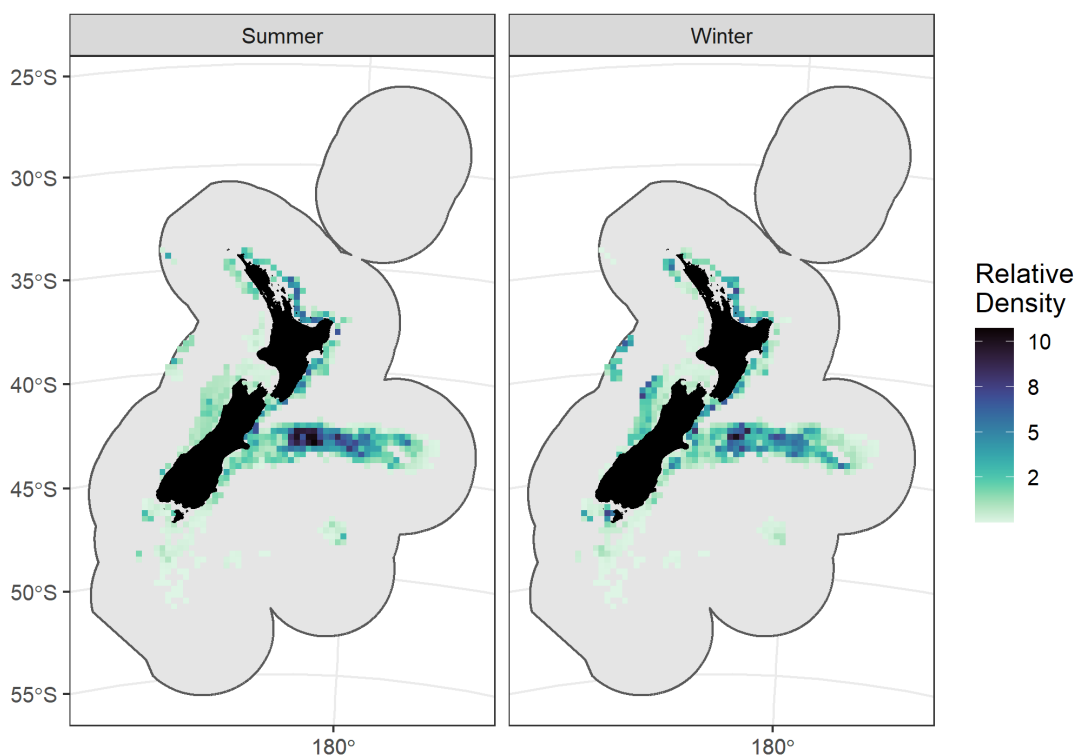


Figure 32: Posterior prediction of the relative density per grid cell and season for sea perch. Posterior median values are shown on a natural scale in tonnes per square kilometre.

Table 14: Total predicted bycatch (tonnes) per method for sea perch. Posterior median values are given, with the 95% equal-tailed credibility intervals in brackets.

Fishing year	BLL	TWL	Total
2000/01	144 (123 - 170)	1 323 (1 227 - 1 459)	1 468 (1 371 - 1 607)
2001/02	173 (150 - 206)	1 392 (1 285 - 1 638)	1 565 (1 456 - 1 820)
2002/03	87 (75 - 104)	1 398 (1 302 - 1 514)	1 487 (1 385 - 1 605)
2003/04	105 (90 - 125)	1 110 (1 020 - 1 243)	1 216 (1 120 - 1 346)
2004/05	174 (148 - 209)	1 072 (993 - 1 187)	1 250 (1 159 - 1 360)
2005/06	127 (108 - 151)	1 087 (1 000 - 1 400)	1 214 (1 125 - 1 515)
2006/07	115 (98 - 136)	1 051 (962 - 1 186)	1 166 (1 073 - 1 301)
2007/08	127 (104 - 194)	1 399 (1 287 - 1 550)	1 531 (1 405 - 1 695)
2008/09	116 (100 - 149)	1 337 (1 217 - 1 527)	1 455 (1 330 - 1 653)
2009/10	149 (126 - 192)	1 582 (1 436 - 1 780)	1 732 (1 581 - 1 940)
2010/11	137 (114 - 236)	1 558 (1 410 - 1 752)	1 701 (1 540 - 1 920)
2011/12	124 (103 - 222)	1 813 (1 637 - 2 034)	1 943 (1 762 - 2 202)
2012/13	107 (89 - 162)	1 793 (1 606 - 2 045)	1 904 (1 708 - 2 169)
2013/14	143 (120 - 237)	1 774 (1 609 - 1 988)	1 920 (1 749 - 2 163)
2014/15	132 (106 - 276)	2 074 (1 862 - 2 342)	2 215 (1 991 - 2 529)
2015/16	174 (148 - 245)	1 986 (1 778 - 2 256)	2 166 (1 951 - 2 445)
2016/17	195 (164 - 324)	1 650 (1 492 - 1 857)	1 850 (1 678 - 2 084)
2017/18	147 (125 - 206)	1 613 (1 468 - 1 853)	1 765 (1 615 - 2 064)
2018/19	153 (124 - 323)	1 853 (1 652 - 2 100)	2 016 (1 809 - 2 313)

4.3.11 Pale ghost shark (*Hydrolagus bemisi*)

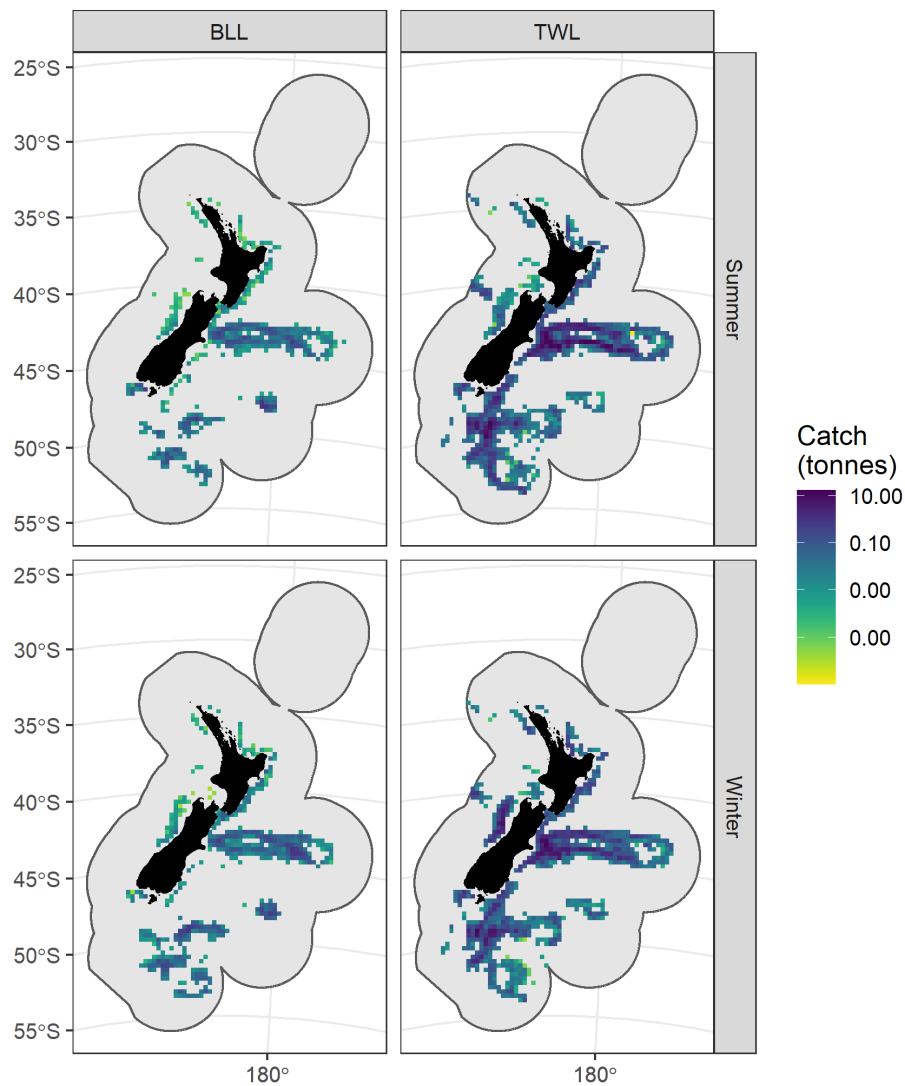


Figure 33: Posterior prediction of the average total catches for pale ghost shark by grid cell and method for each season. Average annual catches per season were calculated as the sum across gear types per grid cell and method. Posterior median values are shown, with catches in tonnes on a log₁₀ scale.

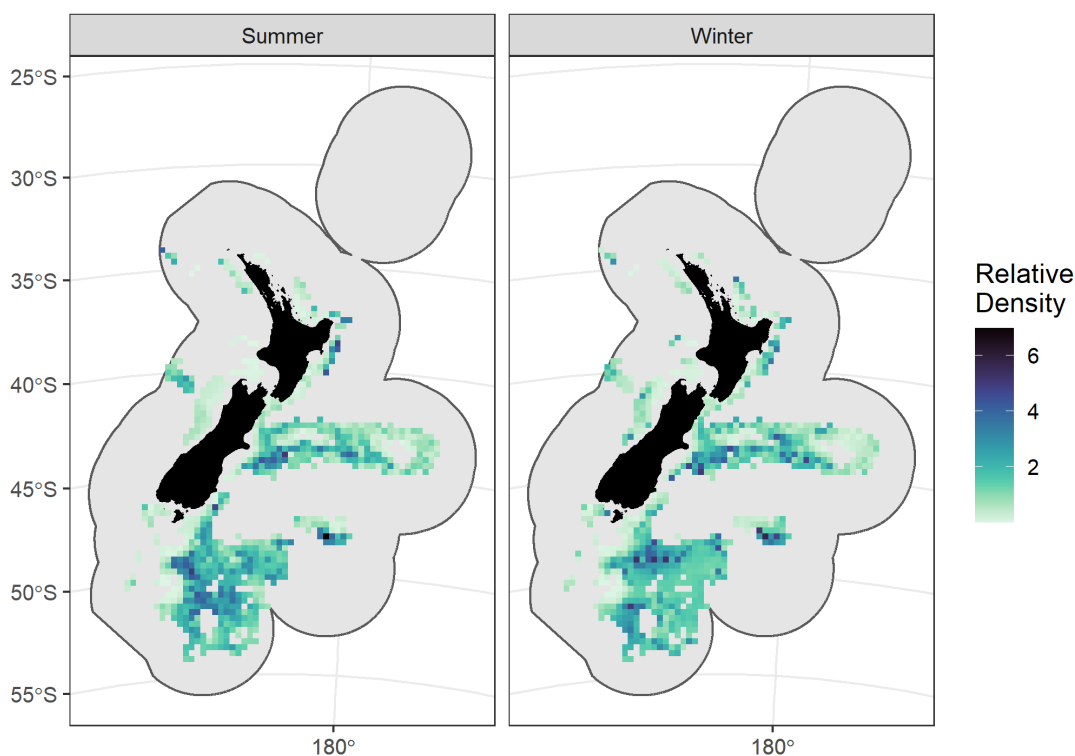


Figure 34: Posterior prediction of the relative density per grid cell and season for pale ghost shark. Posterior median values are shown on a natural scale in tonnes per square kilometre.

Table 15: Total predicted bycatch (tonnes) per method for pale ghost shark. Posterior median values are given, with the 95% equal-tailed credibility intervals in brackets.

Fishing year	BLL	TWL	Total
2000/01	62 (53 - 76)	1 380 (1 278 - 1 510)	1 442 (1 342 - 1 576)
2001/02	63 (54 - 75)	1 429 (1 323 - 1 563)	1 492 (1 385 - 1 629)
2002/03	43 (36 - 52)	1 494 (1 383 - 1 633)	1 537 (1 425 - 1 672)
2003/04	62 (53 - 74)	1 162 (1 067 - 1 277)	1 225 (1 131 - 1 340)
2004/05	45 (38 - 55)	841 (768 - 927)	886 (812 - 971)
2005/06	30 (26 - 37)	692 (634 - 766)	722 (663 - 797)
2006/07	25 (21 - 33)	676 (621 - 747)	701 (647 - 772)
2007/08	33 (27 - 45)	786 (723 - 863)	818 (753 - 900)
2008/09	33 (27 - 48)	802 (733 - 883)	836 (765 - 919)
2009/10	39 (32 - 54)	848 (771 - 940)	888 (810 - 992)
2010/11	37 (31 - 56)	798 (726 - 880)	836 (764 - 922)
2011/12	42 (34 - 58)	769 (702 - 847)	812 (741 - 893)
2012/13	17 (14 - 31)	738 (674 - 816)	757 (691 - 835)
2013/14	50 (40 - 80)	871 (798 - 968)	922 (847 - 1 030)
2014/15	32 (25 - 49)	887 (813 - 983)	920 (846 - 1 022)
2015/16	48 (40 - 64)	824 (752 - 909)	873 (800 - 962)
2016/17	70 (57 - 96)	880 (804 - 962)	951 (871 - 1 033)
2017/18	53 (44 - 72)	946 (866 - 1 045)	1 000 (917 - 1 108)
2018/19	63 (53 - 85)	782 (713 - 877)	848 (775 - 943)

4.3.12 Gemfish (*Rexea solandri*)

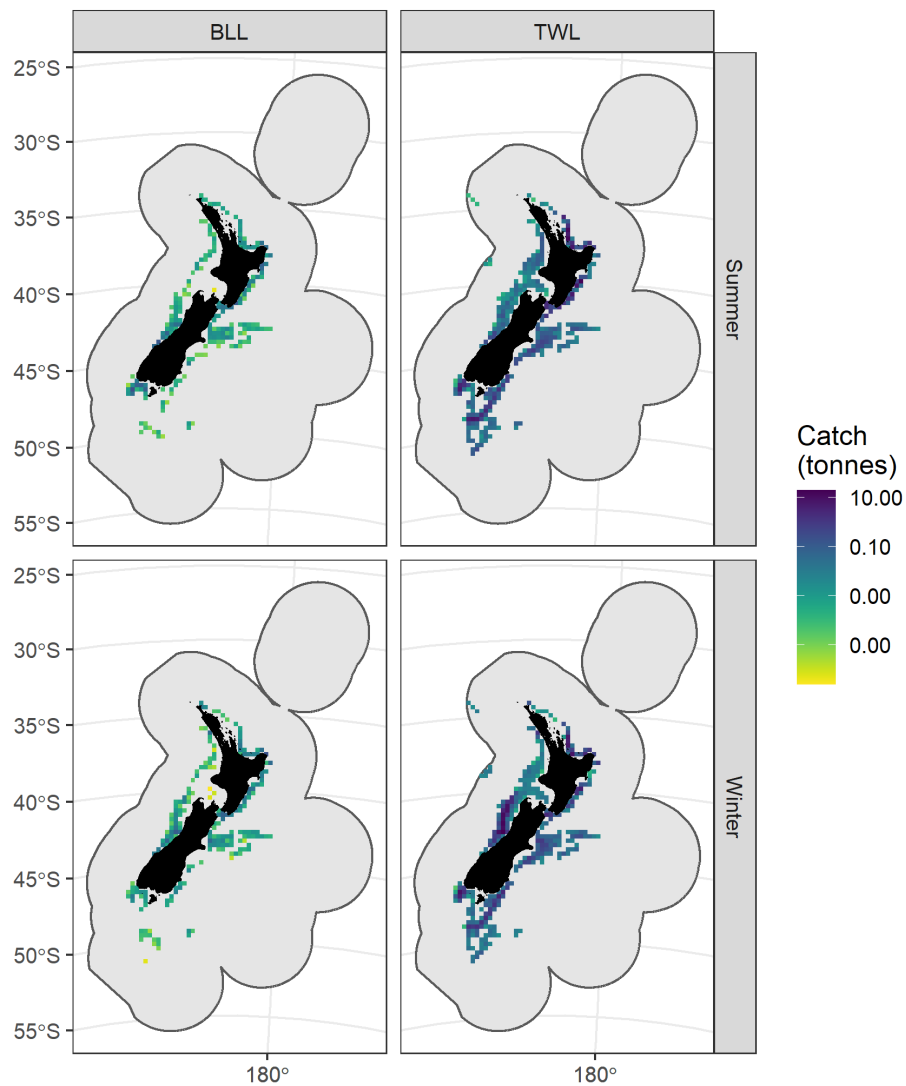


Figure 35: Posterior prediction of the average total catches for gemfish by grid cell and method for each season. Average annual catches per season were calculated as the sum across gear types per grid cell and method. Posterior median values are shown, with catches in tonnes on a log₁₀ scale.

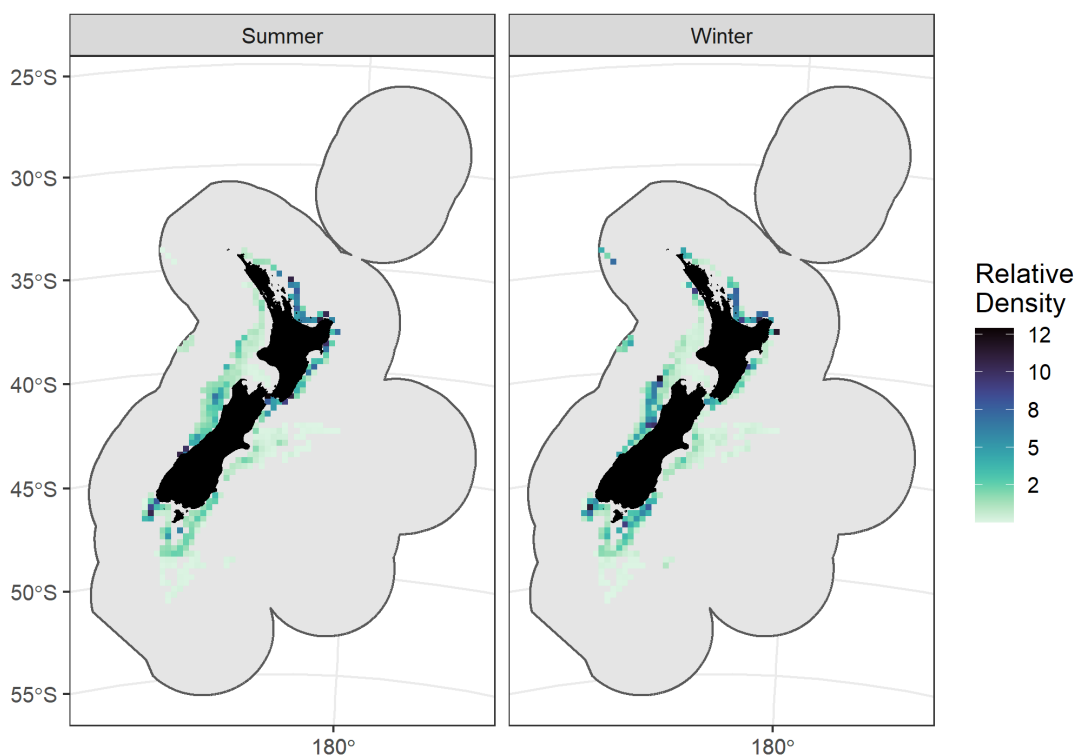


Figure 36: Posterior prediction of the relative density per grid cell and season for gemfish. Posterior median values are shown on a natural scale in tonnes per square kilometre.

Table 16: Total predicted bycatch (tonnes) per method for gemfish. Posterior median values are given, with the 95% equal-tailed credibility intervals in brackets.

Fishing year	BLL	TWL	Total
2000/01	2 (0 - 46)	463 (421 - 543)	469 (425 - 573)
2001/02	1 (0 - 29)	511 (463 - 601)	516 (465 - 630)
2002/03	1 (0 - 15)	561 (497 - 1 031)	563 (499 - 1 033)
2003/04	2 (0 - 39)	391 (352 - 489)	397 (355 - 544)
2004/05	3 (0 - 58)	378 (341 - 437)	386 (345 - 474)
2005/06	3 (0 - 51)	376 (339 - 437)	383 (341 - 463)
2006/07	3 (0 - 58)	269 (242 - 310)	276 (245 - 335)
2007/08	8 (2 - 169)	276 (242 - 341)	289 (250 - 528)
2008/09	5 (1 - 85)	295 (257 - 446)	303 (263 - 565)
2009/10	4 (1 - 127)	423 (368 - 560)	430 (372 - 639)
2010/11	6 (2 - 125)	378 (331 - 767)	386 (336 - 859)
2011/12	4 (2 - 37)	315 (276 - 498)	320 (280 - 535)
2012/13	4 (2 - 50)	330 (289 - 540)	336 (293 - 579)
2013/14	5 (2 - 64)	362 (316 - 480)	372 (322 - 534)
2014/15	6 (2 - 89)	376 (327 - 541)	385 (333 - 610)
2015/16	6 (2 - 93)	369 (320 - 490)	379 (326 - 584)
2016/17	6 (2 - 106)	419 (367 - 489)	429 (374 - 562)
2017/18	5 (2 - 36)	450 (393 - 532)	457 (397 - 556)
2018/19	6 (2 - 48)	403 (356 - 470)	411 (363 - 506)

4.3.13 Ghost shark (*Hydrolagus novaezealandiae*)

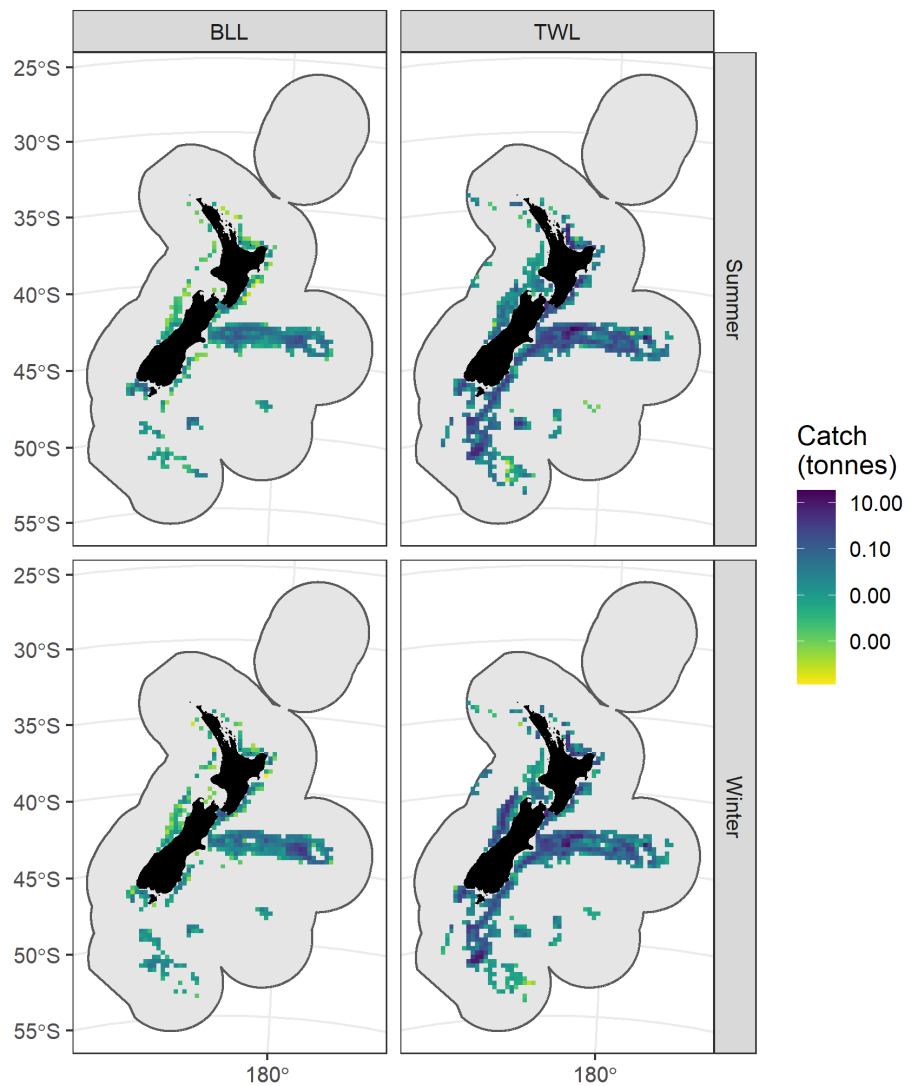


Figure 37: Posterior prediction of the average total catches for ghost shark by grid cell and method for each season. Average annual catches per season were calculated as the sum across gear types per grid cell and method. Posterior median values are shown, with catches in tonnes on a log₁₀ scale.

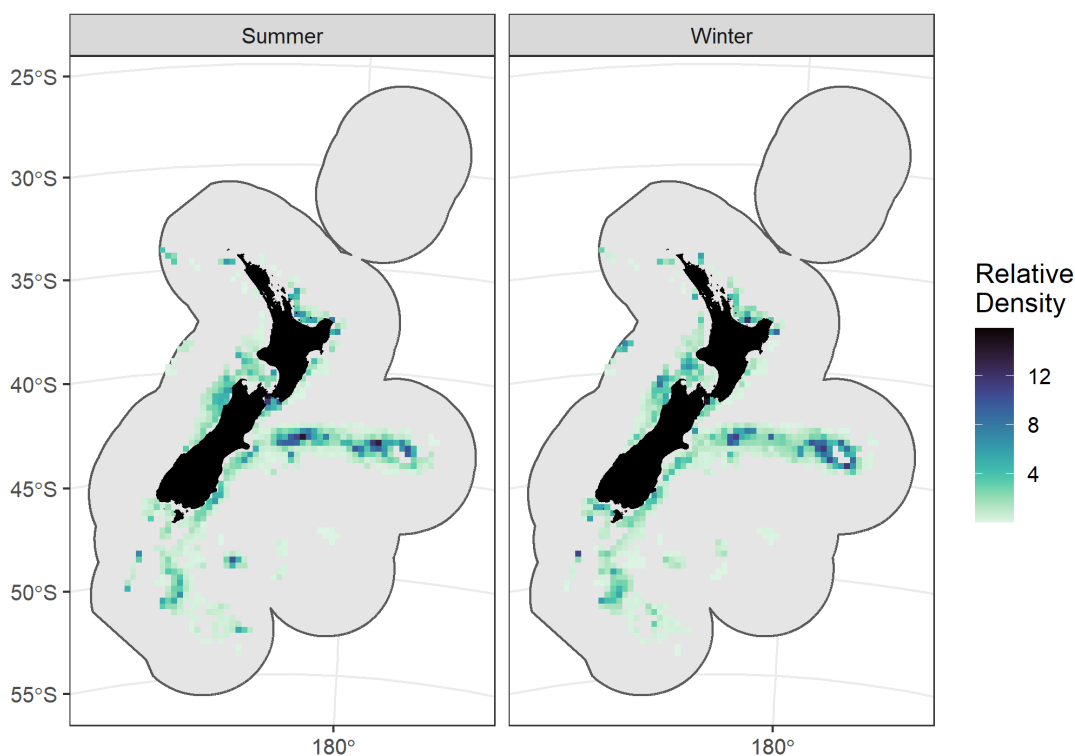


Figure 38: Posterior prediction of the relative density per grid cell and season for ghost shark. Posterior median values are shown on a natural scale in tonnes per square kilometre.

Table 17: Total predicted bycatch (tonnes) per method for ghost shark. Posterior median values are given, with the 95% equal-tailed credibility intervals in brackets.

Fishing year	BLL	TWL	Total
2000/01	31 (26 - 37)	395 (354 - 959)	426 (384 - 992)
2001/02	28 (24 - 34)	408 (365 - 537)	437 (393 - 567)
2002/03	21 (17 - 26)	430 (380 - 1 930)	452 (402 - 1 951)
2003/04	27 (22 - 33)	366 (326 - 521)	392 (351 - 549)
2004/05	26 (21 - 32)	368 (331 - 638)	394 (355 - 665)
2005/06	22 (18 - 27)	416 (366 - 2 456)	437 (388 - 2 478)
2006/07	19 (16 - 23)	409 (358 - 638)	428 (378 - 655)
2007/08	25 (20 - 375)	489 (430 - 772)	516 (455 - 1 354)
2008/09	24 (20 - 30)	456 (400 - 565)	480 (425 - 590)
2009/10	26 (21 - 38)	534 (456 - 3 441)	559 (481 - 3 466)
2010/11	23 (19 - 513)	511 (450 - 1 806)	538 (474 - 2 752)
2011/12	23 (19 - 73)	572 (504 - 1 383)	596 (527 - 1 436)
2012/13	19 (16 - 24)	518 (454 - 2 039)	537 (473 - 2 064)
2013/14	20 (16 - 76)	561 (488 - 1 763)	579 (508 - 2 045)
2014/15	29 (23 - 37)	579 (499 - 934)	608 (527 - 965)
2015/16	38 (32 - 48)	627 (539 - 1 320)	665 (575 - 1 360)
2016/17	33 (27 - 42)	566 (494 - 1 389)	599 (528 - 1 426)
2017/18	30 (25 - 75)	517 (456 - 1 093)	547 (485 - 1 171)
2018/19	23 (19 - 166)	551 (483 - 1 991)	575 (508 - 3 384)

4.3.14 Silver dory (*Cyttus novaezealandiae*)

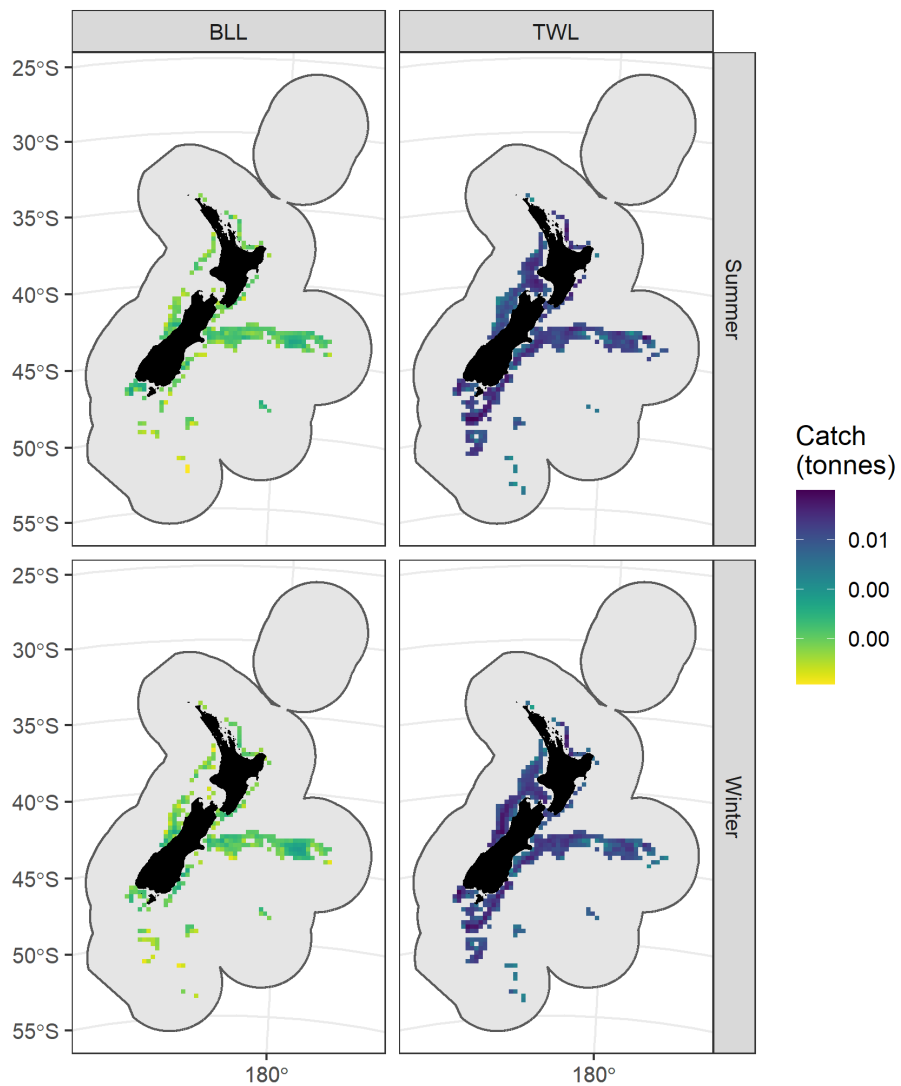


Figure 39: Posterior prediction of the average total catches for silver dory by grid cell and method for each season. Average annual catches per season were calculated as the sum across gear types per grid cell and method. Posterior median values are shown, with catches in tonnes on a log₁₀ scale.

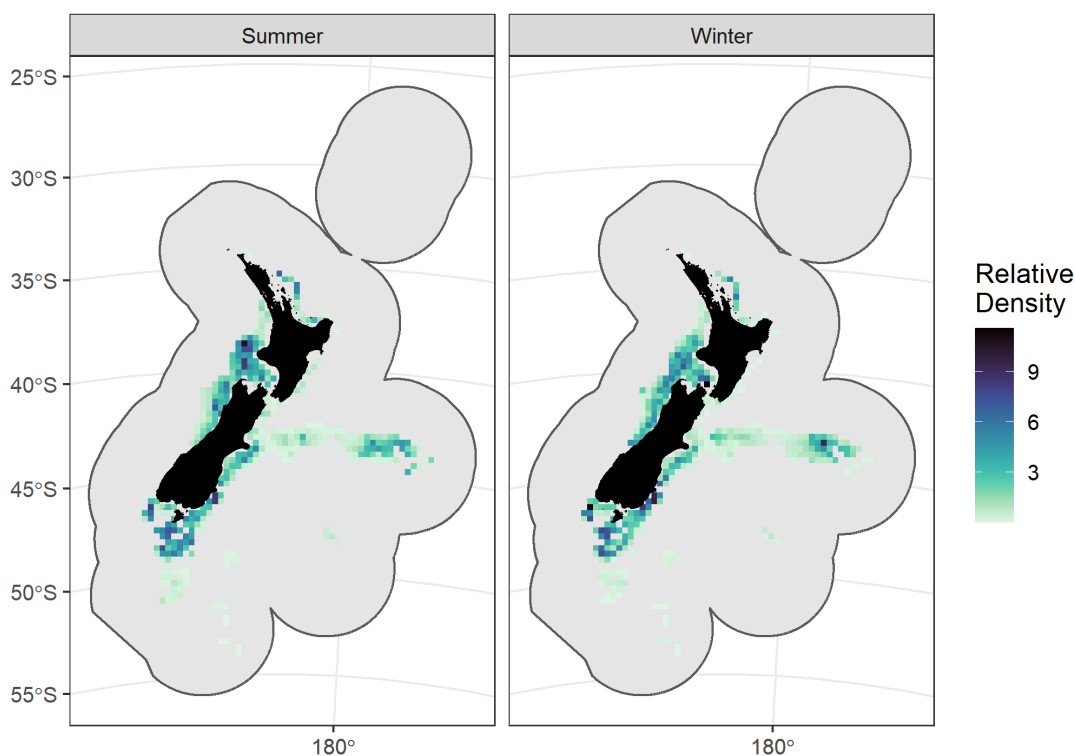


Figure 40: Posterior prediction of the relative density per grid cell and season for silver dory. Posterior median values are shown on a natural scale in tonnes per square kilometre.

Table 18: Total predicted bycatch (tonnes) per method for silver dory. Posterior median values are given, with the 95% equal-tailed credibility intervals in brackets.

Fishing year	BLL	TWL	Total
2000/01	0 (0 - 0)	197 (172 - 233)	197 (172 - 233)
2001/02	0 (0 - 0)	202 (178 - 238)	202 (178 - 238)
2002/03	0 (0 - 0)	232 (201 - 271)	232 (201 - 271)
2003/04	0 (0 - 0)	183 (161 - 216)	183 (161 - 216)
2004/05	0 (0 - 0)	216 (189 - 257)	216 (189 - 257)
2005/06	0 (0 - 0)	193 (166 - 275)	193 (166 - 275)
2006/07	0 (0 - 0)	148 (130 - 176)	148 (130 - 176)
2007/08	0 (0 - 0)	142 (123 - 199)	142 (123 - 199)
2008/09	0 (0 - 0)	121 (106 - 142)	121 (106 - 142)
2009/10	0 (0 - 0)	158 (137 - 196)	158 (137 - 196)
2010/11	0 (0 - 0)	154 (134 - 182)	154 (134 - 182)
2011/12	0 (0 - 0)	142 (124 - 167)	142 (124 - 167)
2012/13	0 (0 - 0)	141 (121 - 167)	141 (121 - 167)
2013/14	0 (0 - 0)	143 (122 - 187)	143 (122 - 187)
2014/15	0 (0 - 0)	137 (118 - 163)	137 (118 - 163)
2015/16	0 (0 - 0)	129 (110 - 174)	129 (110 - 174)
2016/17	0 (0 - 0)	146 (127 - 180)	146 (127 - 180)
2017/18	0 (0 - 0)	132 (115 - 154)	132 (115 - 154)
2018/19	0 (0 - 0)	139 (122 - 165)	139 (122 - 165)

4.3.15 Giant stargazer (*Kathetostoma* spp.)

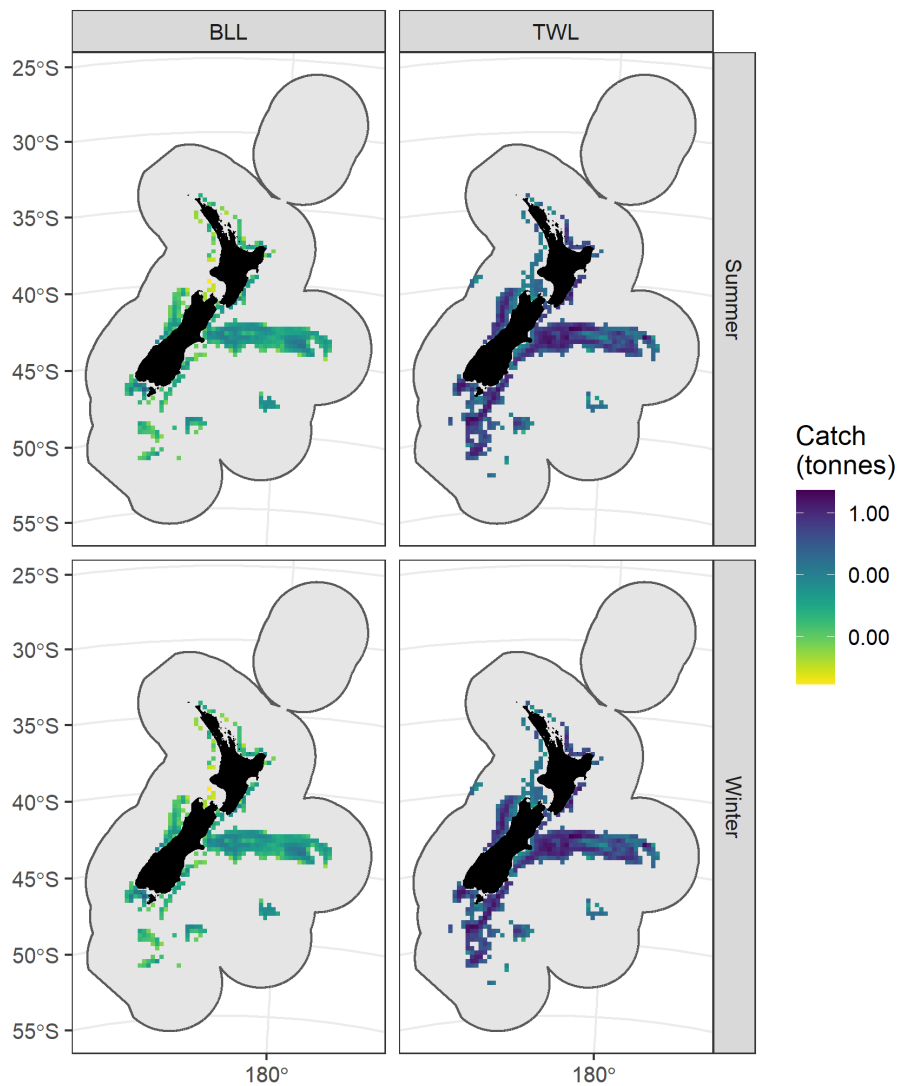


Figure 41: Posterior prediction of the average total catches for giant stargazer by grid cell and method for each season. Average annual catches per season were calculated as the sum across gear types per grid cell and method. Posterior median values are shown, with catches in tonnes on a log₁₀ scale.

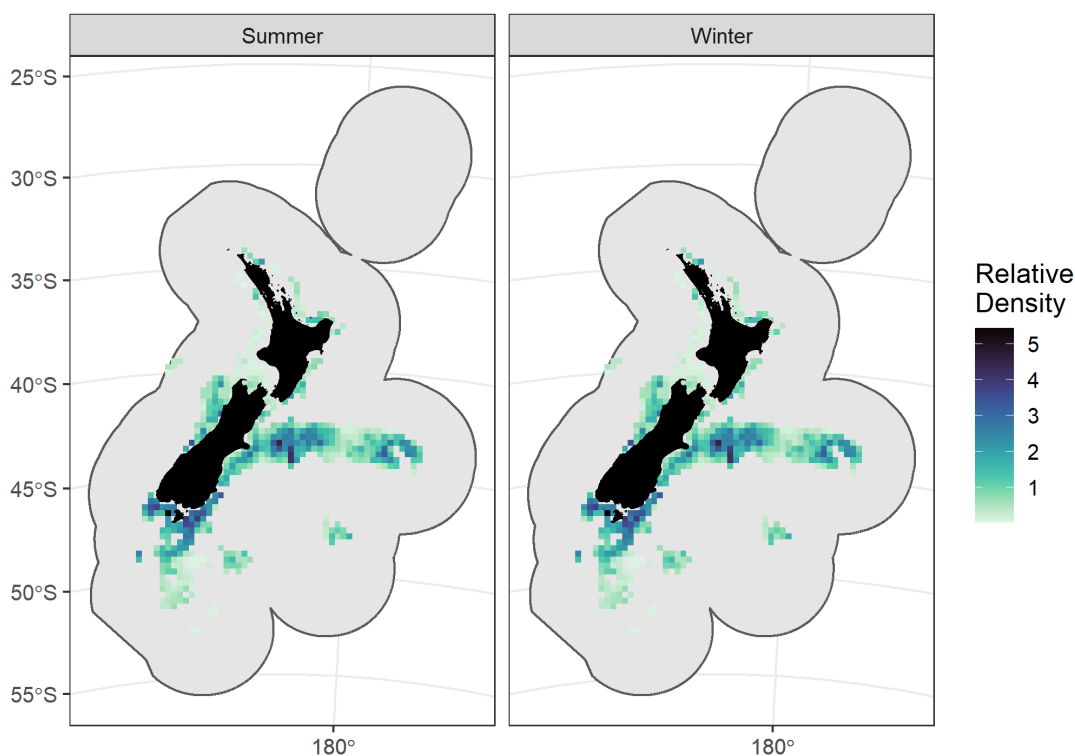


Figure 42: Posterior prediction of the relative density per grid cell and season for giant stargazer. Posterior median values are shown on a natural scale in tonnes per square kilometre.

Table 19: Total predicted bycatch (tonnes) per method for giant stargazer. Posterior median values are given, with the 95% equal-tailed credibility intervals in brackets.

Fishing year	BLL	TWL	Total
2000/01	0 (0 - 0)	641 (603 - 682)	641 (603 - 682)
2001/02	0 (0 - 0)	603 (569 - 643)	603 (569 - 643)
2002/03	0 (0 - 0)	658 (622 - 700)	659 (622 - 700)
2003/04	0 (0 - 0)	456 (433 - 483)	456 (434 - 483)
2004/05	0 (0 - 0)	509 (482 - 538)	510 (482 - 538)
2005/06	0 (0 - 0)	519 (490 - 556)	519 (490 - 556)
2006/07	0 (0 - 0)	465 (437 - 495)	465 (437 - 495)
2007/08	0 (0 - 1)	485 (455 - 526)	485 (455 - 527)
2008/09	0 (0 - 1)	431 (406 - 465)	431 (407 - 465)
2009/10	0 (0 - 1)	522 (491 - 563)	522 (491 - 563)
2010/11	0 (0 - 1)	511 (482 - 541)	512 (482 - 541)
2011/12	0 (0 - 1)	524 (493 - 559)	524 (493 - 559)
2012/13	0 (0 - 1)	496 (466 - 531)	496 (467 - 531)
2013/14	0 (0 - 1)	497 (465 - 535)	497 (466 - 535)
2014/15	0 (0 - 1)	545 (513 - 583)	546 (513 - 583)
2015/16	0 (0 - 1)	517 (484 - 550)	517 (484 - 551)
2016/17	0 (0 - 1)	531 (500 - 569)	532 (500 - 569)
2017/18	0 (0 - 1)	479 (453 - 510)	479 (453 - 510)
2018/19	0 (0 - 1)	500 (470 - 532)	500 (470 - 532)

4.3.16 Shovelnose spiny dogfish (*Deania calcea*)

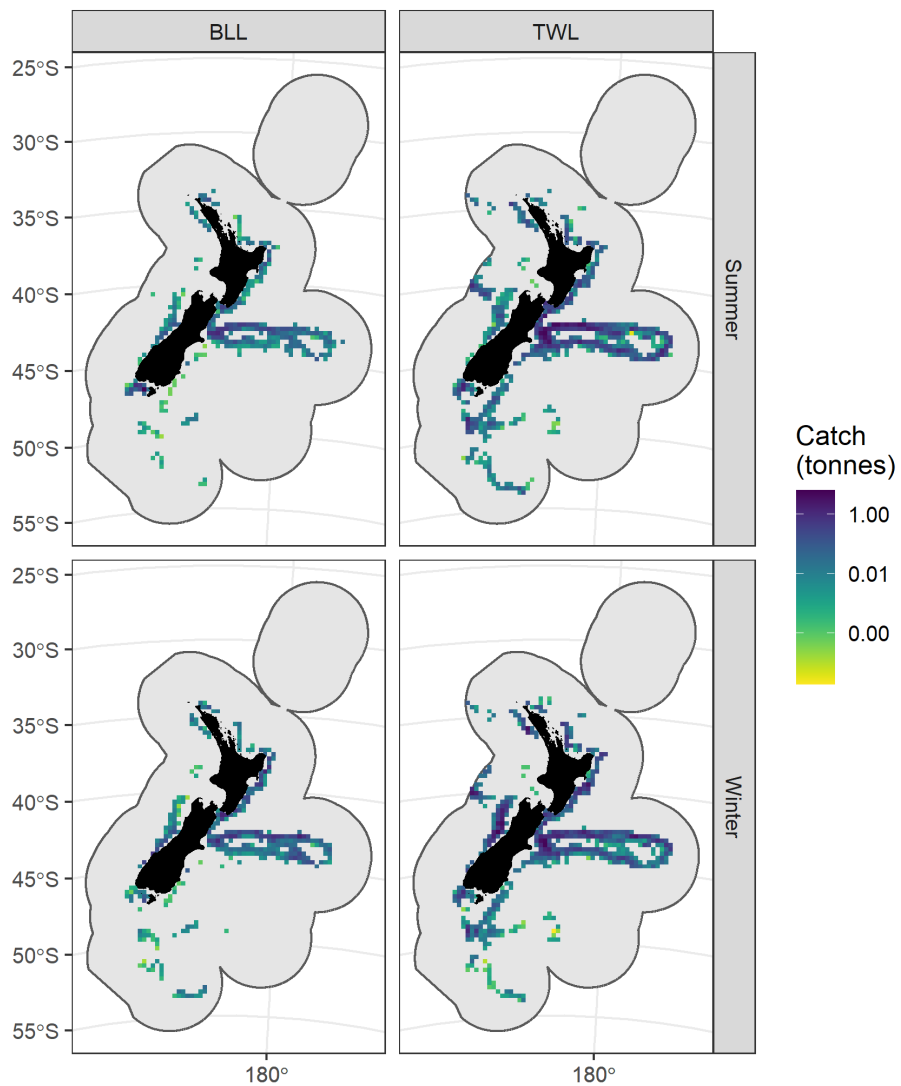


Figure 43: Posterior prediction of the average total catches for shovelnose spiny dogfish by grid cell and method for each season. Average annual catches per season were calculated as the sum across gear types per grid cell and method. Posterior median values are shown, with catches in tonnes on a log₁₀ scale.

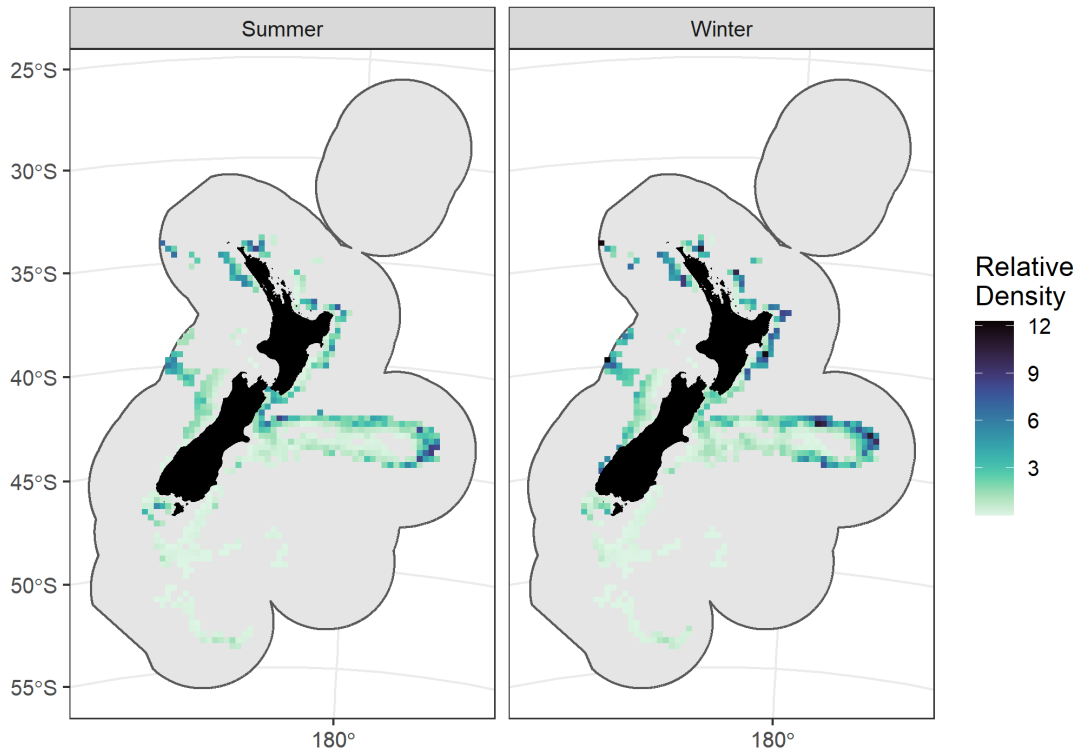


Figure 44: Posterior prediction of the relative density per grid cell and season for shovelnose spiny dogfish. Posterior median values are shown on a natural scale in tonnes per square kilometre.

Table 20: Total predicted bycatch (tonnes) per method for shovelnose spiny dogfish. Posterior median values are given, with the 95% equal-tailed credibility intervals in brackets.

Fishing year	BLL	TWL	Total
2000/01	59 (47 - 80)	398 (361 - 443)	457 (421 - 507)
2001/02	75 (58 - 104)	363 (330 - 407)	440 (398 - 496)
2002/03	30 (24 - 39)	381 (350 - 421)	411 (380 - 452)
2003/04	48 (36 - 65)	344 (314 - 426)	392 (361 - 475)
2004/05	59 (45 - 78)	276 (251 - 306)	335 (307 - 368)
2005/06	45 (36 - 58)	257 (234 - 296)	303 (276 - 345)
2006/07	60 (47 - 78)	228 (208 - 252)	288 (264 - 318)
2007/08	68 (50 - 108)	255 (232 - 284)	324 (292 - 376)
2008/09	64 (48 - 106)	263 (241 - 293)	328 (298 - 378)
2009/10	67 (49 - 117)	235 (214 - 272)	304 (273 - 374)
2010/11	74 (54 - 136)	218 (199 - 245)	294 (264 - 364)
2011/12	60 (42 - 115)	189 (170 - 2 172)	252 (220 - 2 231)
2012/13	55 (40 - 94)	192 (174 - 235)	249 (224 - 309)
2013/14	101 (73 - 148)	233 (208 - 279)	336 (297 - 406)
2014/15	71 (50 - 123)	258 (230 - 323)	333 (294 - 412)
2015/16	80 (58 - 132)	292 (261 - 389)	375 (333 - 485)
2016/17	73 (51 - 135)	288 (260 - 335)	361 (324 - 442)
2017/18	64 (45 - 113)	291 (258 - 373)	358 (315 - 459)
2018/19	77 (55 - 126)	287 (247 - 369)	369 (320 - 457)

4.3.17 Lookdown dory (*Cyttus traversi*)

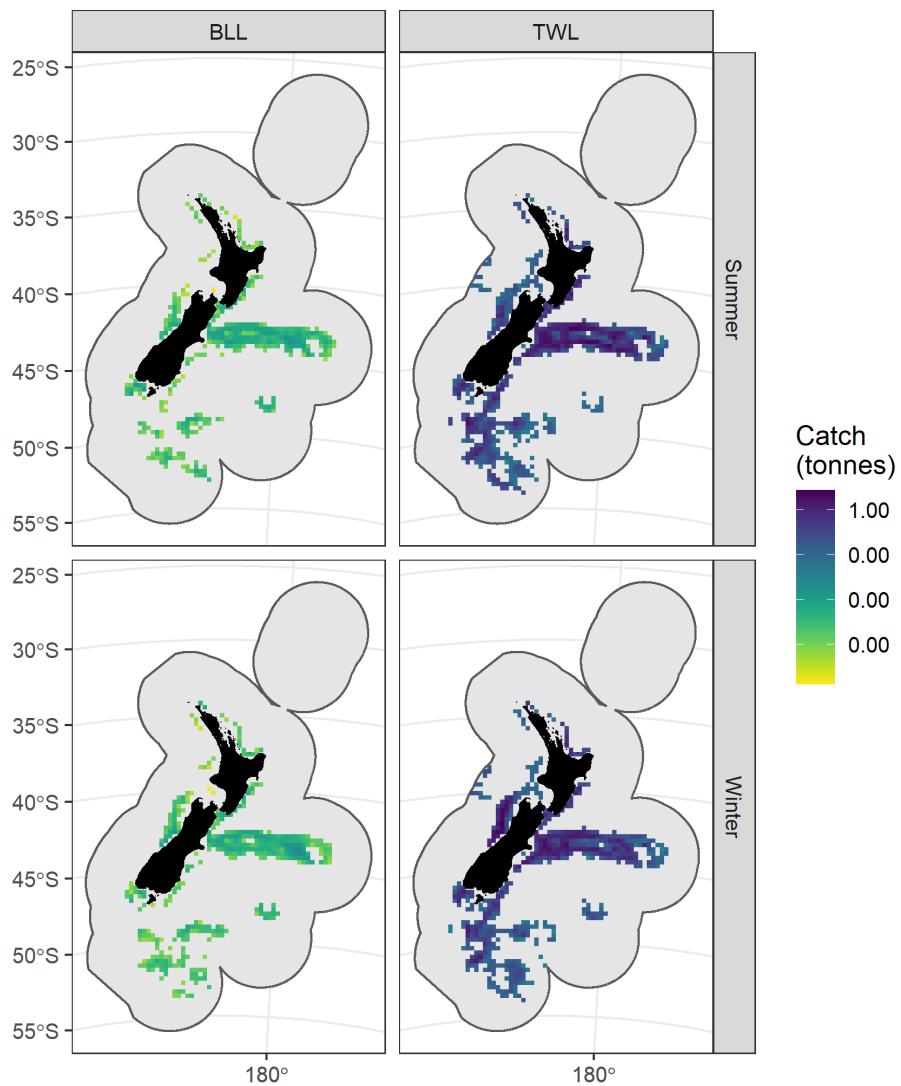


Figure 45: Posterior prediction of the average total catches for lookdown dory by grid cell and method for each season. Average annual catches per season were calculated as the sum across gear types per grid cell and method. Posterior median values are shown, with catches in tonnes on a log₁₀ scale.

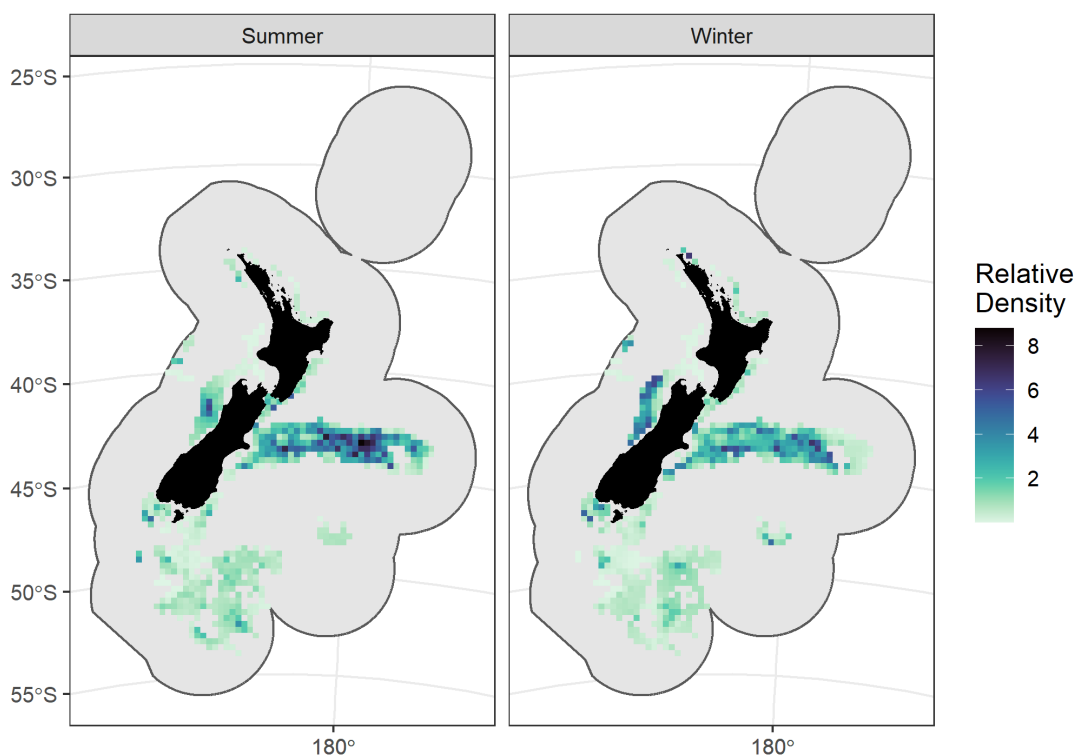


Figure 46: Posterior prediction of the relative density per grid cell and season for lockdown dory. Posterior median values are shown on a natural scale in tonnes per square kilometre.

Table 21: Total predicted bycatch (tonnes) per method for lockdown dory. Posterior median values are given, with the 95% equal-tailed credibility intervals in brackets.

Fishing year	BLL	TWL	Total
2000/01	0 (0 - 0)	782 (727 - 1 658)	782 (727 - 1 658)
2001/02	0 (0 - 0)	754 (698 - 844)	754 (698 - 844)
2002/03	0 (0 - 0)	838 (781 - 1 509)	838 (781 - 1 509)
2003/04	0 (0 - 0)	719 (651 - 847)	719 (651 - 847)
2004/05	0 (0 - 0)	573 (525 - 961)	573 (525 - 961)
2005/06	0 (0 - 0)	549 (499 - 3 506)	549 (499 - 3 506)
2006/07	0 (0 - 0)	491 (453 - 642)	491 (453 - 642)
2007/08	0 (0 - 0)	601 (548 - 1 064)	601 (548 - 1 064)
2008/09	0 (0 - 0)	555 (501 - 757)	555 (501 - 757)
2009/10	0 (0 - 0)	560 (516 - 1 374)	560 (516 - 1 374)
2010/11	0 (0 - 0)	527 (493 - 616)	527 (493 - 616)
2011/12	0 (0 - 0)	592 (551 - 643)	592 (551 - 643)
2012/13	0 (0 - 0)	559 (521 - 942)	559 (521 - 942)
2013/14	0 (0 - 0)	571 (528 - 1 070)	571 (528 - 1 070)
2014/15	0 (0 - 0)	642 (595 - 1 185)	642 (595 - 1 185)
2015/16	0 (0 - 0)	633 (579 - 2 861)	633 (579 - 2 861)
2016/17	0 (0 - 0)	643 (596 - 1 267)	643 (596 - 1 267)
2017/18	0 (0 - 0)	639 (593 - 3 408)	639 (593 - 3 408)
2018/19	0 (0 - 0)	559 (519 - 620)	559 (519 - 620)

4.3.18 Smooth skate (*Dipturus innominatus*)

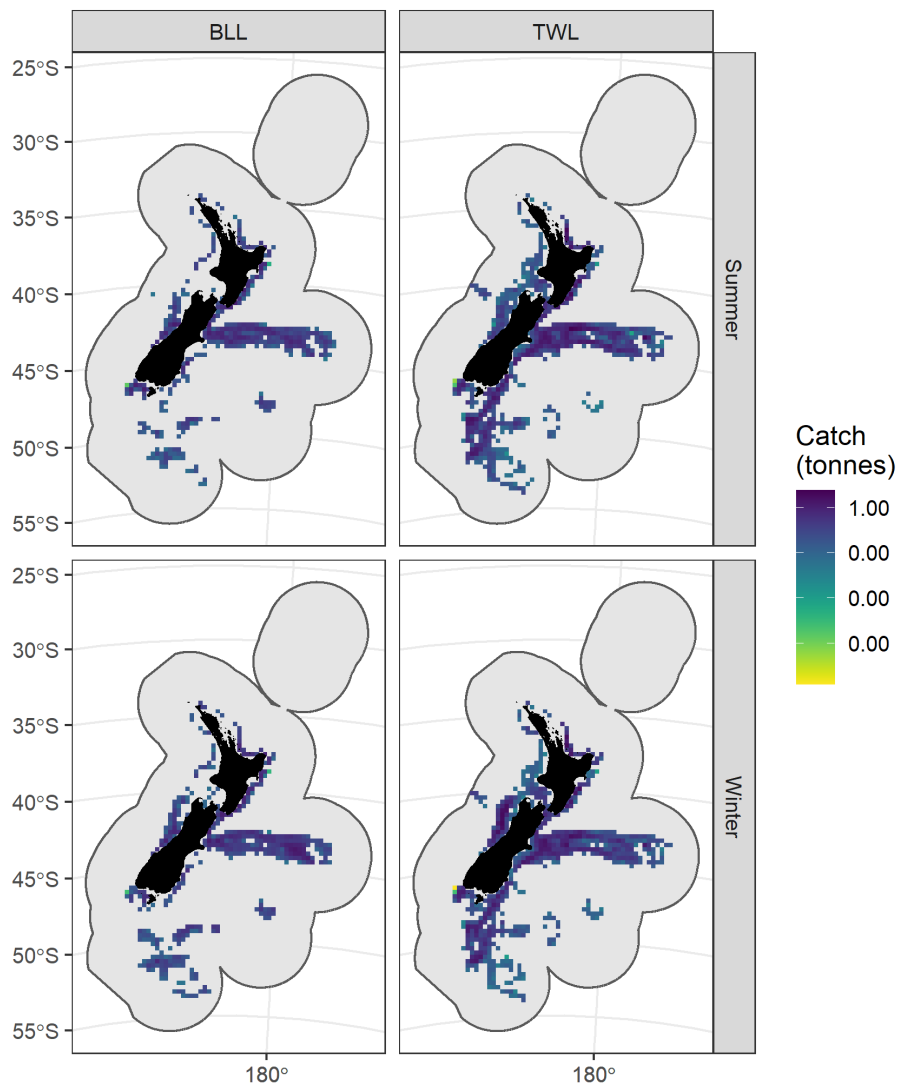


Figure 47: Posterior prediction of the average total catches for smooth skate by grid cell and method for each season. Average annual catches per season were calculated as the sum across gear types per grid cell and method. Posterior median values are shown, with catches in tonnes on a log₁₀ scale.

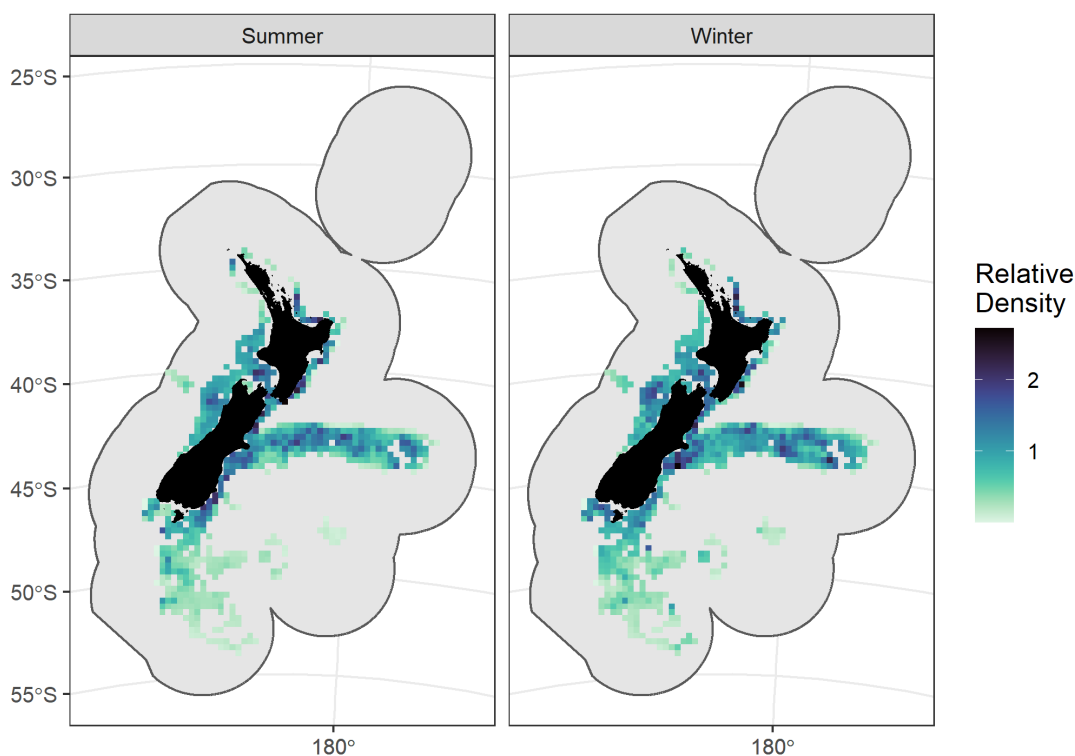


Figure 48: Posterior prediction of the relative density per grid cell and season for smooth skate. Posterior median values are shown on a natural scale in tonnes per square kilometre.

Table 22: Total predicted bycatch (tonnes) per method for smooth skate. Posterior median values are given, with the 95% equal-tailed credibility intervals in brackets.

Fishing year	BLL	TWL	Total
2000/01	91 (79 - 106)	511 (475 - 555)	604 (563 - 648)
2001/02	95 (83 - 109)	522 (485 - 566)	617 (577 - 666)
2002/03	58 (50 - 67)	502 (470 - 538)	560 (527 - 597)
2003/04	80 (69 - 93)	399 (373 - 426)	479 (450 - 509)
2004/05	88 (76 - 104)	382 (358 - 405)	470 (443 - 499)
2005/06	68 (59 - 80)	382 (357 - 408)	450 (424 - 478)
2006/07	65 (56 - 77)	340 (318 - 362)	405 (380 - 430)
2007/08	107 (88 - 137)	364 (341 - 390)	473 (440 - 511)
2008/09	103 (86 - 126)	365 (340 - 391)	469 (437 - 507)
2009/10	112 (93 - 141)	432 (402 - 477)	545 (506 - 596)
2010/11	126 (103 - 164)	404 (378 - 432)	531 (493 - 577)
2011/12	108 (90 - 142)	406 (379 - 437)	515 (480 - 558)
2012/13	105 (84 - 138)	398 (371 - 432)	503 (467 - 552)
2013/14	137 (111 - 178)	413 (384 - 447)	551 (510 - 603)
2014/15	136 (109 - 179)	444 (413 - 492)	582 (537 - 645)
2015/16	152 (125 - 195)	451 (416 - 511)	604 (560 - 676)
2016/17	157 (130 - 200)	462 (431 - 510)	621 (577 - 680)
2017/18	144 (117 - 186)	438 (407 - 484)	582 (541 - 642)
2018/19	162 (129 - 243)	400 (370 - 437)	565 (518 - 653)

4.3.19 Slender tuna (*Allothunnus fallai*)

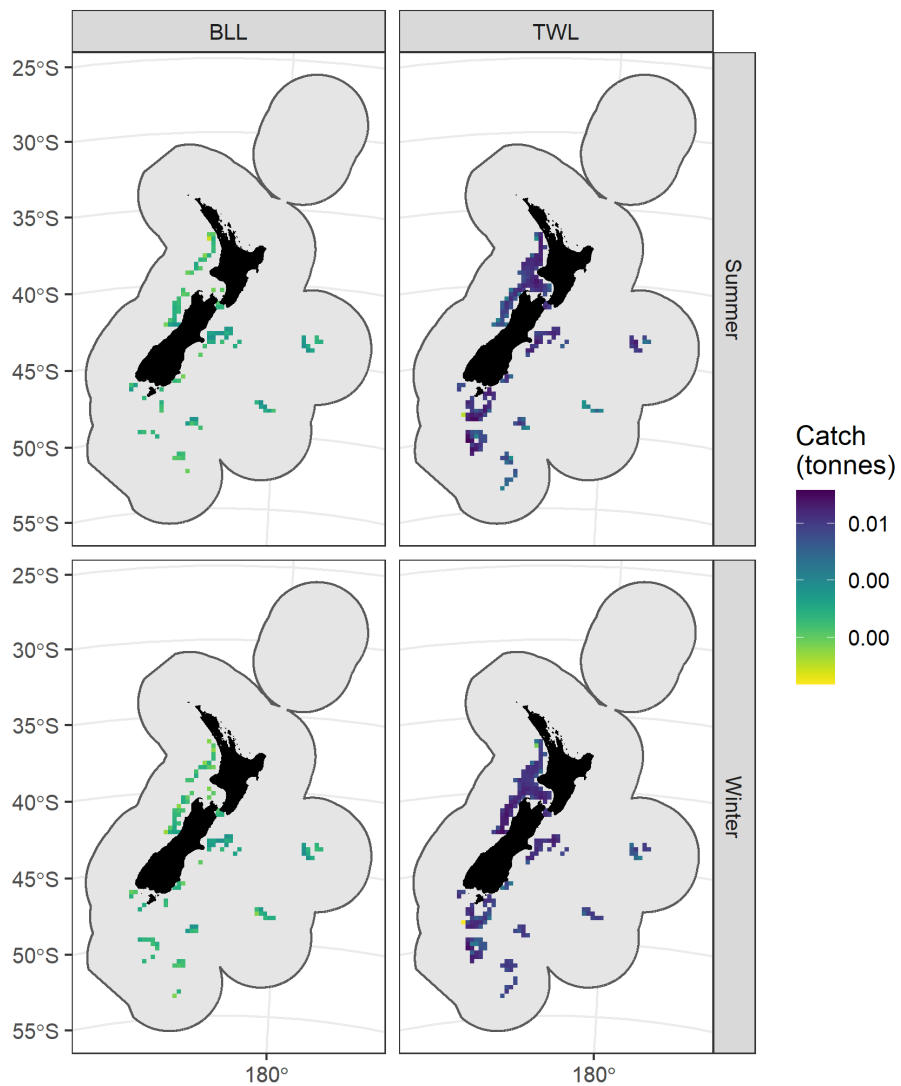


Figure 49: Posterior prediction of the average total catches for slender tuna by grid cell and method for each season. Average annual catches per season were calculated as the sum across gear types per grid cell and method. Posterior median values are shown, with catches in tonnes on a log₁₀ scale.

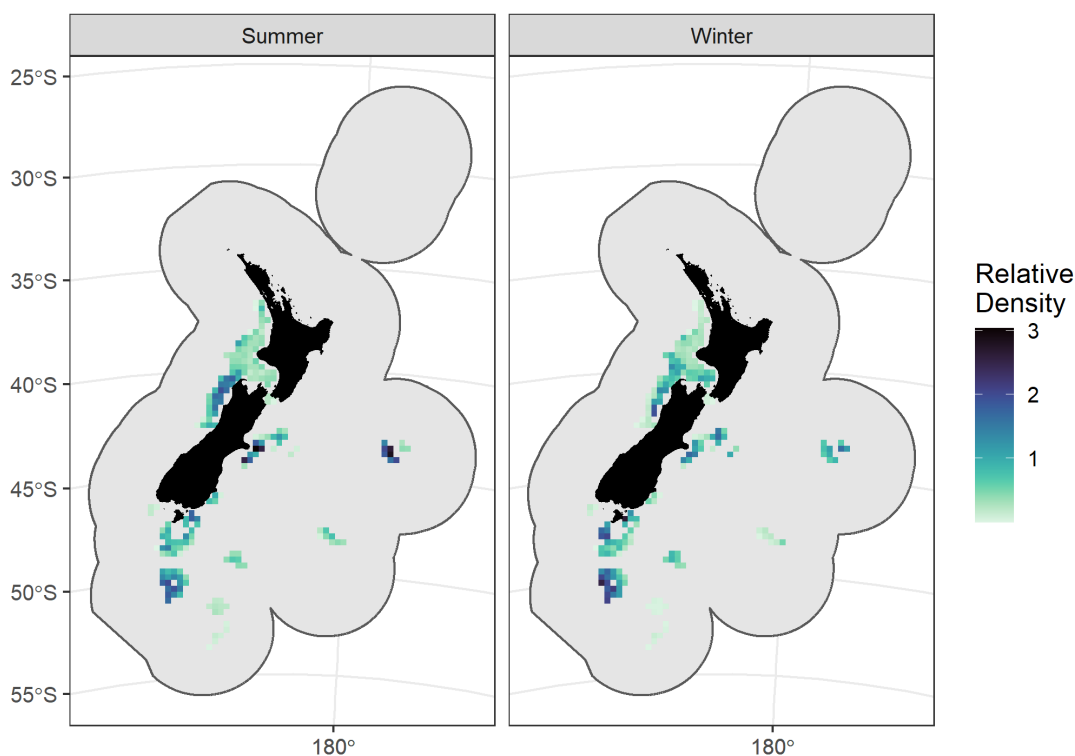


Figure 50: Posterior prediction of the relative density per grid cell and season for slender tuna. Posterior median values are shown on a natural scale in tonnes per square kilometre.

Table 23: Total predicted bycatch (tonnes) per method for slender tuna. Posterior median values are given, with the 95% equal-tailed credibility intervals in brackets.

Fishing year	BLL	TWL	Total
2000/01	0 (0 - 0)	26 (23 - 29)	26 (23 - 29)
2001/02	0 (0 - 0)	31 (28 - 35)	31 (28 - 35)
2002/03	0 (0 - 0)	29 (26 - 33)	29 (26 - 33)
2003/04	0 (0 - 0)	30 (27 - 35)	30 (27 - 35)
2004/05	0 (0 - 0)	31 (28 - 35)	31 (28 - 35)
2005/06	0 (0 - 0)	24 (22 - 28)	24 (22 - 28)
2006/07	0 (0 - 0)	25 (22 - 28)	25 (22 - 28)
2007/08	0 (0 - 0)	22 (20 - 25)	22 (20 - 25)
2008/09	0 (0 - 0)	25 (22 - 28)	25 (22 - 28)
2009/10	0 (0 - 0)	14 (12 - 16)	14 (12 - 16)
2010/11	0 (0 - 0)	16 (14 - 18)	16 (14 - 18)
2011/12	0 (0 - 0)	17 (15 - 20)	17 (15 - 20)
2012/13	0 (0 - 0)	17 (15 - 19)	17 (15 - 19)
2013/14	0 (0 - 0)	24 (21 - 28)	24 (21 - 28)
2014/15	0 (0 - 0)	20 (18 - 23)	20 (18 - 23)
2015/16	0 (0 - 0)	19 (17 - 22)	19 (17 - 22)
2016/17	0 (0 - 0)	17 (15 - 20)	17 (15 - 20)
2017/18	0 (0 - 0)	18 (16 - 22)	18 (16 - 22)
2018/19	0 (0 - 0)	22 (19 - 28)	22 (19 - 28)

4.3.20 Ray's bream (*Brama brama*)

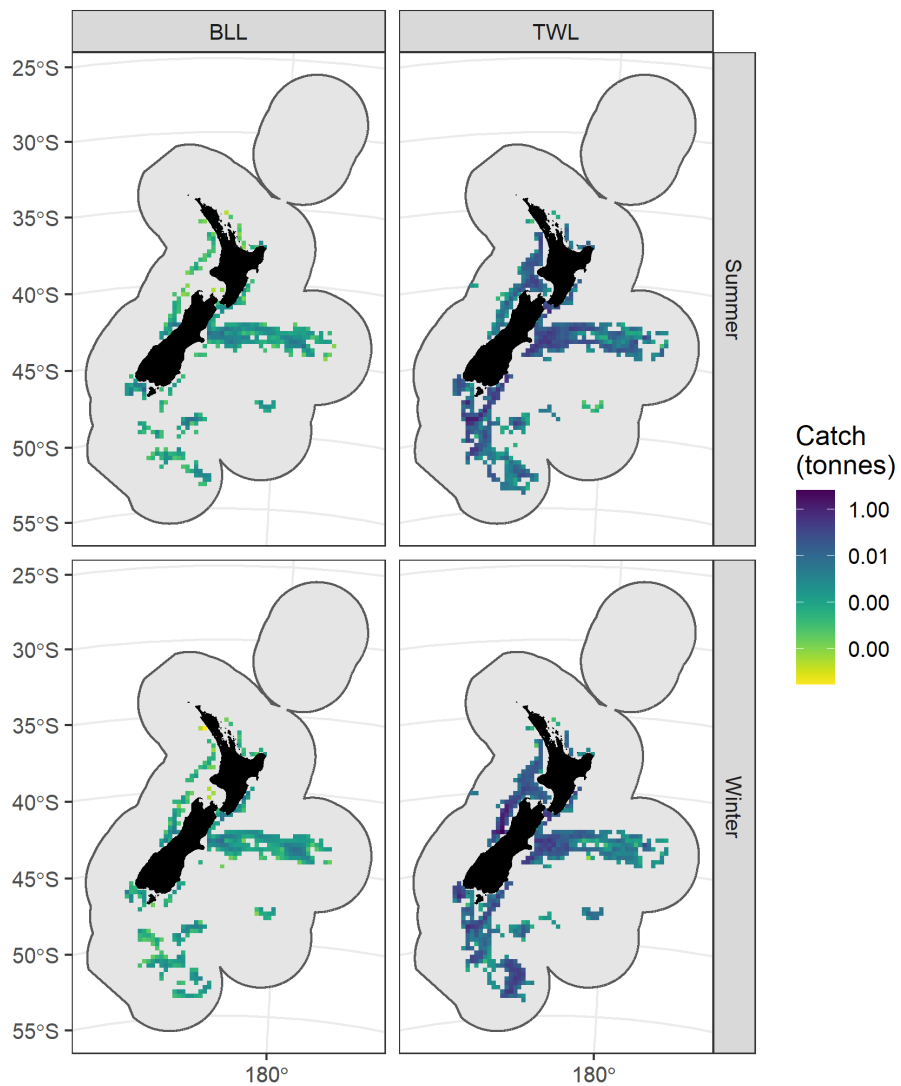


Figure 51: Posterior prediction of the average total catches for Ray's bream by grid cell and method for each season. Average annual catches per season were calculated as the sum across gear types per grid cell and method. Posterior median values are shown, with catches in tonnes on a log₁₀ scale.

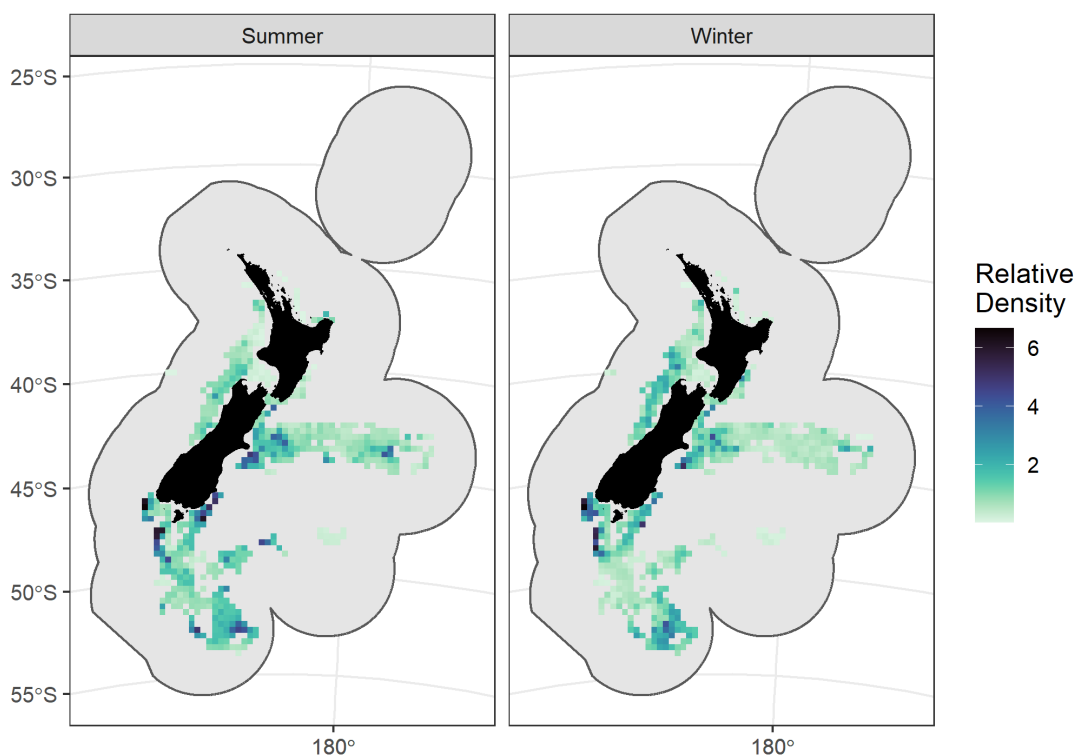


Figure 52: Posterior prediction of the relative density per grid cell and season for Ray's bream. Posterior median values are shown on a natural scale in tonnes per square kilometre.

Table 24: Total predicted bycatch (tonnes) per method for Ray's bream. Posterior median values are given, with the 95% equal-tailed credibility intervals in brackets.

Fishing year	BLL	TWL	Total
2000/01	0 (0 - 1)	128 (117 - 179)	128 (117 - 179)
2001/02	0 (0 - 1)	106 (98 - 116)	106 (98 - 116)
2002/03	0 (0 - 0)	107 (98 - 123)	107 (98 - 123)
2003/04	0 (0 - 1)	97 (89 - 127)	98 (89 - 128)
2004/05	0 (0 - 0)	78 (72 - 84)	78 (73 - 84)
2005/06	0 (0 - 0)	66 (61 - 71)	66 (61 - 72)
2006/07	0 (0 - 0)	61 (56 - 66)	61 (56 - 66)
2007/08	0 (0 - 1)	51 (47 - 55)	51 (47 - 56)
2008/09	0 (0 - 1)	51 (47 - 56)	51 (48 - 57)
2009/10	0 (0 - 1)	53 (49 - 59)	54 (49 - 60)
2010/11	0 (0 - 1)	55 (51 - 61)	56 (51 - 61)
2011/12	0 (0 - 1)	57 (53 - 63)	57 (53 - 63)
2012/13	0 (0 - 1)	55 (51 - 60)	55 (51 - 61)
2013/14	0 (0 - 1)	62 (57 - 67)	62 (58 - 68)
2014/15	0 (0 - 1)	67 (63 - 75)	68 (63 - 75)
2015/16	0 (0 - 1)	59 (55 - 64)	59 (55 - 64)
2016/17	1 (0 - 1)	59 (55 - 65)	59 (55 - 65)
2017/18	0 (0 - 1)	54 (50 - 60)	54 (50 - 60)
2018/19	0 (0 - 1)	63 (58 - 69)	63 (59 - 70)

4.3.21 Rough skate (*Zearaja nasuta*)

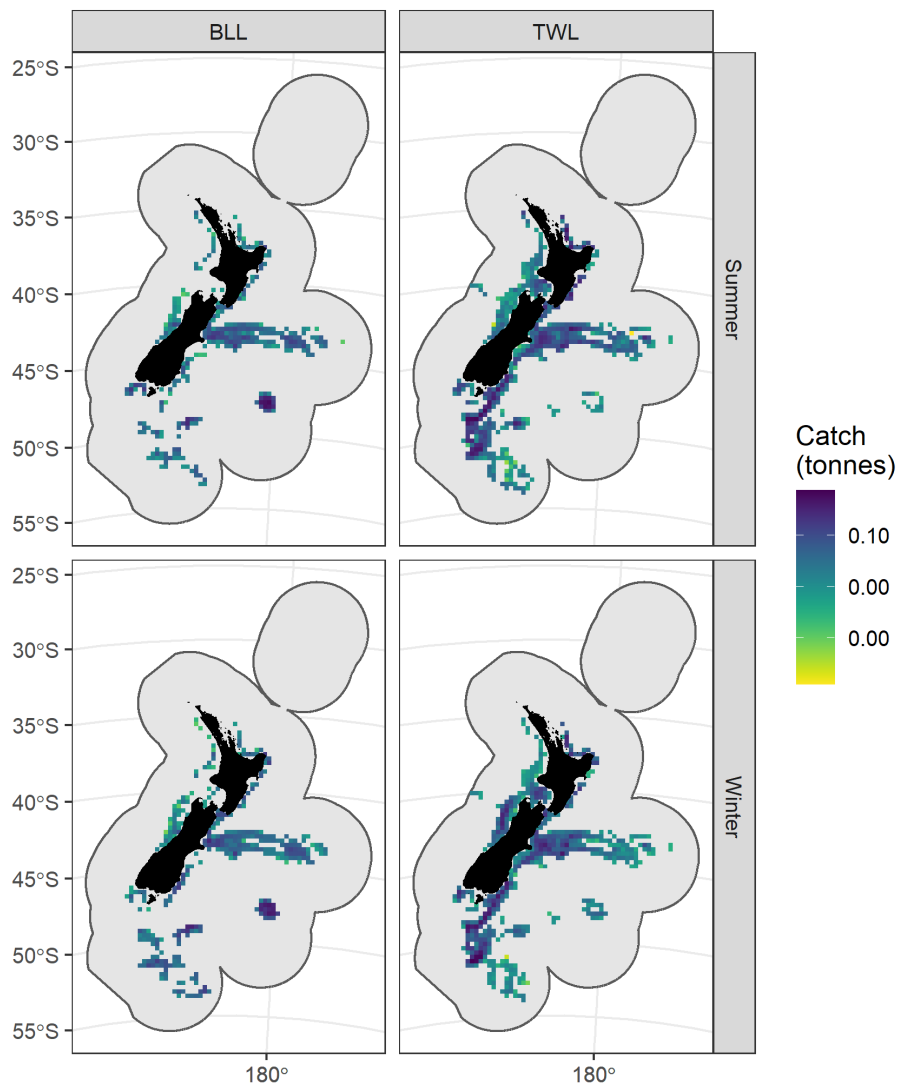


Figure 53: Posterior prediction of the average total catches for rough skate by grid cell and method for each season. Average annual catches per season were calculated as the sum across gear types per grid cell and method. Posterior median values are shown, with catches in tonnes on a log₁₀ scale.

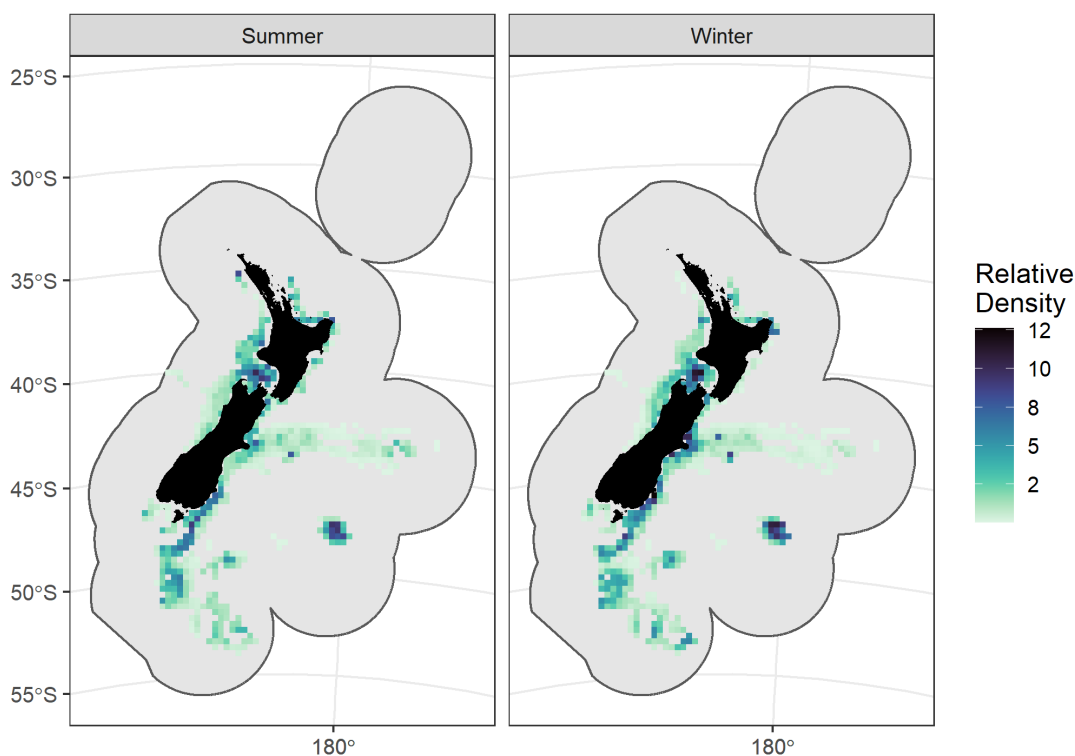


Figure 54: Posterior prediction of the relative density per grid cell and season for rough skate. Posterior median values are shown on a natural scale in tonnes per square kilometre.

Table 25: Total predicted bycatch (tonnes) per method for rough skate. Posterior median values are given, with the 95% equal-tailed credibility intervals in brackets.

Fishing year	BLL	TWL	Total
2000/01	131 (105 - 168)	186 (169 - 213)	319 (285 - 361)
2001/02	93 (75 - 122)	192 (175 - 216)	285 (257 - 323)
2002/03	90 (72 - 118)	175 (161 - 193)	265 (241 - 297)
2003/04	113 (92 - 142)	157 (146 - 172)	270 (246 - 305)
2004/05	32 (24 - 43)	175 (163 - 189)	207 (193 - 225)
2005/06	29 (21 - 39)	172 (159 - 186)	200 (186 - 218)
2006/07	53 (40 - 74)	150 (139 - 162)	203 (185 - 228)
2007/08	98 (73 - 147)	143 (132 - 156)	242 (213 - 292)
2008/09	64 (48 - 93)	158 (146 - 172)	222 (202 - 253)
2009/10	35 (26 - 53)	190 (176 - 217)	227 (208 - 261)
2010/11	42 (30 - 62)	189 (177 - 207)	231 (213 - 257)
2011/12	31 (24 - 43)	176 (164 - 192)	207 (193 - 228)
2012/13	14 (10 - 22)	160 (148 - 181)	174 (162 - 195)
2013/14	49 (36 - 69)	148 (136 - 170)	197 (178 - 232)
2014/15	31 (21 - 53)	149 (136 - 191)	180 (162 - 228)
2015/16	55 (40 - 80)	152 (139 - 208)	208 (185 - 267)
2016/17	115 (82 - 178)	182 (167 - 208)	298 (261 - 367)
2017/18	54 (42 - 73)	175 (162 - 195)	229 (210 - 255)
2018/19	49 (37 - 64)	186 (172 - 202)	235 (215 - 257)

4.3.22 Baxter's lantern dogfish (*Etmopterus baxteri*)

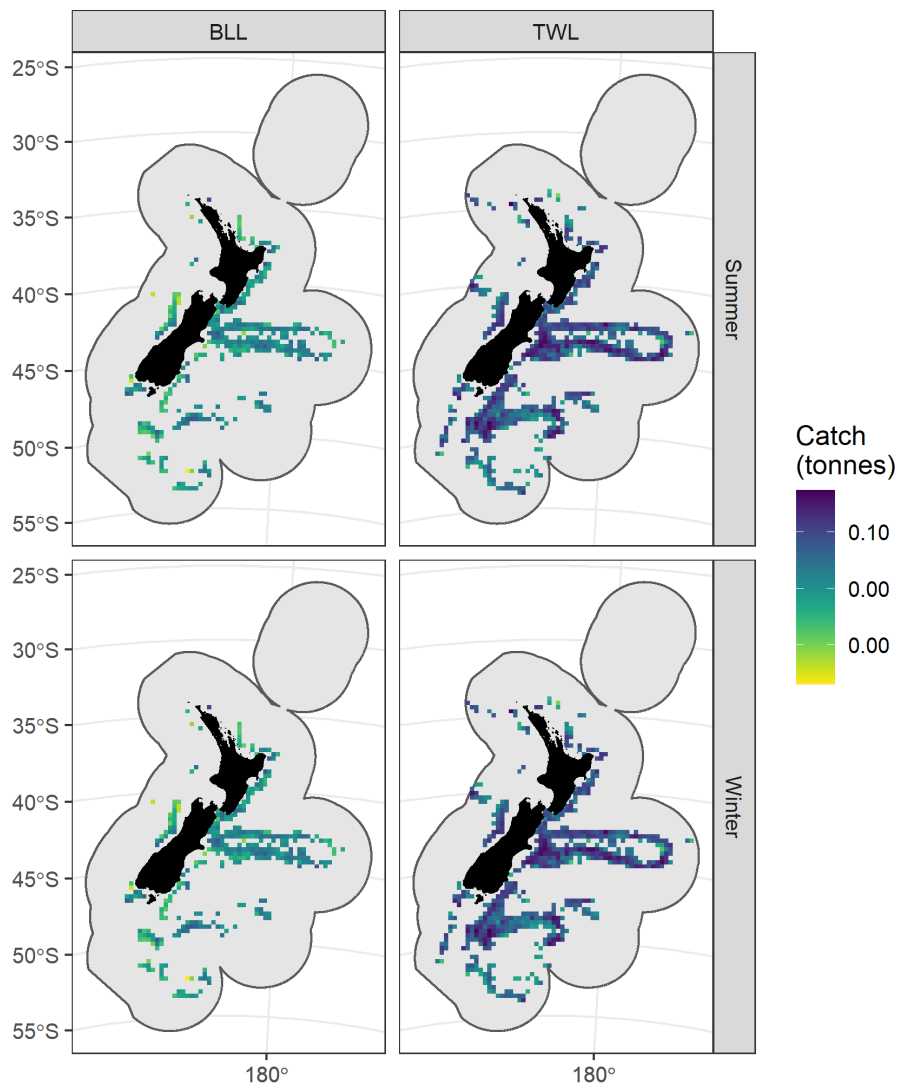


Figure 55: Posterior prediction of the average total catches for Baxter's lantern dogfish by grid cell and method for each season. Average annual catches per season were calculated as the sum across gear types per grid cell and method. Posterior median values are shown, with catches in tonnes on a log₁₀ scale.

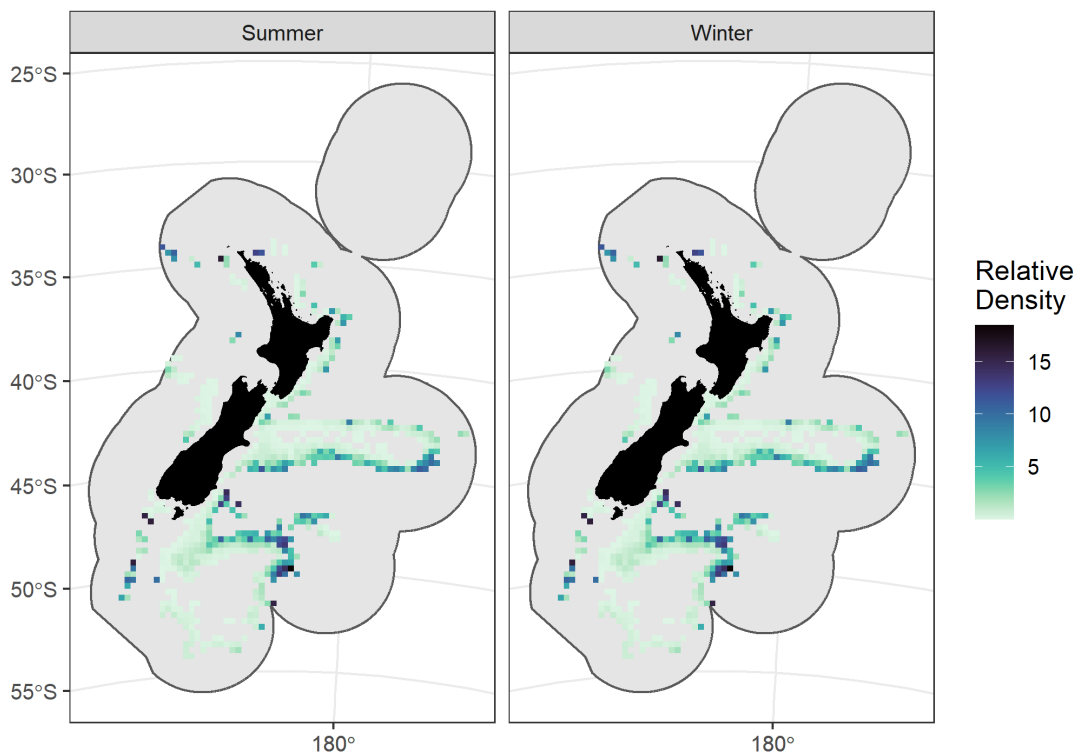


Figure 56: Posterior prediction of the relative density per grid cell and season for Baxter's lantern dogfish. Posterior median values are shown on a natural scale in tonnes per square kilometre.

Table 26: Total predicted bycatch (tonnes) per method for Baxter's lantern dogfish. Posterior median values are given, with the 95% equal-tailed credibility intervals in brackets.

Fishing year	BLL	TWL	Total
2000/01	4 (2 - 9)	302 (275 - 364)	307 (279 - 370)
2001/02	5 (3 - 10)	291 (262 - 346)	295 (266 - 351)
2002/03	2 (1 - 4)	289 (264 - 344)	291 (266 - 346)
2003/04	3 (2 - 6)	276 (248 - 347)	279 (251 - 350)
2004/05	2 (1 - 4)	253 (225 - 308)	255 (228 - 310)
2005/06	2 (1 - 4)	215 (195 - 249)	217 (197 - 251)
2006/07	2 (1 - 5)	221 (202 - 249)	224 (204 - 252)
2007/08	4 (2 - 8)	218 (199 - 248)	222 (203 - 253)
2008/09	2 (1 - 5)	223 (202 - 250)	225 (204 - 253)
2009/10	2 (1 - 6)	242 (220 - 272)	244 (222 - 275)
2010/11	4 (2 - 16)	193 (175 - 215)	198 (178 - 223)
2011/12	4 (2 - 16)	169 (152 - 192)	174 (156 - 200)
2012/13	2 (1 - 8)	164 (148 - 191)	167 (150 - 194)
2013/14	4 (2 - 8)	204 (181 - 237)	208 (185 - 243)
2014/15	3 (1 - 9)	213 (192 - 244)	216 (194 - 249)
2015/16	4 (2 - 9)	197 (178 - 223)	202 (181 - 229)
2016/17	4 (2 - 11)	206 (185 - 237)	211 (189 - 243)
2017/18	3 (1 - 9)	262 (235 - 300)	266 (238 - 307)
2018/19	4 (2 - 9)	220 (191 - 271)	224 (197 - 277)

4.3.23 Hydrocorals (Stylasteridae)

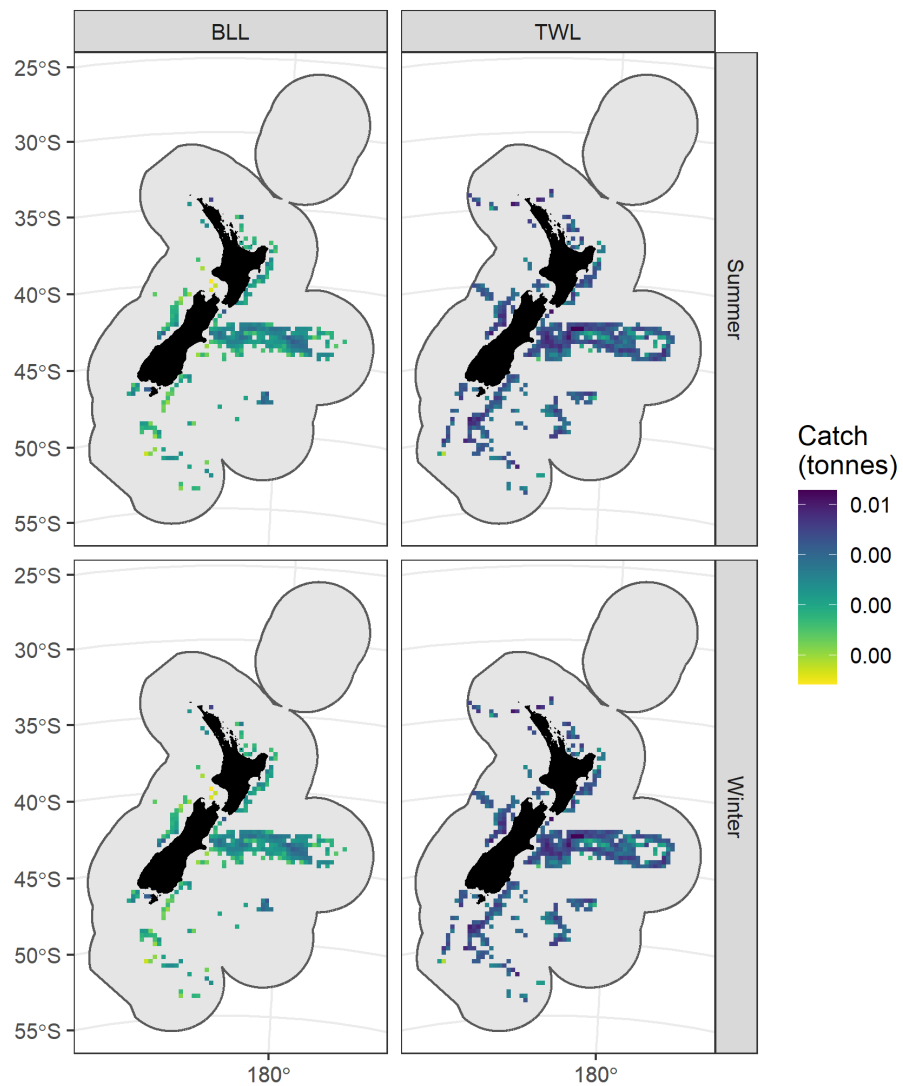


Figure 57: Posterior prediction of the average total catches for hydrocorals by grid cell and method for each season. Average annual catches per season were calculated as the sum across gear types per grid cell and method. Posterior median values are shown, with catches in tonnes on a log₁₀ scale.

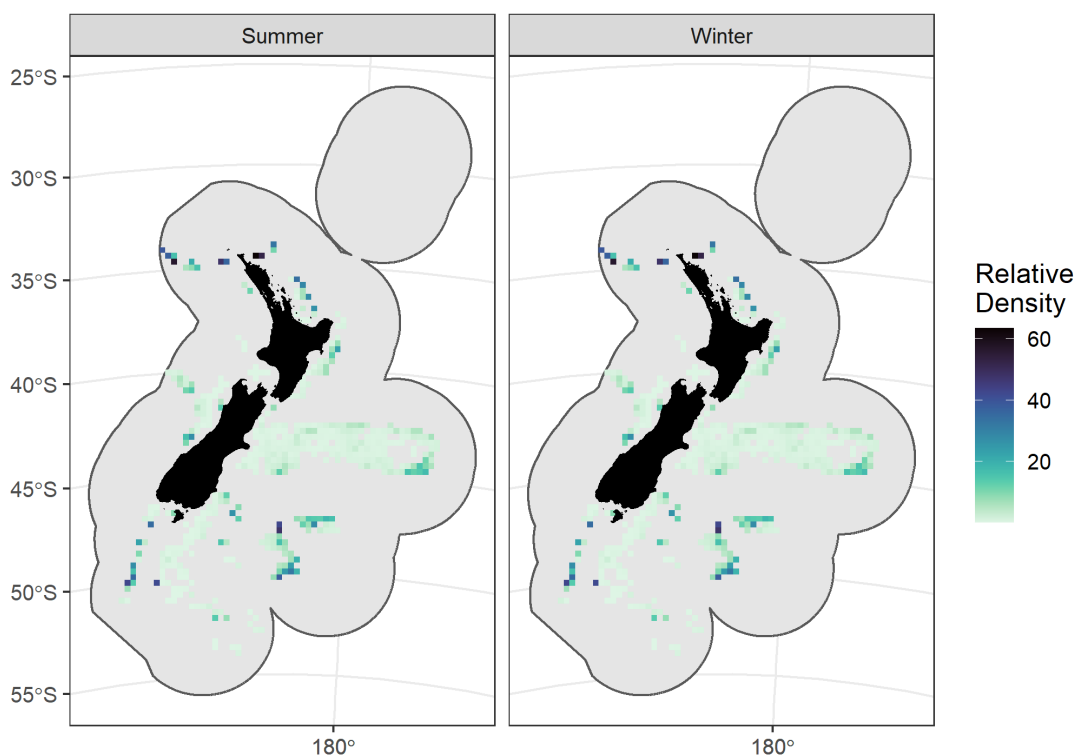


Figure 58: Posterior prediction of the relative density per grid cell and season for hydrocorals. Posterior median values are shown on a natural scale in tonnes per square kilometre.

Table 27: Total predicted bycatch (tonnes) per method for hydrocorals. Posterior median values are given, with the 95% equal-tailed credibility intervals in brackets.

Fishing year	BLL	TWL	Total
2000/01	0 (0 - 1)	1 (1 - 4)	1 (1 - 4)
2001/02	0 (0 - 1)	1 (1 - 3)	1 (1 - 4)
2002/03	0 (0 - 1)	1 (1 - 4)	1 (1 - 5)
2003/04	0 (0 - 1)	1 (1 - 4)	1 (1 - 4)
2004/05	0 (0 - 1)	1 (1 - 4)	1 (1 - 4)
2005/06	0 (0 - 1)	1 (1 - 3)	1 (1 - 3)
2006/07	0 (0 - 1)	1 (1 - 2)	1 (1 - 3)
2007/08	0 (0 - 1)	1 (1 - 3)	1 (1 - 3)
2008/09	0 (0 - 1)	1 (1 - 3)	1 (1 - 3)
2009/10	0 (0 - 1)	1 (1 - 2)	1 (1 - 3)
2010/11	0 (0 - 1)	1 (1 - 2)	1 (1 - 3)
2011/12	0 (0 - 1)	1 (1 - 2)	1 (1 - 3)
2012/13	0 (0 - 0)	1 (1 - 4)	1 (1 - 4)
2013/14	0 (0 - 1)	1 (1 - 2)	1 (1 - 3)
2014/15	0 (0 - 1)	1 (1 - 3)	1 (1 - 3)
2015/16	0 (0 - 1)	1 (1 - 2)	1 (1 - 3)
2016/17	0 (0 - 1)	1 (1 - 2)	1 (1 - 3)
2017/18	0 (0 - 1)	1 (1 - 4)	1 (1 - 4)
2018/19	0 (0 - 1)	1 (1 - 2)	1 (1 - 3)

Table 28: Model estimates of the average annual catch (tonnes) by the offshore Tier 1 fisheries, per gear, per non-target species, excluding the TAN and KAH trawl surveys. Posterior median values are given, with the 95% equal-tailed credibility intervals in brackets. Estimates for LIN are included for purposes of validation.

Species	AUT	MAN	BT	MB	MW	PRB	PRM	Total
LIN	3 057 (2 940 - 3 665)	1 228 (1 032 - 1 579)	8 390 (8 033 - 8 811)	453 (415 - 498)	384 (351 - 418)	46 (37 - 55)	5 (3 - 9)	13 592 (13 132 - 14 420)
BAR	0 (0 - 0)	0 (0 - 0)	1 130 (965 - 1 493)	3 311 (2 859 - 3 876)	450 (382 - 547)	1 (0 - 10)	0 (0 - 1)	4 910 (4 406 - 5 640)
RAT	7 (7 - 8)	0 (0 - 1)	11 747 (11 116 - 12 654)	103 (92 - 115)	40 (36 - 46)	98 (79 - 127)	7 (4 - 12)	12 005 (11 381 - 12 900)
SPD	712 (633 - 815)	142 (85 - 592)	2 497 (2 353 - 2 696)	139 (129 - 149)	132 (120 - 145)	15 (11 - 22)	3 (2 - 6)	3 644 (3 457 - 4 236)
FRO	0 (0 - 0)	0 (0 - 0)	16 (14 - 18)	1 006 (905 - 1 119)	243 (220 - 272)	0 (0 - 1)	2 (1 - 3)	1 269 (1 159 - 1 389)
EMA	0 (0 - 0)	0 (0 - 0)	70 (5 - 1 020)	254 (212 - 311)	211 (167 - 277)	1 (0 - 13)	0 (0 - 4)	552 (433 - 1 502)
MOD	290 (250 - 354)	103 (69 - 247)	1 585 (1 510 - 2 224)	28 (25 - 31)	6 (6 - 7)	5 (4 - 7)	1 (1 - 2)	2 029 (1 924 - 2 728)
RBT	0 (0 - 0)	0 (0 - 0)	26 (22 - 39)	226 (200 - 265)	107 (87 - 265)	1 (0 - 1)	0 (0 - 0)	364 (326 - 536)
WAR	0 (0 - 0)	0 (0 - 0)	13 (11 - 46)	200 (169 - 246)	24 (19 - 31)	0 (0 - 3)	0 (0 - 0)	238 (207 - 306)
NCB	0 (0 - 0)	0 (0 - 0)	409 (337 - 509)	14 (11 - 17)	1 (1 - 2)	0 (0 - 0)	0 (0 - 0)	424 (352 - 525)
SPE	115 (103 - 132)	24 (16 - 79)	1 514 (1 420 - 1 655)	1 (1 - 1)	0 (0 - 0)	10 (8 - 13)	0 (0 - 0)	1 665 (1 561 - 1 834)
GSP	44 (39 - 50)	1 (0 - 11)	915 (862 - 977)	0 (0 - 0)	0 (0 - 0)	12 (9 - 17)	0 (0 - 0)	975 (919 - 1 037)
RSO	1 (0 - 32)	2 (1 - 37)	332 (296 - 443)	27 (23 - 30)	24 (21 - 28)	7 (4 - 12)	0 (0 - 1)	396 (357 - 588)
GSH	26 (22 - 60)	0 (0 - 37)	492 (445 - 2 439)	1 (0 - 1)	0 (0 - 0)	1 (1 - 3)	0 (0 - 0)	520 (473 - 2 510)
SDO	0 (0 - 0)	0 (0 - 0)	130 (116 - 158)	27 (24 - 32)	4 (3 - 4)	0 (0 - 1)	0 (0 - 1)	162 (146 - 191)
STA	0 (0 - 0)	0 (0 - 0)	514 (489 - 538)	4 (3 - 4)	1 (0 - 1)	3 (2 - 4)	0 (0 - 2)	522 (497 - 546)
SND	49 (40 - 61)	16 (7 - 43)	269 (250 - 394)	1 (0 - 1)	1 (1 - 1)	7 (4 - 13)	0 (0 - 1)	346 (318 - 472)
LDO	0 (0 - 0)	0 (0 - 0)	608 (567 - 2 677)	8 (7 - 10)	4 (3 - 5)	7 (5 - 24)	0 (0 - 0)	627 (587 - 2 695)
SSK	69 (61 - 77)	42 (29 - 67)	419 (395 - 446)	1 (0 - 1)	0 (0 - 0)	2 (2 - 3)	0 (0 - 3)	534 (503 - 570)
STU	0 (0 - 0)	0 (0 - 0)	0 (0 - 0)	14 (13 - 16)	8 (7 - 9)	0 (0 - 1)	0 (0 - 0)	23 (21 - 25)
RBM	0 (0 - 0)	0 (0 - 0)	25 (23 - 29)	27 (24 - 30)	17 (16 - 22)	0 (0 - 0)	0 (0 - 0)	71 (66 - 77)
RSK	59 (49 - 72)	3 (1 - 9)	168 (158 - 182)	1 (1 - 1)	0 (0 - 0)	0 (0 - 1)	0 (0 - 1)	233 (217 - 254)
ETB	2 (1 - 4)	1 (0 - 4)	221 (205 - 238)	3 (0 - 32)	0 (0 - 0)	3 (2 - 7)	0 (0 - 0)	233 (215 - 267)
COR	0 (0 - 1)	0 (0 - 0)	1 (1 - 1)	0 (0 - 2)	0 (0 - 0)	0 (0 - 0)	0 (0 - 0)	1 (1 - 3)

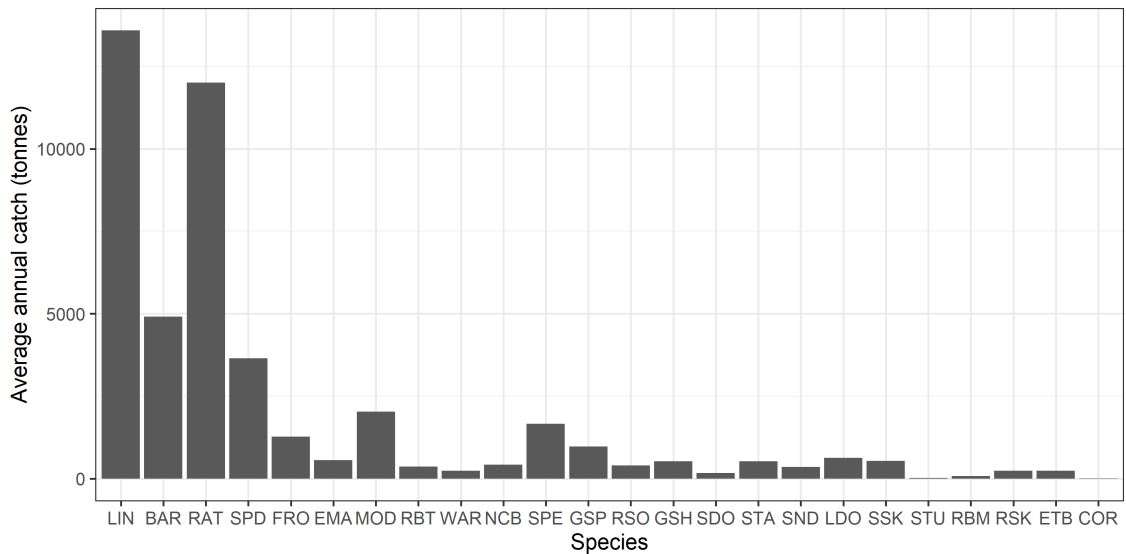


Figure 59: Model estimated annual catch per species (tonnes) ordered according to the total observed catch (Figure 1). Estimated annual catch for LIN is included only for purposes of validation.

4.4 Summary of estimated catches

In almost all instances, the model was able to reproduce the observer catch data, with the exception of giant spider crab, for which the model did not converge. We validated the catch predictions using vessel reported and landings data, which highlighted the strengths and weaknesses of the approach, as well as shortcomings of the landings data. These results are listed in full in by Edwards & Mormede (2023). In interpreting the model estimated catches per species, the following points should be considered:

- to better diagnose performance in instances where observer coverage is high, the model is used to predict catches using the total effort (not the residual effort);
- the statistical framework is generic and is more or less suitable for each species depending on the particular qualities of the data being presented;
- the biomass density surface is assumed constant over years and therefore any annual variation in the catches is due only to changes in the quantity and distribution of the fishing effort.

We further need to consider limitations in the data being used to validate the model. The vessel reported data are limited because only the most frequently caught species are recorded (i.e., the top species by biomass) and therefore often underestimate the actual catch. For this reason, the landings data are more reliable; but these latter data also include an uncertain discard component, which was necessary for comparison with the model outputs. The model outputs represent a third catch time series, which we must assess as being more or less reliable than the other two. For example (with reference to Edwards & Mormede 2023), for pale ghost shark (Figure S121), lookdown dory (Figure S187) and smooth skate (Figure S198), the model overestimates the vessel reported catches but accurately predicts the landings; for spiny dogfish (Figure S33), morid cods (Figure S66), ghost shark (Figure S143), giant stargazer (Figure S165) and rough skate (Figure S231), the model overestimates the vessel reported catches but underestimates the landings; for frostfish (Figure S44), the model accurately predicts the vessel reported catches but underestimates the landings. In all

these instances, the model appears to be performing well, since it is reproducing either the vessel reported catches or the landings, or is between the two. Further, if landings are considered the most accurate of the three time series, the model outputs are at least as good as, or in most instances better than, the vessel reported catches, being a closer match to the landings data.

In addition to the spatial component of model predictions, the strength of the approach and validity of the outputs can be seen from instances in which there are deficiencies also in the landings data, which are evident from apparent discontinuities in the landings time series. Discontinuities in the landings data can be due to species entering the QMS, improved species identification, or changes in the reporting code (for example to a higher taxonomic resolution). The best example of such a discontinuity is Baxter's dogfish (Figure S242). For this species, accurate landings data are only recorded from 2014 onward, which is evident from a large change in the landings recorded at that time. The model is able to reproduce the landings data from 2014 onward, but further extends the time series of catches backwards to 2001. For rough skate (Figure S231), landings appear to be underestimated prior to 2004 when rough skate entered the QMS. The model is able to reproduce the catches for 2001 – 2003. A similar reconstruction of the catch time series occurs for red swimming crab prior to 2010 (Figure S99), and shovelnose dogfish prior to 2014 (Figure S176). For these species, the model is able to generate an arguably better time series of catches compared with both the landings data and vessel reported estimates. This is also true for the hydrocorals (Figure S253), which have no useful landings data but for which the model can generate a catch time series.

Performance of the model is however dependent on representativeness of the observer data. An illustration of this is provided by gemfish (Figure S132). Here the prediction of the landings is accurate up until 2016. For 2017 – 2019 the model underestimates the landings. This corresponds to a time when precision harvesting gear became an important method in the gemfish fishery, yet the observed catch rates for PRB and PRM were lower than the corresponding vessel reported catch rates (Figure S122). The observed catch rates for BT, MB and MW were higher than the vessel reported catch rates. This indicates that the observer data may not be representative of the precision fishing methods. If this has led to an underestimate of the catches in recent years, it highlights the importance of representative observer data for the model to be successful in predicting catches. Distribution of the observer data across fishing effort has been typically considered when estimating the bycatch (Anderson & Edwards 2018) but was not evaluated directly here and is left for future and more directed application of the approach.

When comparing model outputs to the vessel reported catches and landings, we can conclude poor model performance when predicted catches are below both the landings and vessel reported catches. This can occur due to fluctuations in the catch time series that are not captured by the model when it is otherwise performing well, for example, Ray's bream (Figure S220), but also when the predicted catches are systemically low. In general, the model appears to perform better when catches are from the bottom trawl fisheries, and less well when catches are predominantly mid-water. For barracouta (Figure S11), blue mackerel (Figure S55), redbait (Figure S77), common warehou (Figure S88) and slender tuna (Figure S209), catch estimates are much lower than both the vessel reported and landings data. These are all predominantly mid-water fisheries. From inspection of the observer data, this failure appears to be due to the statistical properties of the observations and inability of the model in its current form to adequately represent these data. Specifically, when viewed across grid cells, mid-water catches show a much stronger positive skew, meaning that the total catch can be predominated by infrequent large catch events in a small part of the spatial distribution.

The model may not be able to adjust the biomass density sufficiently in those grid cells with a strong positive skew in the captures or, more likely, the variance structure of the observation model is of insufficient spatial resolution. To illustrate this point we use frostfish and redbait, both of which are predominantly mid-water fisheries, but with contrasting model performance. From Figure 60, it can be seen that the data from redbait show a much stronger positive skew than the data from frostfish. The data from frostfish are comparable with the data from smooth skate, which is caught predominantly in the bottom trawl fisheries and is included for illustrative purposes. When the data are skewed in this way, the distributional assumptions of the model cannot accurately represent the large catch values, which in turn leads to underestimation of the catch rate and poor model performance. This may also be the reason for poor performance of the model when applied to data from giant spider crab, which is characterised by low frequency, high catch events.

Overall, we can conclude the model performs well, but only when the statistical properties of the data are adequately represented. Since the work is developmental and the model generic, this variability in performance is to be expected. In Section 6 we discuss improvements that could be made in further work.

4.5 Summary of density estimates

The biomass density distributions are assumed seasonal but constant across years. The seasonal changes are difficult to discern visually, but we can draw qualitative conclusions regarding the overall estimated spatial distributions. Since both the catches and biomass density combine to determine the exploitation rate, it is interesting to note instances where catches are concentrated in regions of high density, or where large catches occur despite the density being low.

Rough and smooth skates provide a good illustration of how the estimated density can reflect the known biology of the species. For rough skate (Figure 54), the density is predominantly inshore, including around the Auckland and Bounty islands, whereas smooth skate (Figure 48) is estimated to have a much wider distribution, extending onto the Chatham Rise, and to be less abundant at the higher latitudes. The chimeras are similarly resolved spatially. The pale ghost shark (*H. bemisi*, Figure 34) is estimated to be on the southern edge of the Chatham Rise, and extending to higher latitudes on the Campbell Plateau. The ghost shark (*H. novaezealandiae*, Figure 38), is more confined to shallower regions of the Chatham Rise and also found at lower latitudes. In both instances, we note that relatively large catches are estimated to occur off the west coast of the South Island (Figures 33 and 37), in a region of low density for both species.

Species found in shallower inshore regions include the barracouta (Figure 14), blue mackerel (Figure 22), gemfish (Figures 36) and common warehou (Figure 28). We can also see that rattails (Figure 16), morid cods (Figure 24), shovelnose dogfish (Figure 44), and Baxter's dogfish (Figure 56) show a higher density at the deeper edges of the fished distribution, around the Chatham Rise and Campbell Plateau. For these species, higher catches appear to occur in shallower regions where the biomass density is lower. For spiny dogfish (Figures 17 and 18), sea perch (Figures 31 and 32) and lookdown dory (Figures 45 and 46) catches are concentrated in regions of higher biomass. These predictions have implications for our understanding of the exploitation of each species and highlight the potential benefits of an integrated spatial approach.

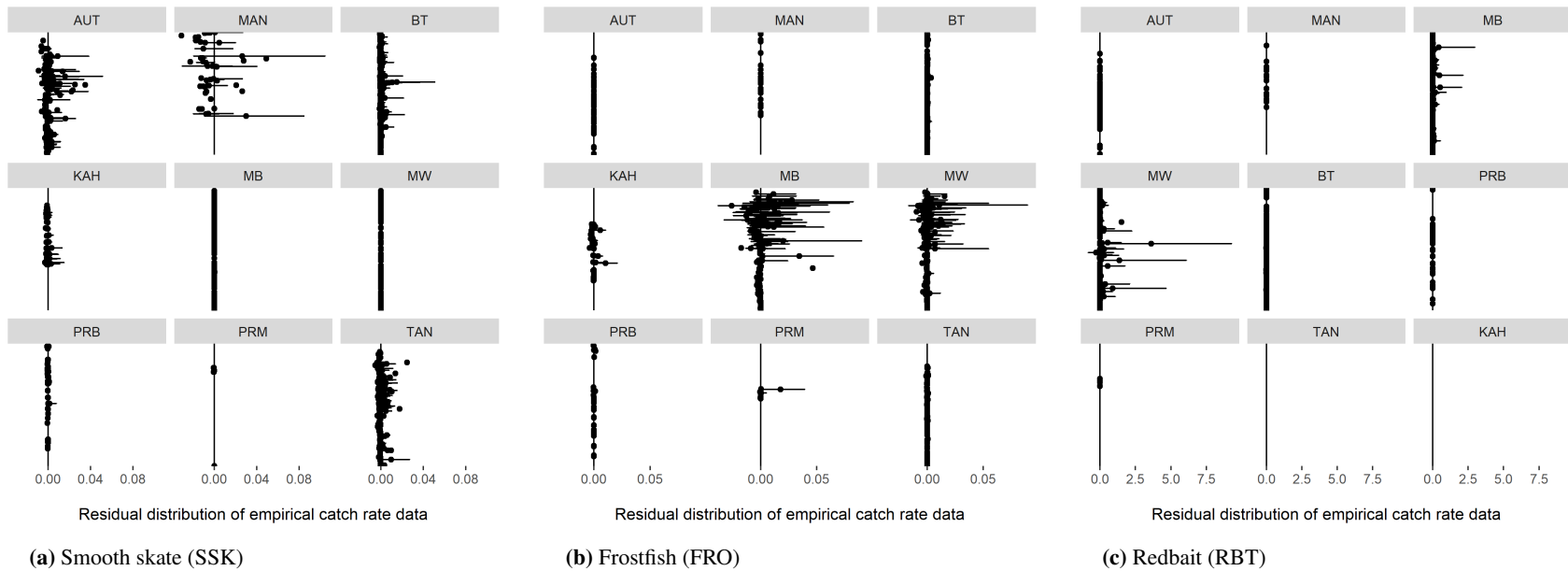


Figure 60: Residual distributions from model fits to smooth skate, frostfish and redbait. For each grid cell and fishing method, the distribution of empirical catch rate values is shown relative to the model estimated mean catch rate. The empirical distribution is represented by the mean and upper and lower 90% quantile values. The empirical data for redbait shows a strong positive skew (noting the difference in scale).

5. DISCUSSION

Estimates of the non-target catch have so far been typically conducted per fishery (Anderson et al. 2017a,b, Anderson & Edwards 2018, Anderson et al. 2019, Finucci et al. 2020), with the work of Anderson (2017) and Finucci et al. (2019) being exceptions. Finucci et al. (2019) applied a model to data from each of the major fisheries to estimate bycatch for the top 50 non-target species per fishery. If required, the non-target catch estimates for a species could be added across fisheries to generate a total over time. The current work has provided an opportunity to further develop this approach, but specifically allowing estimation of the total non-target catch per species by simultaneous integration of the data from multiple fisheries, and using these combined data to predict catches at a higher spatial resolution. In developing this approach we have also proposed a means for integrated estimation of the biomass density surface, providing a possible foundation for a spatially explicit fisheries risk assessment (e.g., Edwards 2021). A risk assessment for data-poor bycatch species would be an important step towards ecosystem-based fisheries management.

For species examined in detail (see Sections 4.1 and 4.2) the model is able to accurately predict the observed catch data and to use the estimated catch rate to predict catches spatially and over time. For the remaining species, the fits are also reasonable, but accurate prediction of the catches is dependent on the representativeness of the observer data and the extent to which statistical structure of the model is able to describe the properties of the data. In both instances, these can lead to poor performance of the model. However, it is also clear that the model can perform well, in some cases generating a catch time series that is superior to the vessel reported catches (i.e., a closer match to the landings). In instances in which the landings time series is incomplete due to changes in the reporting, the model may also be able to provide a better estimate of the total removals than the landings.

6. POTENTIAL RESEARCH

In the current project we have developed and applied a generic framework to a variety of species, in each case integrating across multiple discordant fisheries. This was achieved with a parametrically simple model, representing fishing per gear type with only two parameters: the catch efficiency (π_j) and the encounter rate (γ_j). That the model is able to predict catches despite this simplicity is testament to the importance of the underlying biomass density distribution in describing the catch process.

Although established methods for spatial estimation of the catch rate do exist (e.g., Thorson & Ward 2013, Thorson et al. 2015, 2017, Zhou et al. 2019), to our knowledge the biomass density has never been considered explicitly in previous attempts to model or predict bycatch, either in New Zealand or internationally. Recent iterations of the Vector Autoregressive Spatio-Temporal (VAST) model for example, consider density as the product of an encounter rate and the non-zero catch (i.e., the catch rate). Using the author's own terminology, the expected density is: $\mathbb{E}[d_i] = p_i \cdot r_i$, where p_i is the probability of encounter and r_i is the catch rate per non-zero catch event, at the location and time of fishing event i (Thorson 2018, Grüss & Thorson 2019). The p_i and r_i terms are interpreted as functions of the available numbers and the average weight per individual, respectively. In the current work, biomass density is instead represented explicitly and consistently by the estimated parameter d_{kl} , which is a predictor of both the encounter probability and the catch per non-zero catch event. The catch process is defined by the encounter rate γ_j , efficiency π_j , and an effort scalar proportional to the gear affected area s_{jkl} . This has the advantage of separating estimates of the biomass density from the catch process, and the work presented here indicates that it may

be a fruitful avenue for future research. A number of modifications and improvements present themselves, which we elaborate further here.

Statistical properties of the model could be improved with a more focused application of the approach. When selecting a model for application across a wide range of species and fisheries, it is often required to be more simple than would otherwise be appropriate for optimum performance in each case. In the current setting we have noted that highly skewed data can be problematic. This could potentially be resolved by better representation of the variance spatially, or modifications to the spatial resolution of the model itself (i.e., experimenting with different grid cell sizes).

Expansion of the spatial resolution to grid cells with no observed positive catches. This can be achieved by selecting grid cells that are neighbours to the observed “core” grid cells. Inclusion of a conditional autoregressive (CAR) prior, as well as the use of environmental covariates, can stabilise estimation of the biomass density in these unsampled cells. A wider variety of environmental covariates could naturally be considered as part of this process.

Expansion of the data included in the modelling. Currently the model is applied to the survey and observer catch rate data, which are the best available. However, there are large amounts of vessel reported catches that were not used by the model presented in the current project. Although incomplete, these data contain information on, if not the catch rate, then at least the spatial and temporal distribution of the catches. Future modelling should attempt to make use of this information.

Definitions of the catchability could be improved by including sub-models that can describe γ_j and π_j using predictive coefficients. Currently only gear type, and optionally target, are considered. Other more subtle fishery definitions could easily be included given the available data.

7. ACKNOWLEDGEMENTS

Financial support for this work was provided by Fisheries New Zealand project ENV2020-20, granted to CEscape Consultancy Services (Otaki, New Zealand). We are grateful for the direction given by Marco Milardi and Josh Van Lier (previously Fisheries New Zealand) and to feedback from members of the Aquatic Environment Working Group. A helpful review of the report was provided by Campbell Murray (Fisheries New Zealand).

8. REFERENCES

- Anderson, O.F. (2017). Fish and invertebrate bycatch in New Zealand deepwater fisheries from 1990–91 until 2013–14. *New Zealand Aquatic Environment and Biodiversity Report No. 181*. 75 p.
- Anderson, O.F.; Ballara, S.L.; Edwards, C.T.T. (2017a). Fish and invertebrate bycatch and discards in New Zealand orange roughy and oreo trawl fisheries from 2001–02 until 2014–15. *New Zealand Aquatic Environment and Biodiversity Report No. 190*. 216 p.
- Anderson, O.F.; Edwards, C.T.T. (2018). Fish and invertebrate bycatch and discards in New Zealand arrow squid and scampi trawl fisheries from 2002–03 until 2015–16. *New Zealand Aquatic Environment and Biodiversity Report No. 199*. 135 p.
- Anderson, O.F.; Edwards, C.T.T.; Ballara, S.L. (2019). Non-target fish and invertebrate catch and discards in New Zealand hoki, hake, ling, silver warehou, and white warehou trawl fisheries from 1990–91 to 2016–17. *New Zealand Aquatic Environment and Biodiversity Report No. 220*. 117 p.
- Anderson, O.F.; Edwards, C.T.T.; Roux, M.J. (2017b). Fish and invertebrate bycatch and discards in New Zealand jack mackerel trawl fisheries from 2002–03 until 2013–14. *New Zealand Aquatic Environment and Biodiversity Report No. 177*. 71 p.
- Edwards, C.T.T. (2021). Integrated estimation of density and catchability parameters from fisheries catch-effort data. *New Zealand Fisheries Assessment Report 2021/32*. 32 p.
- Edwards, C.T.T.; Mormede, S. (2023). Temporal and spatial distribution of non-target catch and non-target catch species in deepwater fisheries: supplementary information. *New Zealand Aquatic Environment and Biodiversity Report No. 304*. 264 p.
- Edwards, C.T.T.; Sibanda, N.; Roux, M.J.; Sharp, B. (2018). Estimating capture and retention efficiency for nontarget fish species in commercial trawl fisheries. (Unpublished Final Research Report prepared for MPI project SEA2016-19 and held by Fisheries New Zealand, Wellington.)
- Finucci, B.; Anderson, O.F.; Edwards, C.T.T. (2020). Non-target fish and invertebrate catch and discards in New Zealand ling longline fisheries from 2002–03 to 2017–18. *New Zealand Aquatic Environment and Biodiversity Report No. 241*. 83 p.
- Finucci, B.; Edwards, C.T.T.; Anderson, O.F.; Ballara, S.L. (2019). Fish and invertebrate bycatch in New Zealand deepwater fisheries from 1990–91 until 2016–17. *New Zealand Aquatic Environment and Biodiversity Report No. 210*. 77 p.
- Fisheries New Zealand (2020). Chapter 9: Non-target fish and Invertebrate Catch, pp. 318–362. *In: Aquatic Environment and Biodiversity Annual Review 2019-20*. (Edited by Aquatic Environment Team, Fisheries Science and Information, Fisheries New Zealand, Wellington New Zealand), 765 p.
- Gelfand, A.E.; Vounatsou, P. (2003). Proper multivariate conditional autoregressive models for spatial data analysis. *Biostatistics 4 (1)*: 11–15.
- Gelman, A.; Rubin, D.B. (1992). Inference from Iterative Simulation Using Multiple Sequences. *Statistical Science 7 (4)*: 457–472.

- Grüss, A.; Thorson, J.T. (2019). Developing spatio-temporal models using multiple data types for evaluating population trends and habitat usage. *ICES Journal of Marine Science* 76 (6): 1748–1761.
- Jin, X.; Carlin, B.P.; Banerjee, S. (2005). Generalized hierarchical multivariate CAR models for areal data. *Biometrics* 61 (4): 950–961.
- McCaughran, D.A. (1992). Standardized nomenclature and methods of defining bycatch levels and implications. In: Proceedings of the National Industry Bycatch Workshop, 4–6 February 1992, Oregon (Edited by R.W. Schoning; R.W. Jacobson; D.L. Alverson; T.G. Gentle; J. Auyong), pages 200–201.
- Mormede, S.; Weber, D.N.; Edwards, C.T.T. (2022). Creating standardised grids for New Zealand marine science outputs. *New Zealand Aquatic Environment and Biodiversity Report No. 283*. 7 p.
- Paloheimo, J.E.; Dickie, L.M. (1964). Abundance and fishing success. *Rapports et Proces-Verbaux des Reunions, Conseil International pour L'exploration de la Mer* 155: 152–163.
- Pikitch, E.K.; Santora, C.; Babcock, E.A.; Bakun, A.; Bonfil, R.; Conover, D.O.; Dayton, P.; Doukakis, P.; Fluharty, D.; Heneman, B.; Houde, E.D.; Link, J.; Livingston, P.A.; Mangel, M.; McAllister, M.K.; Pope, J.; Sainsbury, K.J. (2004). Ecosystem based fisheries management. *Science* 305 (5682): 346–347.
- R Core Team (2020). R: A Language and Environment for Statistical Computing. R Foundation for Statistical Computing, Vienna, Austria. Version 4.0.2
- Stan Development Team (2020). RStan: the R interface to Stan. Version 2.21.2
- Thorson, J.T. (2018). Three problems with the conventional delta-model for biomass sampling data, and a computationally efficient alternative. *Canadian Journal of Fisheries and Aquatic Sciences* 75: 1369–1382.
- Thorson, J.T.; Fonner, R.; Haltuch, M.A.; Ono, K.; Winker, H. (2017). Accounting for spatiotemporal variation and fisher targeting when estimating abundance from multispecies fishery data. *Canadian Journal of Fisheries and Aquatic Sciences* 74 (11): 1794–1807.
- Thorson, J.T.; Shelton, A.O.; Ward, E.J.; Skaug, H.J. (2015). Geostatistical delta-generalized linear mixed models improve precision for estimated abundance indices for west coast groundfishes. *ICES Journal of Marine Science* 72 (5): 1297–1310.
- Thorson, J.T.; Ward, E.J. (2013). Accounting for space–time interactions in index standardization models. *Fisheries Research* 147: 426–433.
- Zhou, S.; Campbell, R.A.; Hoyle, S.D. (2019). Catch per unit effort standardization using spatio-temporal models for Australia’s Eastern Tuna and Billfish Fishery. *ICES Journal of Marine Science* 76 (6): 1489–1504.

APPENDIX 1

DATA REQUEST

23 July 2021 (relogs 13468 & 13813)

For ENV2020-20, we require data extracts for all deepwater fishing activity, all years from 1 October 1990 up to 30th September 2020, in all areas, for all form types and by any fishing method, where the target species is one of: ORH, HOK, HAK, LIN, JMA, JMD, JMN, JMM, OEO, SSO, BOE, SOR, WOE, SBW, SQU, ASQ, NOS, NOG, SCI, SWA, WWA.

- Catch and effort data:
 - This includes all data recorded in the CELR, TCER and LCER form types;
 - All fishing event records are required from each trip, with a single data row for each fishing event;
 - Estimated catches for all species recorded are required for each event record;
 - Full accuracy position data are required.

The following fields are required: dcf_key, vessel_key, trip, form_type, event_key, version_seqno, vessel_reg_type, flag_nationality_code, overall_length_metres, draught_metres, beam_metres, gross_tonnes, max_speed_knots, built_year, engine_kilowatts, start_datetime (in yyymmdd and hhmm format if possible), end_datetime (in yyymmdd and hhmm format if possible), haul_start_datetime, primary_method, fishing_duration, start_latitude, start_longitude, end_latitude, end_longitude, start_stats_area_code, target_species, effort_num, effort_total_number, effort_height, effort_width, effort_depth, effort_speed, bottom_depth, total_hook_number, total_net_length, species_estimated_catch, total_catch.

- Landing data:
 - This includes landing data for each fishing trip.

The following fields are required: event_key, trip, state_code, version_seqno, vessel_key, unit_type, group_key, start_datetime, unit_num, specprod_seqno, trip_end_datetime, unit_weight, dcf_key, landing_datetime, conversion_factor, fishstock_code, greenweight_type, form_type_processed_weight (kg), destination_type, species_greenweight (kg)

- An extract of all available observer data:
 - This includes the relevant data tables from the Centralised Observer Database (COD).

The following tables are required (all fields): x_event, x_fishing_event, x_fishing_event_catch, x_fishing_method, x_trip, y_trip_vessel, x_species_codes, x_trawl_effort, x_trawl_gear, x_bottom_lining_effort, x_setnet_effort, x_setnet_gear.

- An extract of the research trawl database for all trawl surveys (inshore and offshore), the data and format described in <https://marlin.niwa.co.nz/files/dataHoldings/scientificResearchDbs/trawl.xls> is likely to be the required type of data.